# CONVERSION OF HAZELNUT SHELL INTO VALUE-ADDED CHEMICALS BY USING SUB-CRITICAL WATER AS A REACTION MEDIUM

**A Thesis Submitted to**
**the Graduate School of Engineering and Sciences of**
**İzmir Institute of Technology**
**in Partial Fulfillment of the Requirements for the Degree of**

**MASTER OF SCIENCE**

**in Chemical Engineering**

**by**
**Gökalp GÖZAYDIN**

**December, 2016**
**İZMİR**

We approve the thesis of **Gökalp GÖZAYDIN**

**Examining Committee Members:**

_____

**Assist. Prof. Dr. Aslı YÜKSEL ÖZŞEN**
Department of Chemical Engineering, İzmir Institute of Technology

_____

**Prof. Dr. Fehime ÇAKICIOĞLU ÖZKAN**
Department of Chemical Engineering, İzmir Institute of Technology

_____

**Assist. Prof. Dr. Meral DÜKKANCI**
Department of Chemical Engineering, Ege University

**26 December 2016**

_____

**Assist. Prof. Dr. Aslı YÜKSEL ÖZŞEN**
Supervisor, Department of Chemical Engineering
İzmir Institute of Technology

_____

**Prof. Dr. Fehime ÇAKICIOĞLU ÖZKAN**
Head of the Department of Chemical Engineering

_____

**Prof. Dr. Bilge KARAÇALI**
Dean of the Graduate School of Engineering and Sciences

# ACKNOWLEDGMENTS

First of all, I would like to express my gratefulness to my supervisor Assist. Prof. Dr. Aslı YÜKSEL ÖZŞEN for her support, guidance and encouragement during my M.Sc. Thesis. I gained significant experience throughout study with her and her research team.

I would like to thank to Filiz KURUCAOVALI for HPLC and TOC analysis, Handan GAYGISIZ for GC-MS analysis and Esra TUZUOĞLU YÜCEL for GC-TCD analysis at Environmental Research and Development Center. Moreover, I wish to thank to Yekta GÜNAY OĞUZ for HPLC and FTIR analysis at Biotechnology and Bioengineering Application and Research Center.

I am also grateful to my workmate Okan AKIN for his support, guidance and friendship during my experiments and analysis period.

Finally, I would like to my special thanks to my parents Yücel ÖZSOY and Esin GÖZAYDIN for their support and encouragements.

# ABSTRACT


## CONVERSION OF HAZELNUT SHELL INTO VALUE-ADDED CHEMICALS BY USING SUB-CRITICAL WATER AS A REACTION MEDIUM

The objective of this study is to clarify the effect of reaction temperature, reaction time, acid concentration and acid type on the hydrothermal conversion of waste hazelnut shell into value-added chemicals under hot compressed water with high temperature/high pressure autoclave. The other aim is to gaining of added value and new utilization field to waste hazelnut shell. This is the first study about the degradation of waste hazelnut shell in order to produce levulinic acid under subcritical water in literature. Reactions were performed at 150-280 °C of reaction temperature, 15-120 min of reaction time with different acid ($H_2SO_4$ and $H_3PO_4$) concentrations that was varied from 0 to 125 mM.

The liquid product distribution was evaluated with High Performance Liquid Chromatography (HPLC) and Gas Chromatography-Mass Spectrometry (GC-MS) and gas products were identified by Gas Chromatography with a Thermal Conductivity Detector (GC-TCD). While levulinic acid, acetic acid and furfural were identified as a major liquid compounds, the main gaseous products were carbon dioxide and carbon monoxide. Increasing reaction temperature and reaction time improved the conversion of hazelnut shell up to 65.40% at 280 °C and 120 min in the presence of 50 mM $H_2SO_4$ and 13.05% of levulinic acid yield was obtained under the similar reaction conditions. Addition of dilute $H_2SO_4$ and $H_3PO_4$ in the reaction medium enhanced different product formation. $H_2SO_4$ treatment promoted the production of levulinic acid whereas addition of $H_3PO_4$ increased the formation of furfural. Furthermore, total phenolic content, antioxidant capacity and possible reaction pathways of hydrothermal conversion of waste hazelnut shell was evaluated.

# ÖZET

## KRİTİK-ALTI SUYU REAKSİYON ORTAMI OLARAK KULLANARAK FINDIK KABUĞUNUN DEĞERLİ KİMYASALLARA DÖNÜŞTÜRÜLMESİ

Bu çalışmanın amacı sıcak basınçlı suda fındık kabuğu atığının değerli kimyasallara dönüştürülmesini yüksek sıcaklık/yüksek basınlı reaktör kullanarak reaksiyon sıcaklığı, reaksiyon süresi, asit miktarı ve asit cinsinin etkisini ortaya çıkarmaktır. Diğer amaç ise fındık kabuğu atığına katma değer ve yeni kullanım alanı kazandırmaktır. Kritik-altı su koşullarında fındık kabuğu atığından levulinik asit üretimi literatürdeki ilk çalışmadır. Reaksiyonlar 150-280 °C reaksiyon sıcaklığı, 15-120 dakika reaksiyon süresi ve 0-125 mM $H_2SO_4$ and $H_3PO_4$ miktarları arasında gerçekleştirilmiştir.

Sıvı ürün dağılımı Yüksek Performans Sıvı Kromatogram (HPLC) ve Gaz Kromatogram-Kütle Spektrometri (GC-MS) ve gaz ürünler Termal İletken Dedektörlü Gaz Kromatogram kullanılarak belirlenmiştir. Levulinik asit, asetik asit ve furfural temel sıvı ürünlerken, ana gaz ürünler ise karbon dioksit ve karbon monoksittir. Reaksiyon sıcaklığının ve reaksiyon süresinin arttırılması, fındık kabuğu dönüşümünün 280 °C, 120 dak. ve 50 mM $H_2SO_4$ içerisinde 65.40%'e kadar yükseltmiştir ve aynı reaksiyon koşullarında 13.05% levulinik asit elde edilmiştir. Reaksiyon ortamına $H_2SO_4$ ve $H_3PO_4$ ilavesi farklı ürünlerin oluşumunu arttırmıştır. Sülfürik asitli işlem levulinik asit üretimi arttırırken, fosforik asit ilavesi furfural oluşumunu arttırmıştır. Ayrıca, fındık kabuğu atığının hidrotermal dönüşümünde toplam fenol miktarı, antioksidant kapasitesi ve olası reaksiyon mekanizmaları belirlenmiştir.

# TABLE OF CONTENTS

# LIST OF FIGURES

# LIST OF TABLES

# CHAPTER 1

# INTRODUCTION

The exploration of new alternative resources has been a significant task for the production of fuel and chemicals due to depletion of fossil fuels resources, global warming and sustainability. Currently, we have provided both energy and chemical requirements from nonrenewable sources such as coal, petroleum and natural gas. Therefore, the usage of renewable energy (e.g. solar, wind, thermal, hydroelectric, biomass, etc.) grows in importance since they are cheap, renewable and non-polluting. Among all renewable resources, biomass is unique because the utilization biomass is a carbon neutral process and also, liquid, solid and gaseous products can be produced from biomass that is unique renewable carbon source. The captured carbon dioxide via photosynthesis is released during the production of fuels, chemicals, power and heat from biomass. Moreover, waste lignocellulosic biomass as a feedstock takes more attention owing to not preferred for food necessity. Scientists and academicians from all countries have focused on developing sustainable green technologies to meet world's technical, economic and social demands (Pandey et al. 2011, Saxena et al. 2009).

## 1.1. The Aim and the Importance of the Study

The aim of this study is to investigate the potential role of waste hazelnut shell as a biomass feedstock for the production of valuable chemicals such as levulinic acid, acetic acid, furfural, etc. bring an added value since Turkey leads in hazelnut production with supplying 75% of the global hazelnut production in the World (650.000 tons/year) (Guney 2013). The other objective is to understand the effects of reaction temperature (150-280 °C), reaction time (15-120 min), acid concentration (0-125 mM), and acid type ($H_2SO_4$ and $H_3PO_4$) on the conversion of hazelnut shell and the yields of valuable chemicals in hot compressed water without any organic solvents. In literature, the hydrothermal conversion of waste hazelnut shell to produce levulinic acid, as a value-added chemical, in subcritical water has not been studied before. Subcritical water is chosen as a reaction media in hydrothermal degradation of waste hazelnut shell into its

building blocks since water is environmentally friendly, cheap, abundant, non-flammable and non-toxic (Chan et al. 2014). In addition, the physicochemical properties of water can be varied with changing temperature and pressure. Therefore, the subcritical water becomes a unique solvent for hydrothermal biomass degradation.

Over the years, significant studies about degradation of waste biomass have been performed. Among the various degradation processes, liquefaction process is more attractive since most of the biomass feedstock has higher water content. Therefore, cost and energy saving can be achieved by liquefaction process than pyrolysis where approximately 2.4 MJ/kg energy is required to evaporate water (Asghari and Yoshida 2010).

## 1.2. Description of Biomass

In a term, biomass is generally called as renewable and sustainable organic material. Besides biomass is the fourth major energy resource with compensating 14% of the world's primary energy requirements, it is commonly refers as a carbon neutral source in contrast to fossil fuels such as coal, petroleum and natural gas. During photosynthesis, $CO_2$ in the air, water and sunlight are reacted with each other to form the building blocks of biomass like carbohydrates. The solar energy is stored in the chemical bonds between carbon, hydrogen and oxygen molecules. This stored chemical energy is released by breakage of bonds with chemical or biological processes. Oxygen oxidizes the carbon in carbohydrate products to produce carbon dioxide and carbon dioxide is reabsorbed by other biomass. Therefore, this process has not any contribution to carbon dioxide in atmosphere. These products can be classified into three main types:

- feedstock for chemicals
- electrical/heat energy
- fuel for transportation

The types of biomass can be categorized as:

- herbaceous plants/grasses
- woody plants
- manures
- aquatic plants

Biomass conversion processes are determined with respect to biomass type. For instance, fermentation is preferred for biomass with high moisture content such as herbaceous plant and sugar cane while gasification, pyrolysis and combustion are more suitable for a dry biomass like woody plants (McKendry 2002a, Saxena et al. 2009).

### 1.2.1. Structure of Biomass

Biomass is heterogeneous mixtures of organic substances including cellulose, hemicellulose, lignin and a small amount of inorganic substances that includes in the ash. Although the composition of lignocellulosic biomass component changes with respect to biomass type, tissue type, growth stage and growing conditions, it generally composes of 38-50% cellulose, 23-32% hemicellulose and 15-25% lignin (Figure 1.1). Cellulose, hemicellulose and lignin distribution of some lignocellulosic biomasses are shown in Table 1.1. Cellulose and hemicellulose form the carbohydrate part of the biomass, however; lignin composes the non-carbohydrate part of it. Furthermore, cellulose and hemicellulose provide structural and mechanical strength to the plant, whereas lignin extends the stability of these structures (Tekin et al. 2014, Lee 2013).

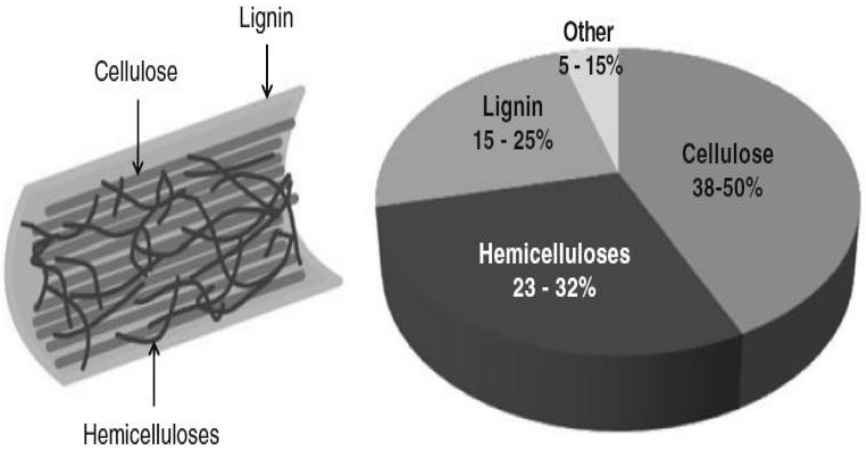


Figure 1.1. Typical composition of lignocellulosic biomass
(Source: Lee 2013)

Table 1.1. Cellulose, hemicellulose and lignin distribution of some lignocellulosic biomasses (Source: Fang and Xu 2014)

| **Biomass** | **Cellulose (wt.%)** | **Hemicellulose (wt.%)** | **Lignin (wt.%)** | **HHV (MJ/kg)** |
|---|---|---|---|---|
| Tobacco leaf | 43.45 | 41.54 | 15.01 | 17.7 |
| Corncob | 52.49 | 32.32 | 15.19 | 17.48 |
| Corn straw | 51.53 | 30.88 | 17.59 | 18.27 |
| Wheat straw | 33.82 | 45.2 | 20.98 | 18.55 |
| Beech wood | 46.27 | 31.86 | 21.87 | 19.23 |
| Hardwood | 45.85 | 32.26 | 21.89 | 18.97 |
| Softwood | 42.68 | 24.82 | 32.5 | 19.55 |
| Spruce wood | 47.11 | 21.31 | 31.58 | 19.77 |
| Hazelnut shell | 26.7 | 30.29 | 43.01 | 20.05 |
| Wood bark | 25.59 | 30.28 | 44.13 | 20.74 |
| Olive cake | 23.08 | 21.63 | 55.29 | 21.53 |

*Cellulose* is the most abundant natural polymer on the earth that founds nearly 35%-50% of most plant material (Sengupta and Pike 2013). Cellulose is a long chain polysaccharide with a high molecular weight (approximately 500,000) and its general formula is $(C_6H_{10}O_5)_n$ (Tekin et al. 2014). Cellulose is formed by the glucose units which are linked by β-1,4-glycosidic bonds which is given in Figure 1.2 and it has a

higher degree of polymerization (approximately 10,000) (Sengupta and Pike 2013). It has also higher degree of crystallinity than starch since cellulose composes of straight chains, which give an opportunity to form either strong intra- and inter-molecular hydrogen bonds. Therefore, cellulose is insoluble in ambient water whereas it is completely soluble and hydrolyzed to its components at subcritical conditions (Toor et al. 2011). Furthermore, cellulose is insoluble in most of the solvents because of hydrogen bonding that gives a strong fiber structure (Tekin et al. 2014).

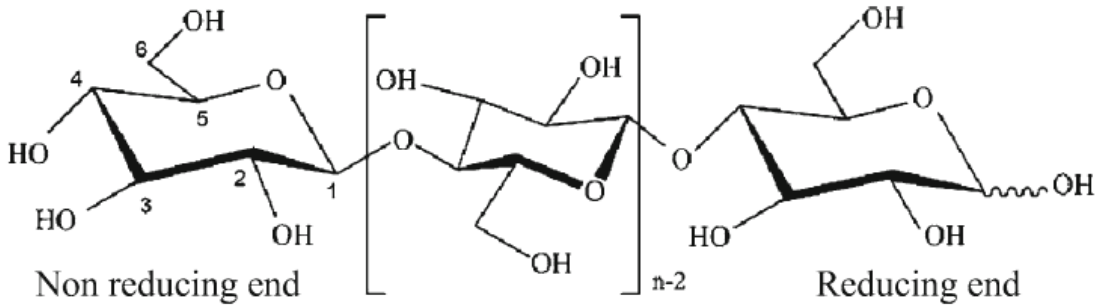


Figure 1.2. Structure of cellulose
(Source: Lee 2013)

*Hemicellulose* is an amorphous heteropolymer including xylose, mannose, glucose and galactose and has a lower degree of polymerization (approximately 100 sugars per hemicelluloses molecule) than cellulose. Hemicellulose creates hydrogen bonds with cellulose, covalent bonds with lignin and ester bonds with acetyl units and hydroxycinnamic acids. It has a lower degree of crystallinity and degrades more easily with heat treatment due to the presence of high amount of side groups and less stable structure than cellulose (Tekin et al. 2014, Toor et al. 2011, Lee 2013). Hemicellulose is a polymer that consists of mixed sugars such as six carbon sugars and five carbon sugars. Six carbon sugars are mannose, galactose, glucose and D-glucuronic acid and five carbon sugars are xylose and arabinose which are shown in Figure 1.3 (Lee 2013, Tekin et al. 2014). Xylan is a typical building block of hemicellulose as shown in Figure 1.4.

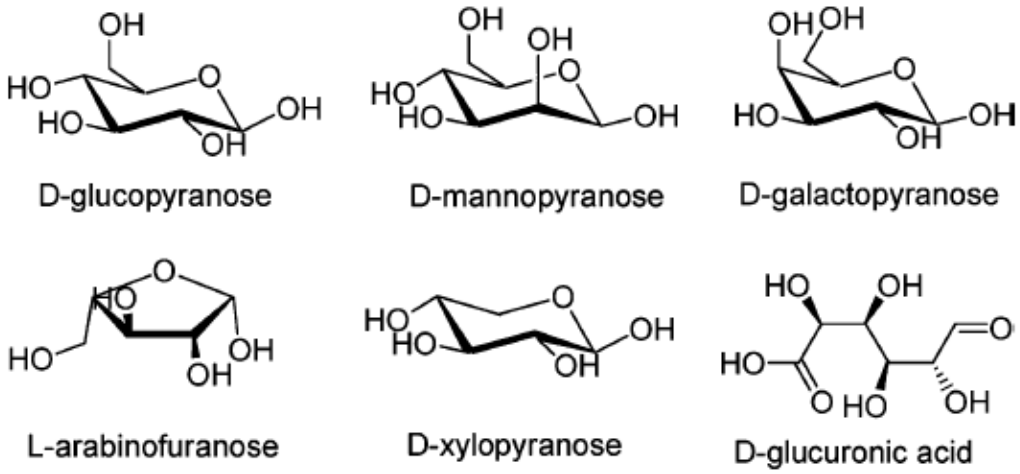


Figure 1.3. Basic structures of hemicellulose monomers
(Source: Gandini 2011)

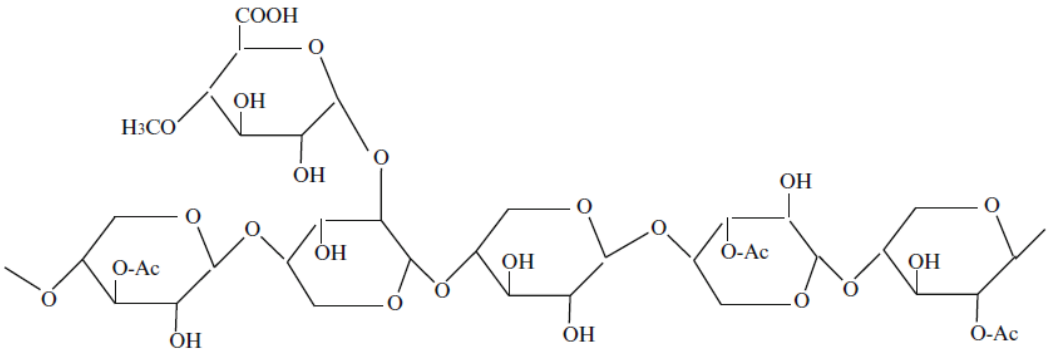

Figure 1.4. Molecular structure of xylan
(Source: Lee 2013)

*Lignin* is a complex aromatic polymer in which phenylpropane units link with hydroxyl and methoxy groups through ether bonds. The structure of basic lignin monomers is shown in Figure 1.5. The lignin polymers have a heterogeneous structure in which basic lignin monomers are linked by C-C and aryl-ether linkages with aryl-glycerol-β-aryl ether. Furthermore, lignin is an amorphous polymer, hydrophobic and less soluble in water (Lee 2013, Tekin et al. 2014).

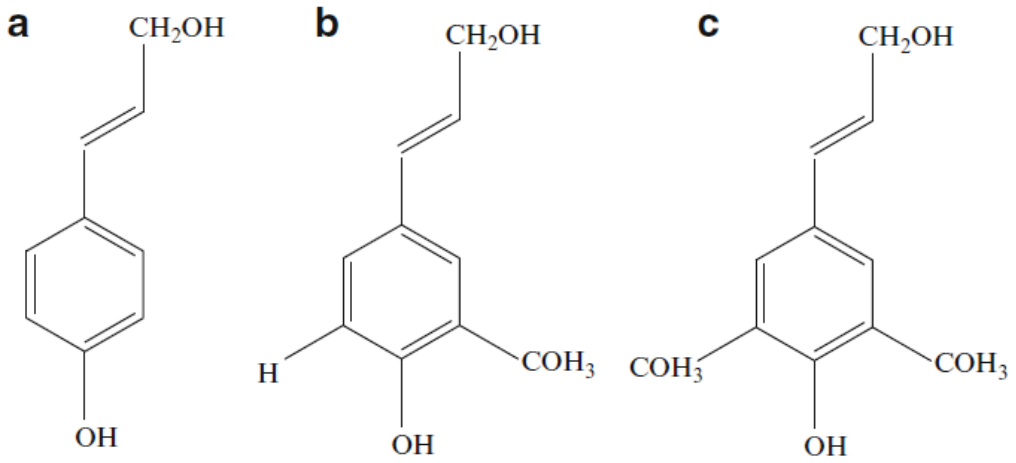


Figure 1.5. Structure of lignin monomers **(a)** *trans*-p-coumaryl alcohol, **(b)** coniferyl alcohol, and **(c)** sinapyl alcohol (Source: Lee 2013)

Lignin has a complex structure and its molecular weight is high, therefore; its degradation with enzymes is very difficult. The chemical structure of lignin polymer is shown in Figure 1.6. Lignin has higher energy content than cellulose and hemicellulose, therefore; heating value of biomass increases with lignin content. Phenolic compounds with ethyl and methyl groups are the main compounds that are produced during hydrothermal degradation of lignin (Lee 2013, Tekin et al. 2014).

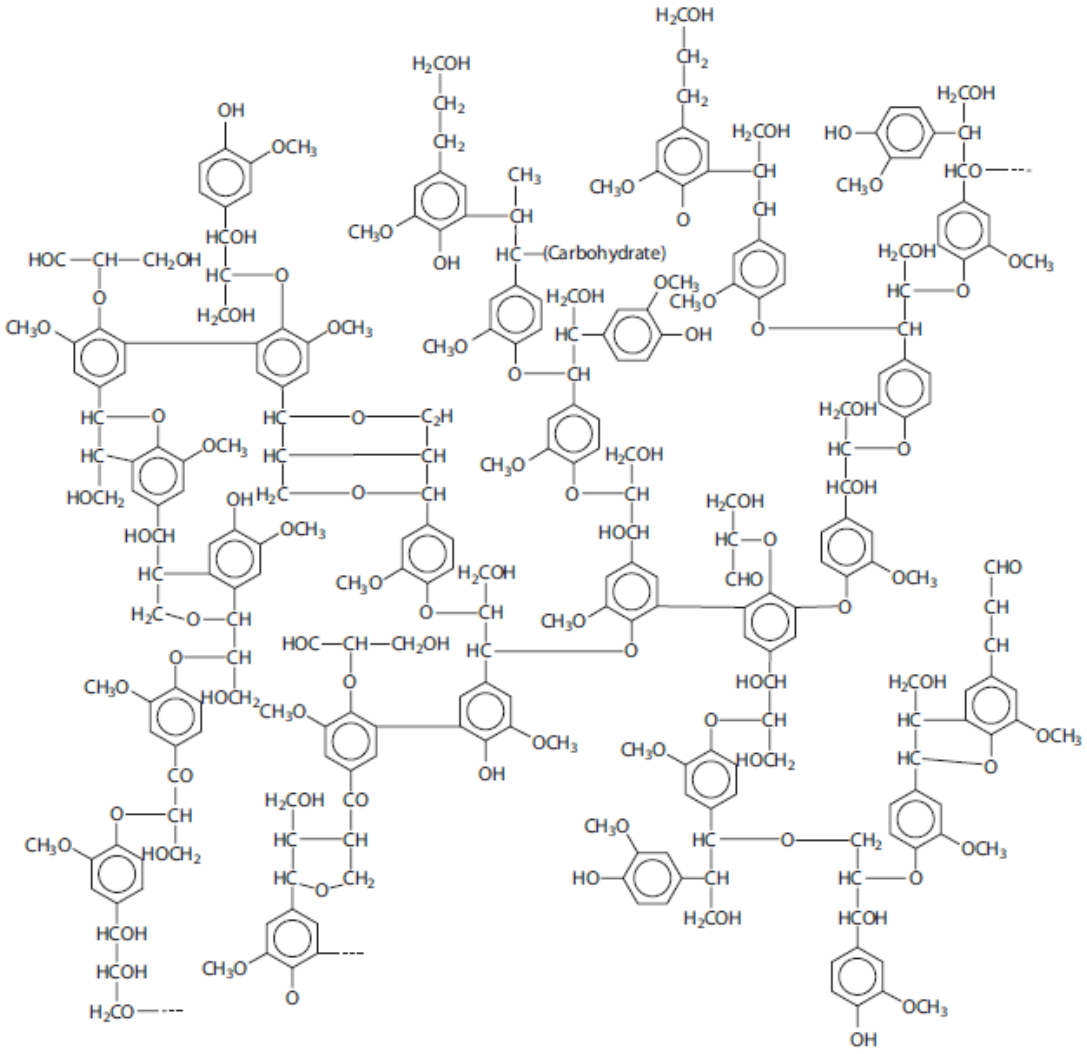


Figure 1.6. Molecular structure of lignin
(Source: Sengupta and Pike 2013)

*Extractives* compose of heterogeneous substances that are soluble in water or organic solvents. Although the composition of extractives varies according to biomass type, proteins, fats, fatty acids, sugars, phenols, terpenes, resin acids and resin are primarily components of extractives. They are responsible for the color, odor, taste and durability of the biomass (Lee 2013, Tekin et al. 2014).

## 1.3. Subcritical Water

***Subcritical water***, also known as hot compressed water and pressurized hot water (Moller et al. 2011), is defined as water exists in liquid state between the boiling point (100 °C) and critical point (374 °C and 22.1 MPa) under enough pressure (Tekin et al. 2014). The phase diagram of water along with temperature and pressure is given in Figure 1.7. Moreover, various substances have been used in different applications and whole substances have a unique critical point, as shown in Table 1.2. Increasing reaction temperature influences both reaction rates and reaction mechanisms, therefore; ionic reactions become dominant at low temperatures whereas radical reactions elevates due to homolytic bond breakage (Moller et al. 2011).

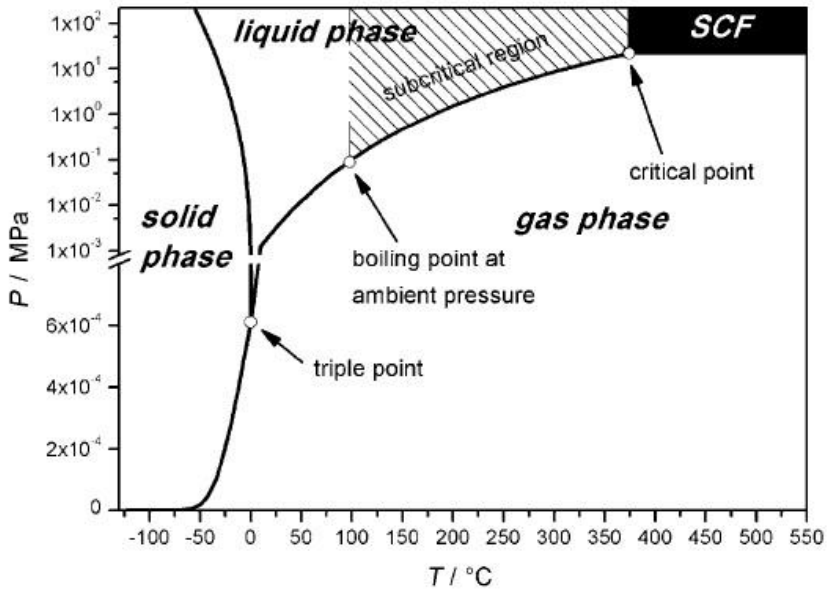


Figure 1.7. Phase diagram of water in different temperature and pressure (Source: Moller et al. 2011)

Table 1.2. The critical points of various substances
(Arai et al. 2002)

| Substances | Critical Temperature (K) | Critical Pressure (atm) | Toxicity and Flammability |
|---|---|---|---|
| Argon | 151 | 49 | --- |
| Methane | 191 | 45 | Highly flammable |
| Carbon dioxide | 304 | 73 | --- |
| Ethane | 305 | 48 | Highly flammable |
| Propane | 370 | 42 | Extremely flammable |
| Ammonia | 406 | 111 | Toxic |
| Water | 647 | 218 | --- |

Near critical point, solvation properties and physicochemical properties of water including dielectric constant, ion product, density, viscosity and diffusivity vary with temperature and pressure (Tekin et al. 2014). With increasing temperature, the polarity of water changes and becomes non-polar which enables the solubilization of organic compounds. Additionally, the hydrogen bonds are weakening, become less stable and found in separate clusters because of water thermal movement (Lee 2013, Kruse and Dahmen 2015). The ion product ($K_w$) of water increases with temperature and reaches to $10^{-11}$ that is approximately three orders of magnitude higher than the ion product of ambient water and the dielectric constant ($\varepsilon$) of ambient water is reduced from 80 to 10 at around 374 °C (Moller et al. 2011, Akiya and Savage 2002) since water self-dissociation is endothermic process (Kruse and Dinjus 2007). Thus, high concentration of $H_3O^+$ and $OH^-$ ions enables to water acts as an acid or base catalyst in subcritical water region (Kruse and Dinjus 2007, Akiya and Savage 2002). Furthermore, the viscosity of water decreases with increasing temperature and it reaches the viscosity of water vapor near the critical point, therefore; the rate of mass-transfer-limited chemical reactions enhance because of the high diffusion coefficient which accelerates the reaction rates (Moller et al. 2011, Kruse and Dinjus 2007). The change of dielectric constant, ionic product and viscosity of water with temperature is shown in Figure 1.8.

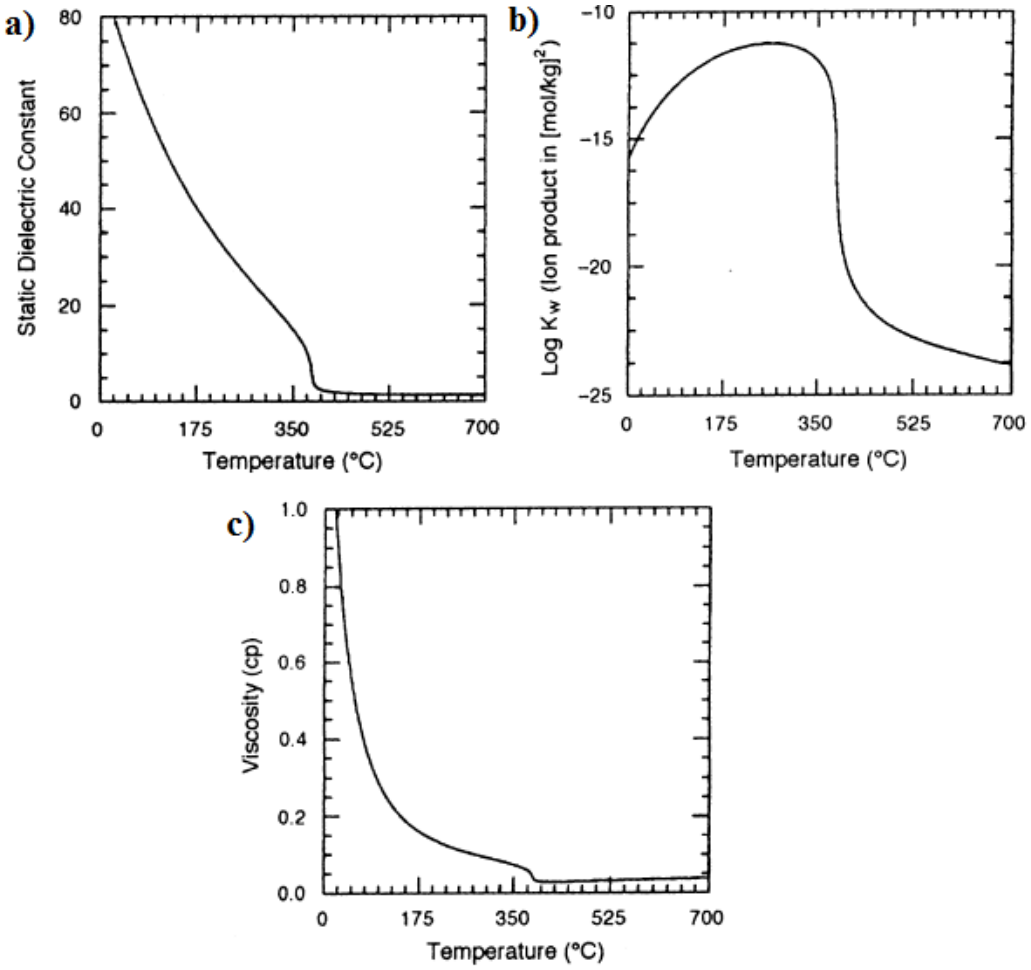


Figure 1.8. The change of **a)** dielectric constant, **b)** ionic product and **c)** viscosity of water at various temperatures (Source: Akiya and Savage 2002)

## 1.4. Reaction Mechanisms of Biomass

During hydrothermal liquefaction of biomass, the complex structure of biomass (mixture of cellulose, hemicelluloses and lignin) leads to occurrence of several complex reaction mechanisms. Besides, the basic degradation mechanisms can be identified by (Tekin et al. 2014):

- depolymerization of the biomass
- degradation of monomers by cleavage, dehydration, decarboxylation and deamination
- recombination of fragments

A possible reaction mechanism of cellulose in hydrothermal treatment is given in Figure 1.9. Firstly, cellulose dissociates to water-soluble, water insoluble and glucose by scission of the glycosidic bonds. There are two types of scission pathways: thermal cleavage through dehydration at reducing-end units (occurs at intermediate temperature and low pressure) and hydrolysis of glycosidic bonds to obtain glucose (take place in the near and supercritical region) (Fang and Xu 2014). Formed soluble oligomers (n = 0-6) decompose into oligomers (n = 0-4) with decomposed endgroup like cellobiose and erythrose by fragmentation and dehydration. In a further degradation steps, glucose isomerizes to fructose. Moreover, both glucose and fructose decompose to a wide variety of organic acids (acetic acid, formic acid, etc.) and hydroxymethylfurfural (5-HMF) by hydration, dehydration and Retro-Aldol reaction. 5-HMF degradates into an equimolar levulinic acid and formic acid and also polyfuranic intermediates may form from 5-HMF polymerization and/or polycondensation. Furthermore, hydrochar which is an insoluble carbonous compound can be produced from both degradation of polyfuranic intermediates and cellulose simultaneously (Moller et al. 2013).

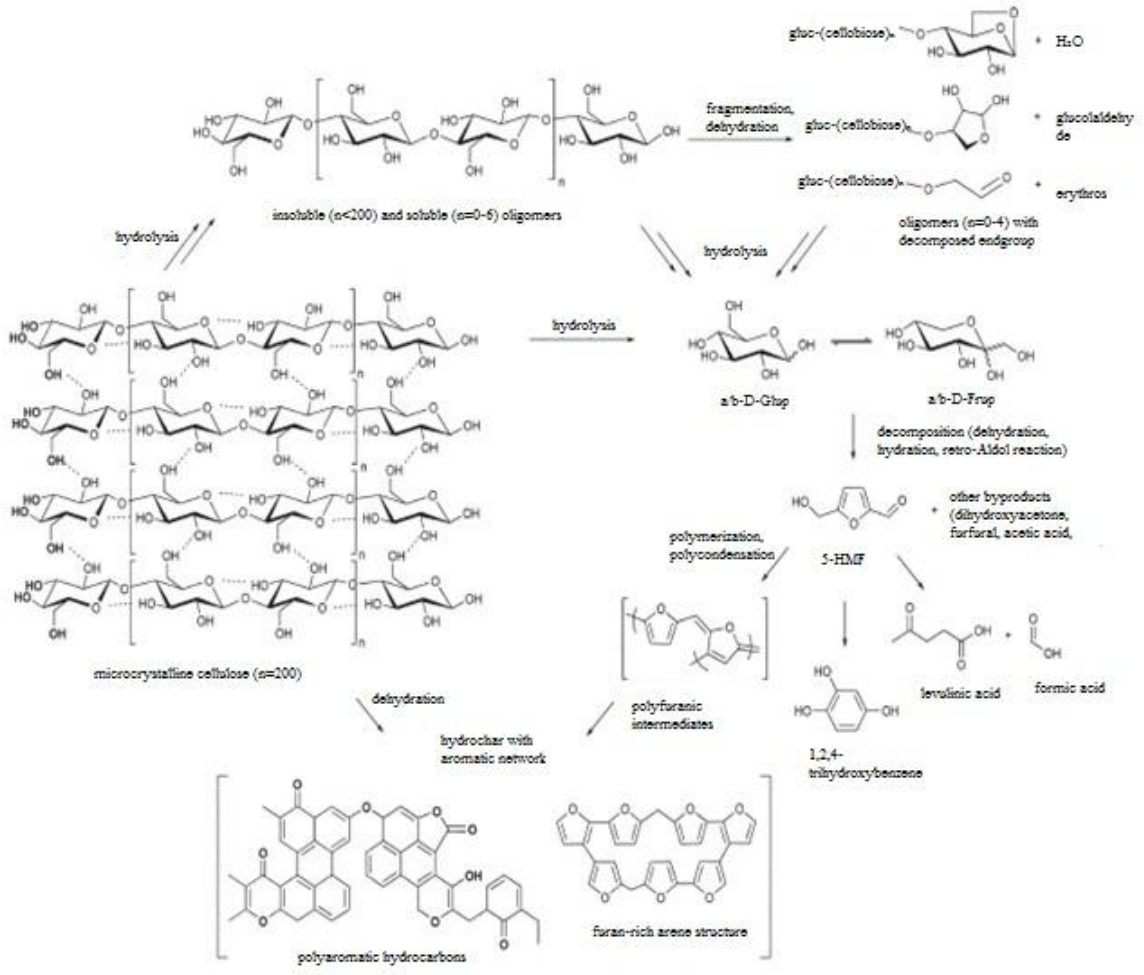


Figure 1.9. Reaction mechanisms of cellulose under hydrothermal conditions (Source: Moller et al. 2013)

Xylan is the main hemicellulose component and it is generally preferred as a representative model compound for summarizing the proposed reaction mechanisms of hemicellulose (Figure 1.10). In a brief, hemicellulose hydrolyzes into low and high molecular weight of oligomers and xylose, and then xylose is formed from the hydrolysis of oligomers. Furthermore, xylose decomposes into furfural by cylcodehydration, which is the main degradation pathway under subcritical water conditions (160-250 °C). Also, acetic acid, glucolaldehyde and glyceraldehyde are the other decomposition products that are produced by Retro-Aldol reaction. In further mechanisms, formic acid is produced from furfural degradation and pyruvaldehyde and lactic acid are formed from the degradation of glyceraldehydes. Moreover, the activation energy of the xylose hydrolysis (in the range of 119-130 KJ/mol) is not affected from improving of the aqueous media acidity, however; the reaction pathway of furfural formation changes towards the formation of acids in the alkaline solution

owing to reducing activation energy to 63 KJ/mol (Moller et al. 2013, Fang and Xu 2014).

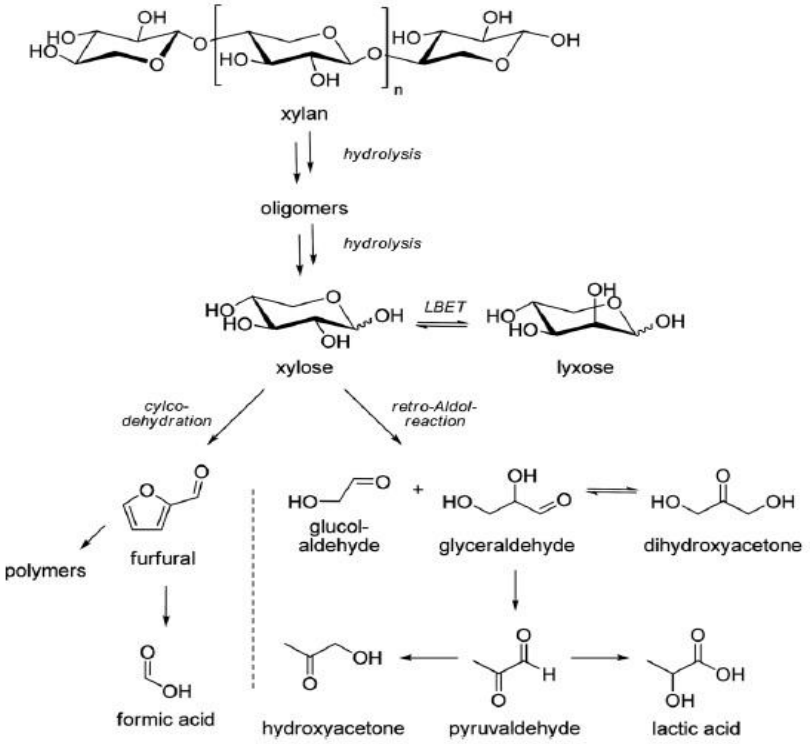


Figure 1.10. Reaction mechanisms of hemicellulose under hydrothermal conditions (Source: Moller et al. 2013)

A proposed reaction pathway of lignin under hydrothermal conditions is given in the Figure 1.11. Lignin degrades to various numbers of phenolic content under decomposition of hot compressed water via hydrolysis and cleavage of the ether and C-C bonds. In addition, formed compounds degrade by hydrolysis or demethoxylation, alkylation into alkylated aromatics and condensation into aromatic oligomers (Christensen 2014).

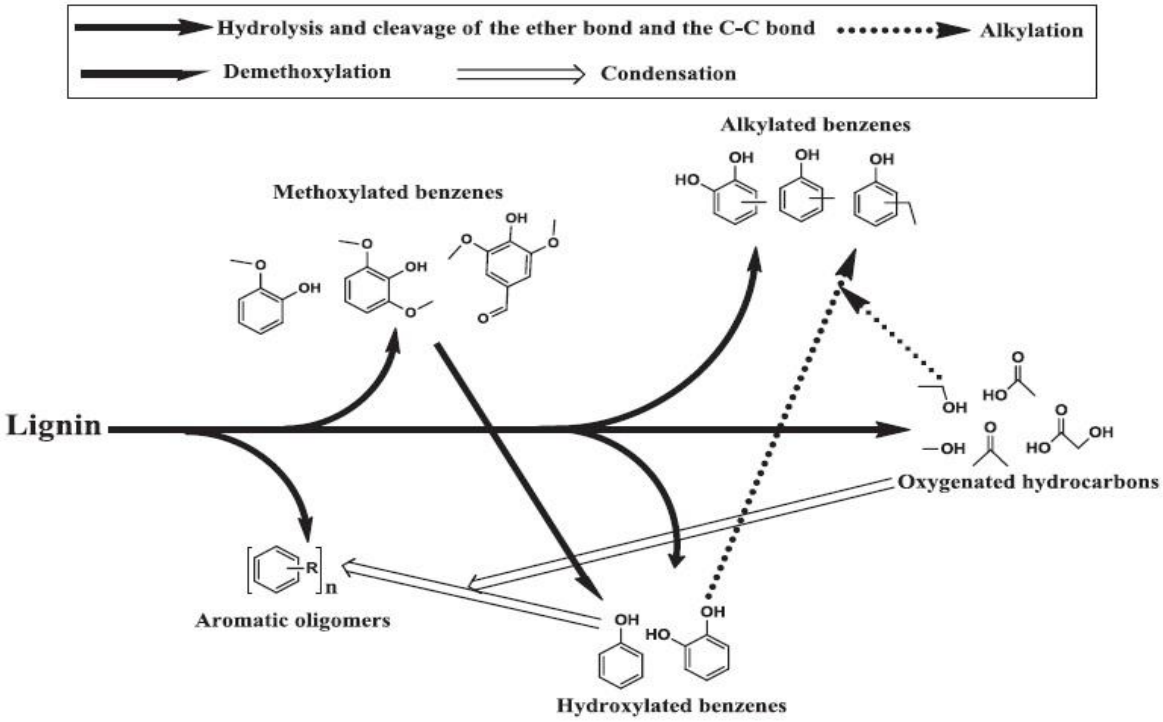


Figure 1.11. Reaction mechanisms of lignin under hydrothermal conditions (Source: Christensen 2014)

## 1.5. Biomass Conversion Technologies

A various different conversion processes are used to convert biomass into value-added chemicals, fuels and power/heat. The choice of conversion technologies can be affected by a several factors such as:

- biomass type quantity
- environmental concerns
- end-use requirements
- economic conditions

Biomass conversion technologies are generally categorized into two groups: thermochemical and biochemical conversion. Thermochemical conversion processes depend on the thermal breakdown of biomass and biochemical conversion processes subject to enzymatic breakdown of biomass (McKendry 2002b, Tekin et al. 2014). Biomass conversion technologies are shown in Figure 1.12.

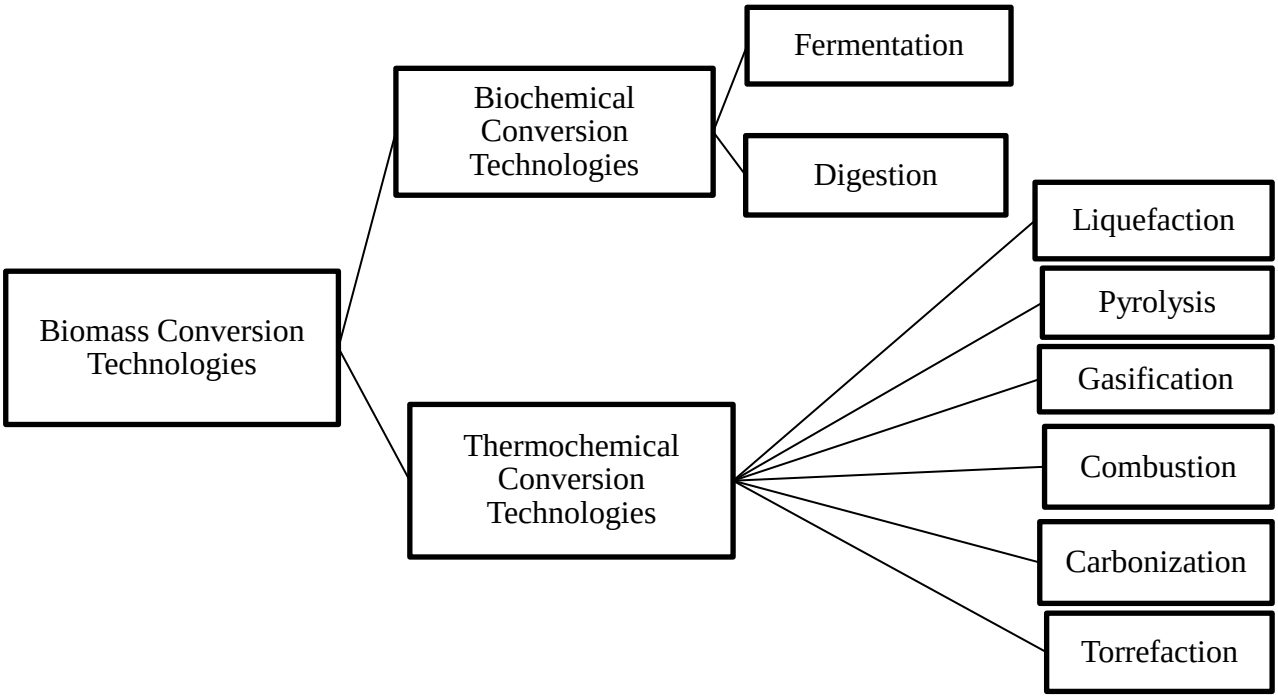


Figure 1.12. Scheme of biomass conversion technologies

### 1.5.1. Thermochemical Conversion Technologies

The thermochemical conversion processes are one of the oldest processes, which have been used from mankind. In thermochemical conversion technologies, biomass degrades into valuable chemicals and fuels with heat. Thermochemical conversion technologies consist of combustion, pyrolysis, gasification, liquefaction, carbonization and torrefaction (McKendry 2002b).

***Combustion*** is the oldest and most preferred process where biomass is burned in the presence of air. Stored energy in the chemical bonds of biomass converted into heat, mechanical power and electricity. Temperatures of produced hot gases are approximately 800-1000 °C and burning a biomass with moisture content less than 50% is more preferable (McKendry 2002b). The combustion reactions are very complicated and they can be classified as devolatilization and char combustion that are shown in Figure 1.13. With drying of biomass in the heating process, the mixture of liquid and volatile fuel gases including volatile hydrocarbon, carbon monoxide and hydrogen are formed in the devolatilization stage. In the combustion process, these produced fuel gases are further oxidized to obtain more heat energy in the presence of oxygen. The produced energy is converted into electricity by boilers, burners, turbines or internal

combustion engine generators. A variety of biomass such as sawdust, barks, forestry waste, and animal droppings can be used for combustion. Furthermore, combustion can be considered as pollutant process due to the generation of nitrogen oxides, sulfur dioxide and carbon dioxide, however; biomass combustion is a carbon neutral process (Clark and Deswarte 2015).

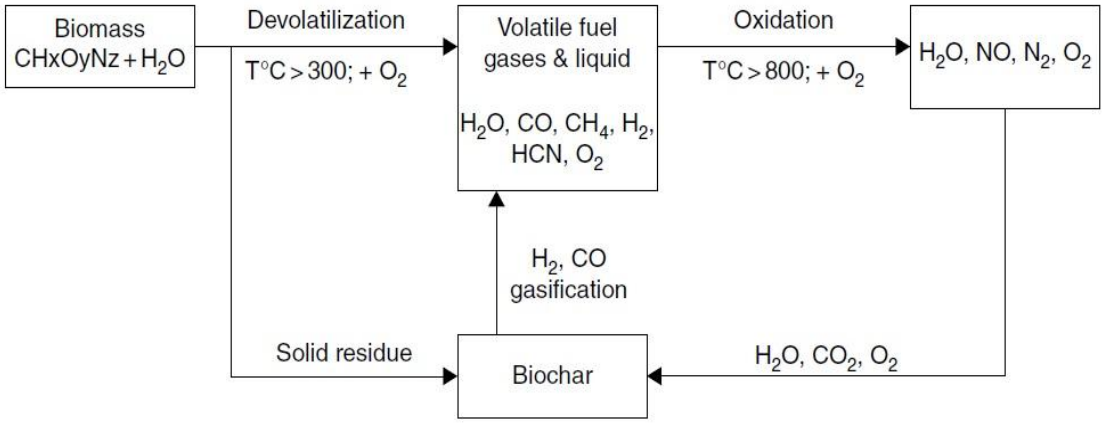


Figure 1.13. Flowchart of biomass combustion
(Source: Clark and Deswarte 2015)

***Pyrolysis*** is the one of the thermochemical process that low molecular weight liquid (bio-oil), solid (char) and gaseous product are produced from the decomposition of organic biomass within the 300-600 °C temperature range. The pyrolysis is performed in the absence of air or oxygen owing to hinder the combustion to form carbon dioxide. The liquid product (bio-oil) consists of water and water-soluble compounds such as organic acids, furfurals, phenols mixture. Major gaseous products are $CO_2$, CO, $CH_4$ and $H_2$. Besides, the solid product is called as bio-char or charcoal and composes of 85% carbon, which is valorized as soil remediation. The by-products of agricultural and forestry residues like rice shells, corn stovers or plant stalks are generally preferred in pyrolysis. Moreover, bio-oil can be used as chemicals, heat and electricity generation and fuel. However, usage of bio-oil in engine as a fuel has limitation because of its incomplete volatility, low heating value, high viscosity, low poor purity and chemical instability (Clark and Deswarte 2015). Usage fields of bio-oil of pyrolysis are shown in Figure 1.14. Ultimate product is greatly depends on operating conditions (e.g. temperature, residence time, heating rate and quenching rate). Hence, pyrolysis can be divided into slow and fast pyrolysis. For slow pyrolysis, highly charcoal is produced by low temperature, high residence time and slow heating rate whereas more bio-oil is

produced by fast pyrolysis with higher temperature (500 °C), short residence time (less than 2 s) and high heating rate (Christensen 2014).

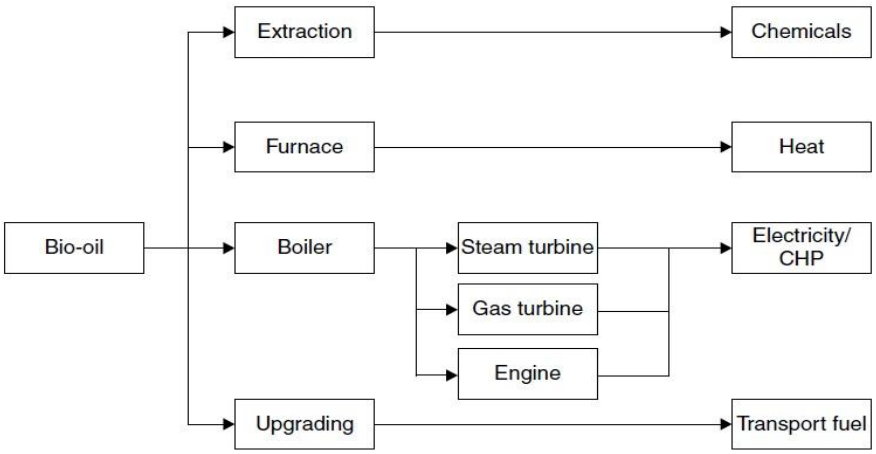


Figure 1.14. Usage fields of pyrolytic bio-oil
(Source: Clark and Deswarte 2015)

A wet biomass is converted into liquid compounds that have high energy content in the ***hydrothermal liquefaction***. Hydrothermal liquefaction is carried out at relatively low temperature (200-400 °C) and high pressure (70-300 bar) than pyrolysis in an aqueous media. A heating value of the liquid product and oxygen content are range from 30 to 38 MJ $kg^{-1}$ and 5 to 15%, respectively. The biomass feedstocks of hydrothermal liquefaction have high moisture content (70-95%). Wood and waste biomass (e.g. municipal waste), industrial by-products, manure or algae are major biomass types. When compared to pyrolysis, bio-oil from hydrothermal liquefaction have much lower oxygen and water content whereas have higher carbon and hydrogen content. Therefore, the heating value of hydrothermal liquefaction bio-oil is much higher than that of pyrolysis bio-oil. Furthermore, bio-oil produced by hydrothermal liquefaction is more viscous and it resembles to conventional crude oil (Christensen 2014).

***Gasification*** is a thermal treatment that biomass is converted into syngas by partial oxidation of biomass in the presence of an oxidizing agent. Gasification is conducted at higher temperatures that range from 700 to 1000 °C with the higher gas yields formation (85%). Complex chemical reactions take place during hydrothermal gasification. Initially, biomass decomposes into low molecular weight products by hydrolysis. Thermal decomposition reaction and devolatilization to form solid carbonized biomass occur above 350 °C and the solid carbonized biomass is oxidized by oxidizing agent such as air, steam, $CO_2$ and $O_2$ at 700-1000 °C. Also, reduction

reactions including water-gas reaction, bounded reaction, shift reaction and methane reaction occur at higher temperature (800-1000 °C) after the consumption of oxidizing agent. Chemical reactions of biomass gasification are summarized in Table 1.3. In consequence of these chemical reactions, a mixture of CO, $CO_2$, $CH_4$ and $H_2$ are produced by breakdown of the bonds in biomass. Besides, some impurities such as tars, char, alkali, sulfur compounds and nitrogen compounds are produced, therefore; carrying out downstream processing like wet scrubbing, hot gas cleaning and barrier filtering is required to remove the impurities. Agricultural and organic municipal wastes, food waste and forestry residues are commonly used for gasification (Clark and Deswarte 2015).

Table 1.3. Reactions of biomass gasification
(Source: Clark and Deswarte 2015)

| | | |
|---|---|---|
| Oxidation | Partial oxidation reaction | $2C + O_2 \rightarrow 2CO$ |
| | Complete oxidation reaction | $C + O_2 \rightarrow CO_2$ |
| Reduction | Water-gas reaction | $C + H_2O \rightarrow CO + H_2$ |
| | Bounded reaction | $C + CO_2 \leftrightarrow 2CO$ |
| | Shift reaction | $CO_2 + H_2 \leftrightarrow CO + H_2O$ |
| | Methane reaction | $C + 2H_2 \leftrightarrow CH_4$ |
| Overall | $CH_xO_y$ (biomass) + $O_2$ (21% of air) + $H_2O$ (steam) → $CH_4 + CO + CO_2 + H_2 + H_2O$ (unreacted steam) + C (char) + tar | |

***Carbonization*** is an environmentally friendly and inexpensive process to produce charcoal from solid biomass in the absence of air or oxygen. Hydrothermal carbonization takes place under mild temperatures (≤ 200 °C) and pressures. Biomass is carbonized quickly into solid carbon by heating. The hydrothermal carbonization includes some advantages than conventional carbonization (Tekin et al. 2014, Pandey et al. 2011);

- require low reaction temperature
- obtain higher product yield in a short time
- use of inexpensive and renewable materials
- aqueous phase synthesis

***Torrefaction*** is the thermal conversion of biomass to charred residue which is also called as char under 240-320 °C process temperature and nonoxidizing conditions. With torrefaction, oxygen content reduces while the energy content increases from 10-17 MJ

$kg^{-1}$ to 19-22 MJ $kg^{-1}$. The other products are water, acetic acid, methanol, carbon monoxide and carbon dioxide which have more oxygen content than biomass. Reaction temperature of torrefaction influences the components of biomass differently. Hemicellulose decomposes at nearly 290 °C and the decomposition of cellulose occurs at relatively higher temperature (360 °C) whereas phenolic compounds like lignin degrades in a wide temperature range (between 250-400 °C) (Clark and Deswarte 2015).

## 1.5.2. Biochemical Conversion Technologies

Fermentation and anaerobic digestion are the two major biochemical conversion technologies, which are conducted by bacterial enzymes and microorganisms. ***Fermentation*** is used to convert sugar crops into variety of products including biofuels, biochemicals or biomaterials by using bacteria and fungi. Commercially, fermentation is used to produce bioethanol from sugar crops (e.g. sugar cane, sugar beet) and starch crops (e.g. maize, wheat). Besides that agricultural by-products of cereals and industrial waste were started to use in biochemical conversion in order to reduce the production cost. The steps of biomass conversion in fermentation are shown in Figure 1.15. Before fermentation, a pretreatment step such as acid or alkaline hydrolysis is required since lignin and hemicellulose can be removed from media and is hydrolyzed into sugars in pretreatment step. By this way, the yield of fermentation product increases and the production cost is reduced (Clark and Deswarte 2015, McKendry 2002b).

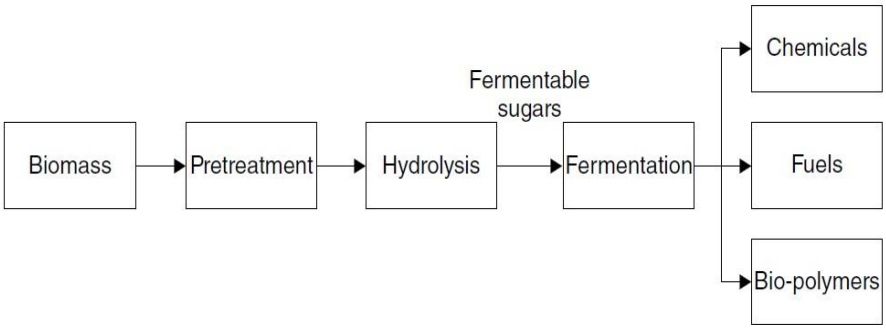


Figure 1.15. The steps of biomass fermentation
(Source: Clark and Deswarte 2015)

In ***anaerobic digestion***, biomass (80-90% moisture content) is decomposed into a gas mixture which composes of mainly methane and carbon dioxide and a trace amount of

hydrogen sulfide in the absence of air (McKendry 2002b). A bacteria mixture like syntrophic bacteria, fermentative bacteria, acetogenic bacteria and methanogenic bacteria is used in the anaerobic digestion process. Anaerobic digestion can be categorized into four stages that are hydrolysis, acidogenesis, acetogenesis and methanogenesis, which are summarized in Figure 1.16. The first stage is hydrolysis in which insoluble organic compounds are converted into soluble compounds by hydrolases. Subsequently, soluble compounds are transformed into short-chain organic acids, alcohols, aldehydes and carbon dioxide in the acidogenesis step and then, acetates, carbon dioxide and hydrogen are produced in the acetogenesis step. In the last stage which is methanogenesis, methane is produced from the products of third stage by methanogenic bacteria. Furthermore, the composition of biogas highly depends on the substrate composition. For instance, the highest methane yield (1014 $m^3$ $ton^{-1}$) can be obtained from lipids whereas the lower methane yield (415-496 $m^3$ $ton^{-1}$) is achieved from the transformation of carbohydrates and proteins (Clark and Deswarte 2015).

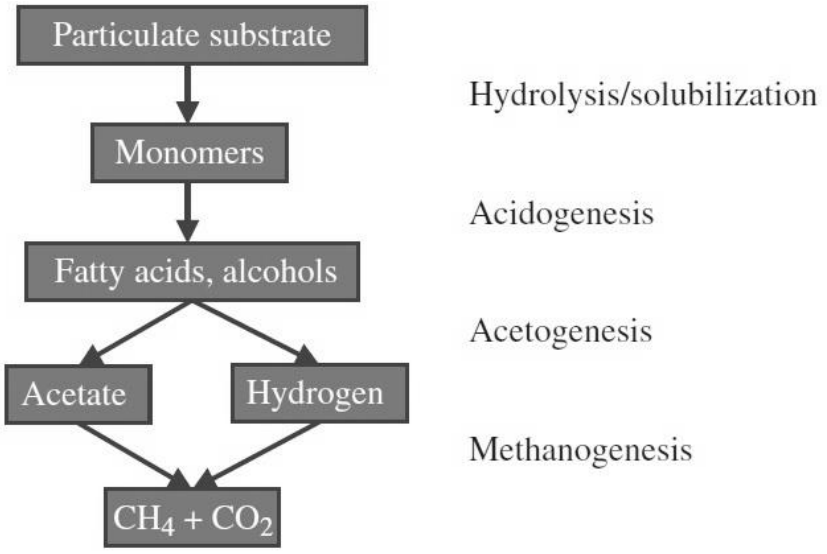


Figure 1.16. Scheme of the anaerobic digestion stages
(Source: Jong and Ommen 2015)

## 1.6. Levulinic Acid

The Dutch professor G. J. Mulder performed the initial levulinic acid synthesis in the 1840's from fructose with hydrochloric acid at high temperature. The US Department of Energy has been defined the levulinic acid into 12 top value-added bio-based chemicals (Sengupta and Pike 2013). Levulinic acid ($C_5H_8O_3$) which is also

known as 4-oxopentanoic acid, β-acetylpropionic acid and γ-ketovaleric acid, is a colorless crystalline molecule and soluble in water and several organic solvents including acetone, ethanol and diethyl ether. Levulinic acid has a ketone (-C=O) and carboxylic group (-COOH) that give behavior of functionality and reactivity. It is an also ideal intermediate compound for the production of ultimate products due to the reactivity of levulinic acid (Rackemann and Doherty 2011, Timokhin et al. 1999). Some physicochemical properties of levulinic acid are presented in Table 1.4.

Table 1.4. Physicochemical properties of levulinic acid
(Source: Timokhin et al. 1999)

| **Physicochemical Properties** | **Values** |
|---|---|
| Melting point | 37 °C |
| Boiling point | 246 °C |
| Surface tension (at 25 °C) | 39.7 $dyne.cm^{-1}$ |
| Heat of vaporization (at 150 °C) | 0.58 $kJ.mol^{-1}$ |
| Heat of fusion | 79.8 $J.mol^{-1}$ |
| Dissociation constant (at 25 °C) | 4.59 |

Levulinic acid can be produced from the acid-catalyzed hydrolyses of hexose sugars. As shown in Figure 1.17, hexose sugars first degraded to glucose and fructose and then 5-HMF that is an intermediate product is formed by dehydration. Ultimately, 5-HMF is converted into levulinic acid and formic acid with the addition of water to the $C_2$-$C_3$ bond (Girisuta 2007).

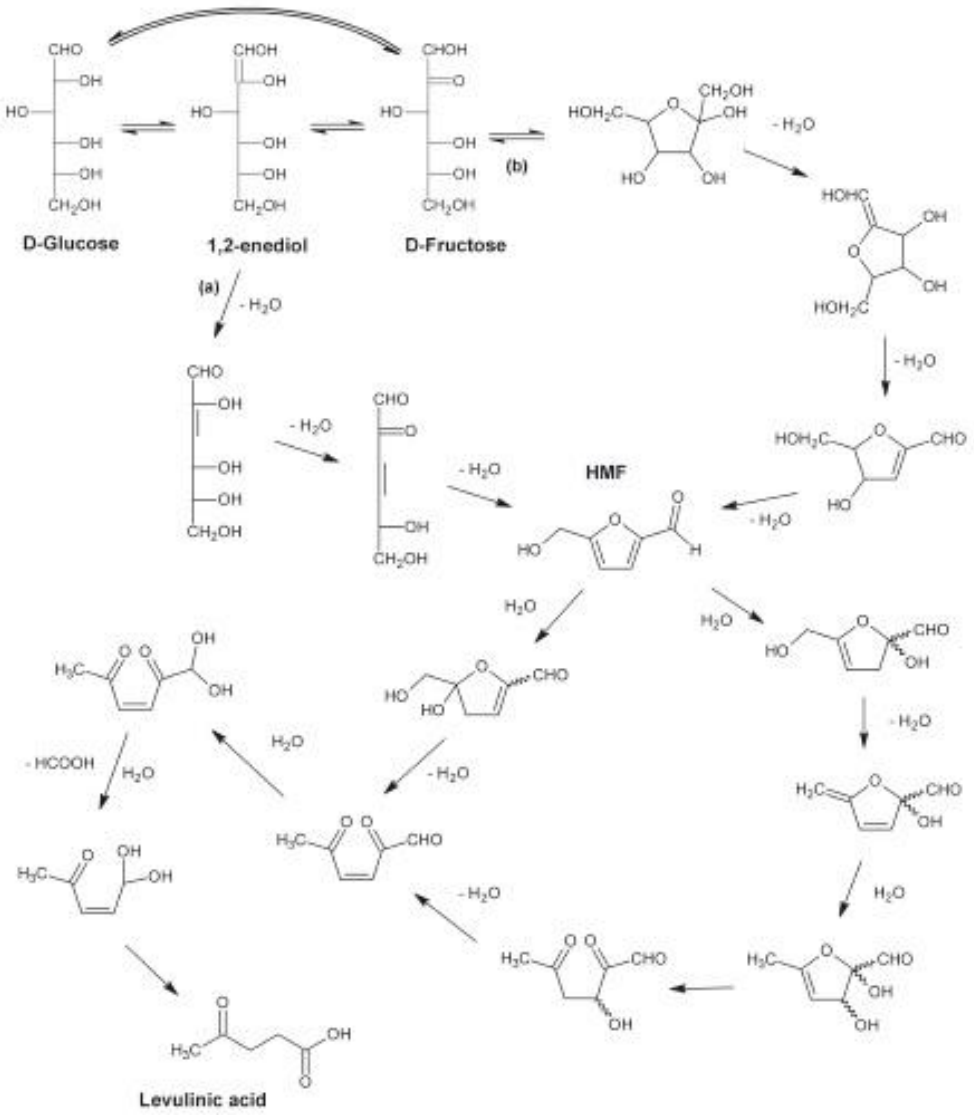


Figure 1.17. Reaction mechanism of the conversion of hexose sugars to levulinic acid (Source: Rackemann and Doherty 2011)

Levulinic acid is a favorable chemical that can be used to produce various chemical derivatives, as shown in Figure 1.18, such as polymer resins, herbicides, pharmaceutical agents, anti-freeze agents, flavoring and fragrance agents, solvents, plasticisers and biofuels additives (Rackemann and Doherty 2011).

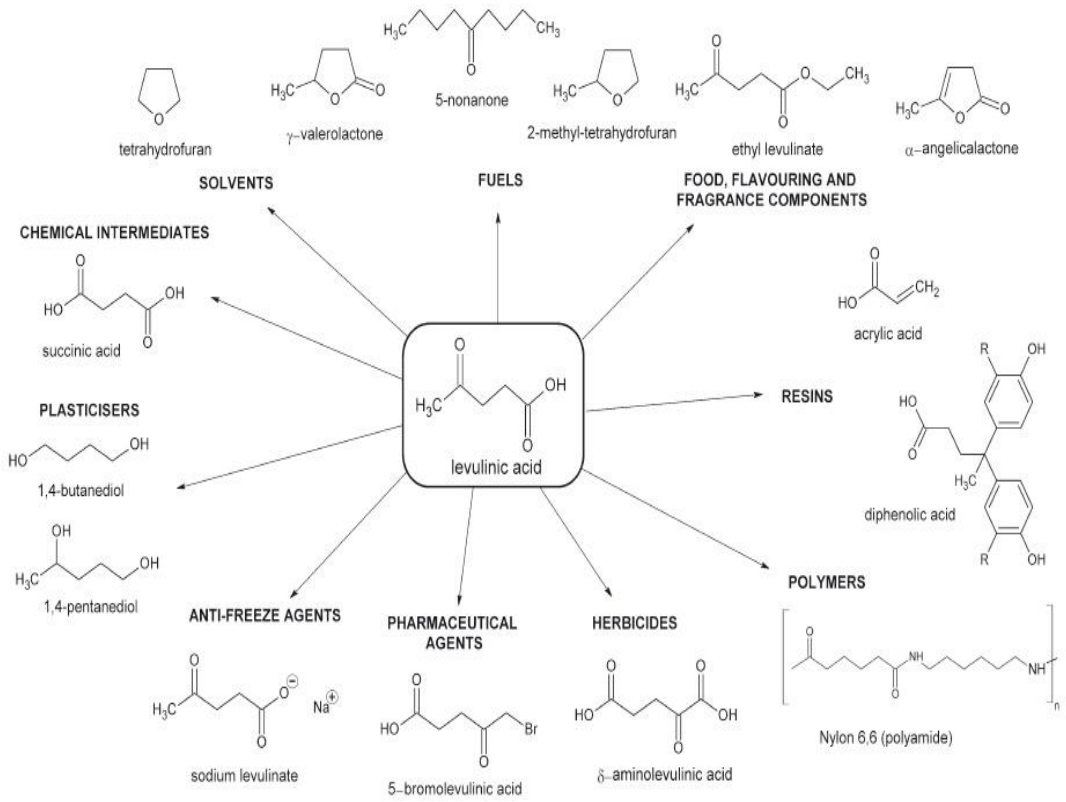


Figure 1.18. End-products from levulinic acid
(Source: Rackemann and Doherty 2011)

Derivative of GVL such as γ-valerolactone (GVL) and methyltetrahydrofuran (MTHF) are produced by catalytic hydrogenation from levulinic acid (Figure 1.19). Platinum oxide, rhenium catalysts, copper-chromite, Raney nickel are most preferred catalyst. Cleaner-burning fuels can be created with blending of petroleum products, γ-valerolactone and methyltetrahydrofuran (Girisuta 2007, Rackemann and Doherty 2011, Timokhin et al. 1999).

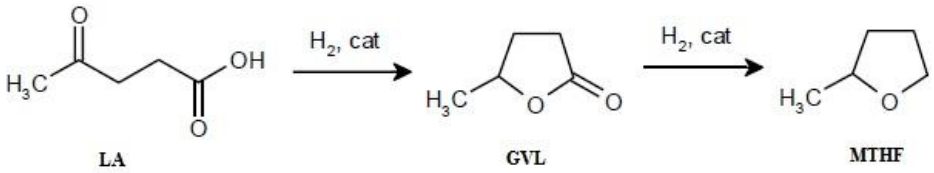


Figure 1.19. Catalytic hydrogenation of LA to MTHF
(Source: Girisuta 2007)

Levulinic acid is oxidized in the presence of $V_2O_5$ catalyst to form succinic acid at high temperatures (365-390 °C). Succinic acid is an important chemical intermediate for many bio-chemicals including γ-butyrolactone (GBL), 1,4-butanediol (BDO) and

tetrahydrofuran (THF). As shown in Figure 1.20, GBL can be formed by hydrogenation of succinic acid which is an intermediate product of agrochemicals and pharmaceuticals. Polyesters, polyurethanes and polyethers are used in a wide range of plastics, fibers, films and adhesives and are produced by 1,4-butanediol. 1,4-butanediol is also produced by the hydrogenation of γ-butyrolactone. Moreover, 1,4-butanediol is dehydrated homogenously to form tetrahydrofuran that is used as solvent for PVC (Girisuta 2007).

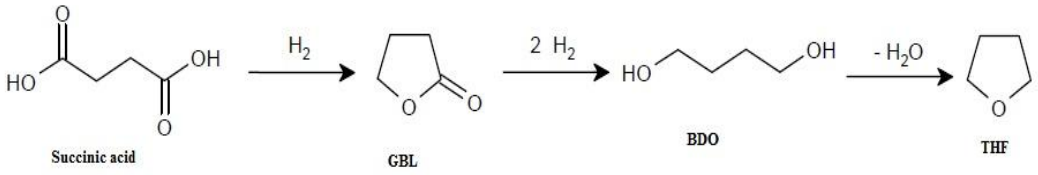


Figure 1.20. Reaction pathway of succinic acid into derivatives
(Source: Girisuta 2007)

Levulinic acid enables chlorination and bromination due to activating of neighbor carbon atoms by the carbonyl and carboxy groups. At moderate temperatures, the reaction of levulinic acid with chlorine leads to the formation of 3,5-dichlorolevulinic acid. In addition, reaction medium severely affects the bromination product of levulinic acid. In the presence of HCl, 2-bromolevulinic acid is formed, however; 3,5-dibromo-derivative is produced in acetic acid medium. The bromination of levulinic acid in the methanol medium causes the formation of 5-bromolevulinic acid which is a pharmaceutical agent for cancer treatment and a precursor for δ-aminolevulinic acid (Girisuta 2007, Timokhin et al. 1999).

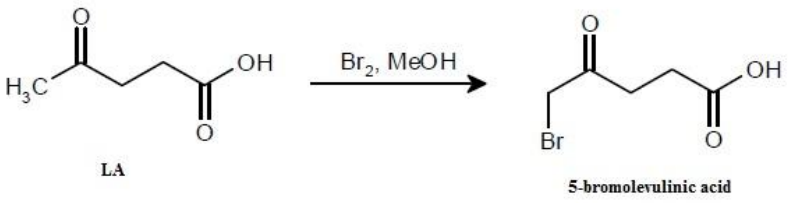


Figure 1.21. Bromination of levulinic acid in methanol
(Source: Girisuta 2007)

## 1.7. Furfural

Furfural ($C_5H_4O_2$) which is also known as furan-2-aldehyde, carboxylic aldehyde, 2-furfural, 2-furancarboxaldehyde, 2-furaldehyde and 2-furyl-methanal, consists of heteroaromatic furan ring and aromatic aldehyde groups. The first time furfural was synthesized by J.W. Döbereiner in 1832 and has been produced in industrial plants since 1922 (Peleteiro et al. 2016). Furfural is a significant selective extractant because of its important physical properties (Table 1.5) so it has been used for the removal of aromatics from lubricant oil to improve viscosity and temperature relation, polymer crosslinking, fungicide and removal of aromatics from diesel to increase ignition properties (Yan et al. 2014). In addition, furfural is also used in the production of flavoring agent of food, alcoholic and non-alcoholic beverages, herbicides, pesticides, fragrances, resins, cosmetics and pharmaceuticals (Peleteiro et al. 2016). Functional groups of furfural, aldehyde (C=O) and furan ring system (C=C-C=C), determine the chemical properties. While acylation, acetalization, decarbonylation, reduction to alcohols, oxidation to carboxylic acids and aldol condensation are occurred due to the presence of aldehyde group, reactions including open-ring, hydrogenation, nitration, alkylation, halogenation and oxidation are caused by conjugated system (Yan et al. 2014).

Table 1.5. Physical properties of furfural
(Source: Yan et al. 2014)

| | |
|---|---|
| Molecular weight | 96.08 |
| Boiling point (°C) | 161.7 |
| Freezing point (°C) | - 36.5 |
| Density at 25 °C | 1.16 |
| Solubility in water (25°C) | 8.3 |
| Dielectric constant at 20 °C | 41.9 |
| Heat of vaporization (kJ/mol) | 42.8 |
| Viscosity at 25 °C (mPa.s) | 1.49 |
| Heat of combustion at 25 °C (kJ/mol) | 234.4 |
| Enthalpy of formation (kJ/mol) | - 151 |
| Surface tension at 29.9 °C (mN/m) | 40.7 |

Furfural cannot be produced with synthetic processes and there are two possible processes for furfural production (Machado et al. 2016). A first process for the furfural production is the dehydration and acid hydrolysis of xylose and arabinose (Figure 1.22) which are the component of hemicelluloses of lignocellulosic biomass. In this process, furfural formation is highly depends on 1,2-enediol intermediate.

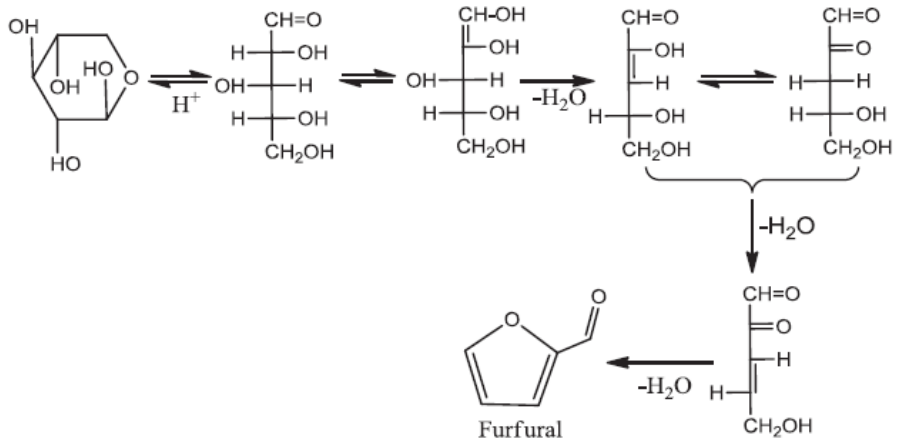


Figure 1.22. Dehydration of pentose to furfural
(Source: Machado et al. 2016)

Second one is acyclic dehydration of xylose (Figure 1.23) and this mechanism has seven steps. First step is protonation of carbon atom with hydroxyl group to form trivalent oxygen. In second step, carbon atom was positively charged by losing one molecular water. Two electrons of C-O bond forms double bond in third step and then C-O bond fission and hydrogen atom migration occur (fourth step). In fifth step, the libaration of another water molecule occur with the protanation of hydroxyl oxygen due to $H^+$. After that ring structure, which is more stable than double bond, is formed by trivalent carbon atom. In the final step, furfural is formed by 1,4-elimination of $H^+$ (Yan et al. 2014).

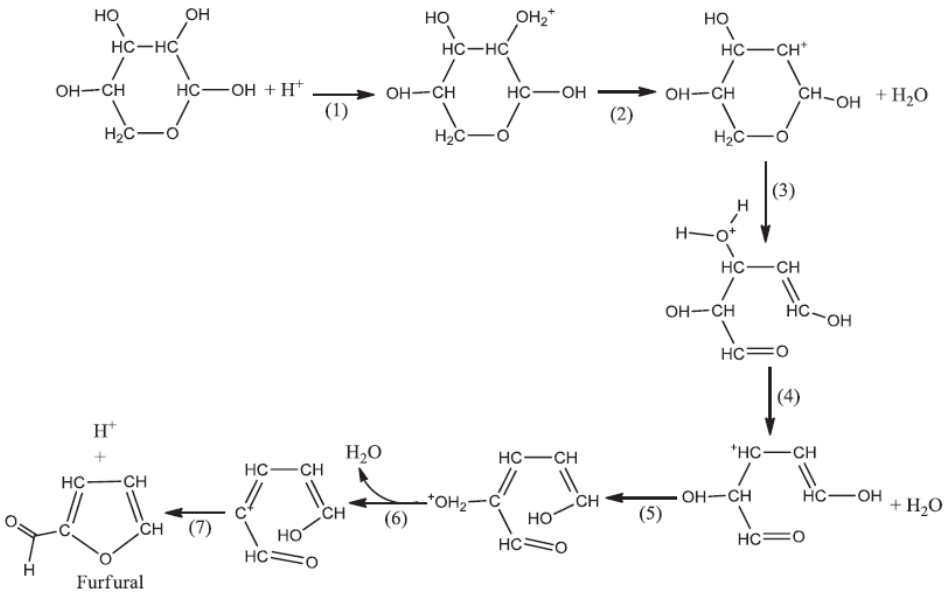


Figure 1.23. Acyclic dehydration of xylose to furfural
(Source: Yan et al. 2014)

## 1.8. Acetic acid

Acetic acid was first produced by the ethyl alcohol fermentation. Some physical properties of acetic acid are shown in Table 1.6. Nearly a half of the acetic acid (44%) is formed from vinyl acetate that is used for the production of plastics, adhesives and paints from polyvinyl acetate and polyvinyl alcohols. 12% of the production of total acetic acid is manufactured acetic anhydride to produce paper sizing agents, aspirin, cellulose acetate and bleach activator; 13% is operated to form acetates and esters to obtain solvents of perfumes, resins, flavorings, coatings, inks and gums; and 12% of that is operated to obtain terephthalic acid which is used in the production of polyethylene teraphthalate (PET) bottles and fibers (Sengupta and Pike 2013).

Table 1.6. Some physical properties of acetic acid
(Source: Agreda 1993)

| Physicochemical Properties | Values |
|---|---|
| Melting point | 16.6 °C |
| Boiling point | 118 °C |
| Heat of combustion (at 25 °C) | 874.2 kJ/mol |
| Heat of vaporization (at 150 °C) | 0.58 $kJ.mol^{-1}$ |
| Heat of fusion | 195.31 $J.mol^{-1}$ |
| Dielectric constant (at 25 °C) | 6.194 |

Oxidation of acetaldehyde, liquid phase oxidation of n-butane or naphtha and methyl alcohol carbonylation are three major commercial processes. Among these three processes, the methyl alcohol carbonylation in the presence of rhodium catalyst iodide catalyst is the most preferred industrial process due to the formation of small amount of by-product, low material cost and energy savings (Sengupta and Pike 2013). The other most used commercial acetic acid production technique is Monsanto process (Figure 1.24) where carbon monoxide and methanol are reacted with each other in the presence of rhodium complex catalyst at 180 °C and 30-40 atm (Shakhashiri).

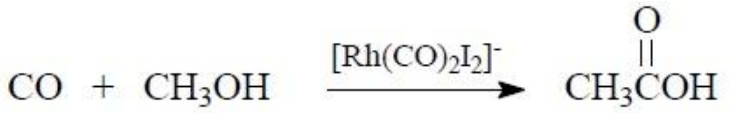


Figure 1.24. Reaction mechanism of Monsanto process
(Source: Shakhashiri)

As mentioned above, some pharmaceuticals are produced from acetic acid like aspirin (acetylsalicylic acid) that is obtained with the reaction of acetic acid and salicylic acid (Figure 1.25). Acetic anhydride can be produced by the hydrolysis of aspirin in the presence of water due to reversible esterification reaction (Shakhashiri). Moreover, acetic anhydride can be prepared by the reaction between acid chloride and sodium acetate which is a salt of acetic acid (Figure 1.26).

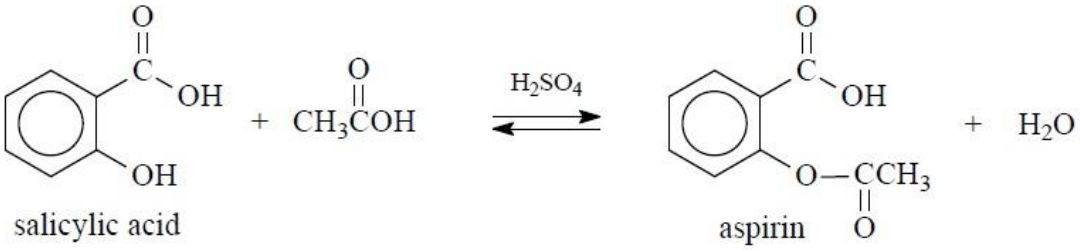


Figure 1.25. Reaction mechanism of the aspirin production
(Source: Shakhashiri)

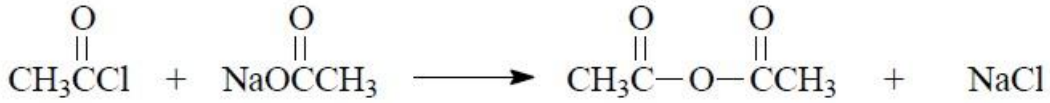


Figure 1.26. Mechanism of the acetic anhydride production
(Source: Shakhashiri)

# CHAPTER 2

# LITERATURE SURVEY

## 2.1. Hydrothermal Liquefaction of Biomass in Subcritical Water

Thermochemical processes (i.e. hydrothermal liquefaction) of wet biomass or waste biomass in sub- or supercritical water have attracted much more attention than traditional treatments for the production of biofuel and valuable chemicals due to requiring no drying process, which cause significant energy consumption. In hydrothermal liquefaction, complex structure of biomass is converted into smaller products, which are highly dependent on composition of biomass and reaction parameters such as reaction temperature, reaction time, pressure and acid addition. Therefore, this section provides experimental results and information about the effect of reaction parameters on the product distribution from literature survey.

Chan et al. (2014) reported the influence of temperature and pressure on the liquefaction of three different oil palm biomass (empty fruit bunch, palm mesocarp fiber and palm kernel shell) in subcritical and supercritical water. They stated that cellulose and hemicellulose degraded nearly at 220 °C and 340 °C, respectively; whereas the degradation of lignin took place in a wide temperature range according to differential thermo-gravimetric curve. Chemical product compositions varied with respect to biomass type because each biomass has different amount of cellulose, hemicellulose and lignin content. Accordingly, more phenolic compounds were produced from palm mesocarp fiber than that of empty fruit bunch and palm kernel shell under supercritical water conditions because of having higher amount of lignin (Figure 2.1). Also, alcohol and ester compounds were only formed from the decomposition of palm kernel shell.

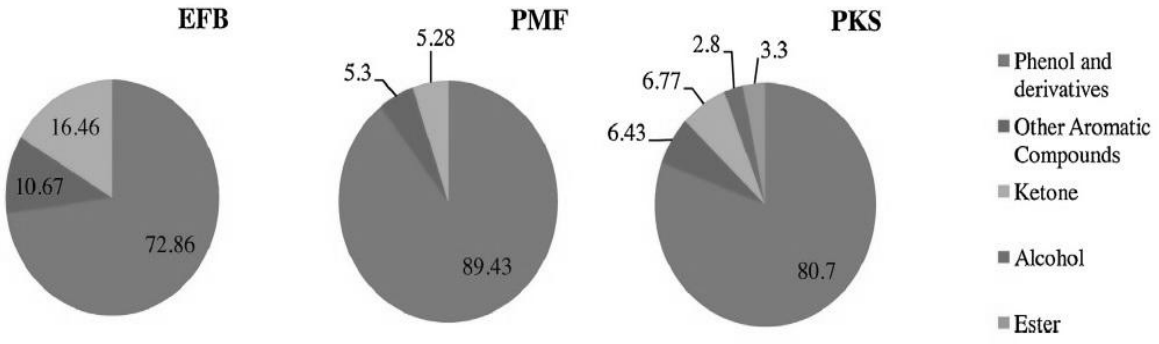


Figure 2.1. Chemical product distribution of bio-oil from EFB, PMF and PKS at 390 °C and 25 MPa (Source: Chan et al. 2014)

The identification of possible reaction pathways of biomass phytomass (cooked carrots and potatoes) degradation in sub- or supercritical water were evaluated (Kruse and Gawlik 2003). In subcritical water, the formation of levulinic acid via acid-catalyzed reaction and the production of 1,2,4-benzenetriol pathways are favor. On the contrary, the degaradation of HMF to furfural is dominant beyond the critical point, therefore; levulinic acid concentration decreased (Figure 2.2.).

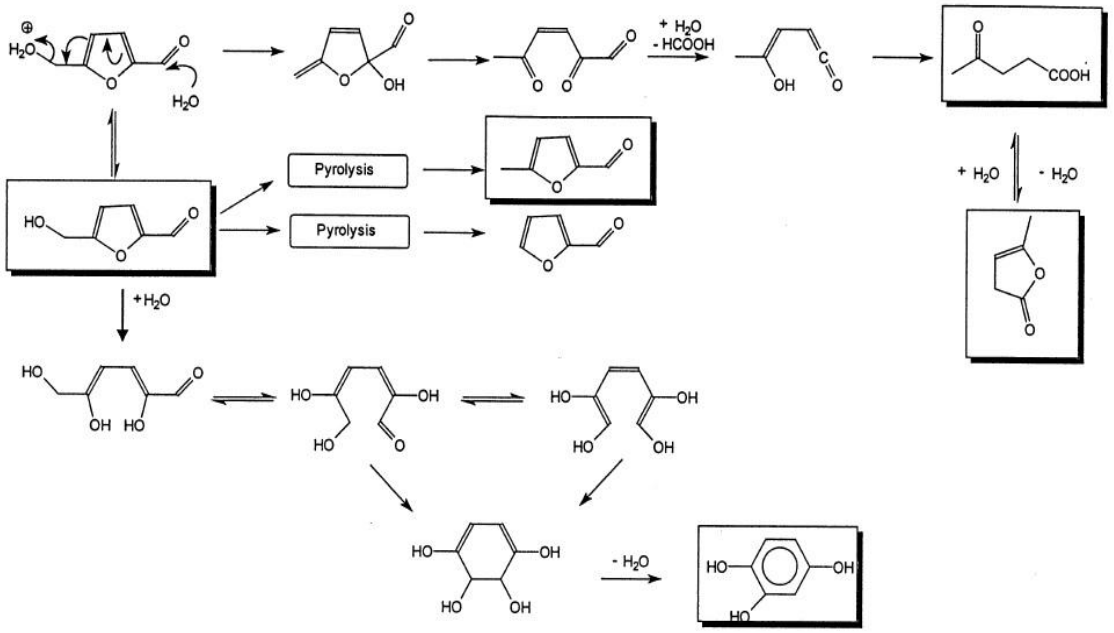


Figure 2.2. Degradation mechanism of HMF
(Source: Kruse and Gawlik 2003)

Cheng et al. (2009) investigated the conversion of switchgrass at 250-350 °C and 20 MPa with 1-300 s residence time. They concluded that the decomposition rate of switchgrass in subcritical water was extremely rapid even at lower temperature. At 350

°C, the conversion of switchgrass reached approximately to 90% in a short reaction time and the gas yield increased significantly with the further degradation of water soluble products into gas products. Also, they indicated that the decomposition rate of glucose and xylose enhanced at higher temperatures while the formation rate of 5-HMF and furfural increased. The detailed composition of main compounds is given in Table 2.1.

Table 2.1. The composition of main compounds in liquid
(Source: Cheng et al. 2009)

| **Temperature (°C)** | **Reaction time (s)** | **Glucose (wt.%)** | **Xylose (wt.%)** | **5-HMF (wt.%)** | **Furfural (wt.%)** |
|---|---|---|---|---|---|
| | 1 | 3.19 | 9.59 | 0.94 | 1.63 |
| | 30 | 2.81 | 9.22 | 1.01 | 2.88 |
| 250 | 45 | 5.42 | 13.20 | 2.42 | 11.3 |
| | 60 | 5.92 | 9.82 | 3.54 | 14.01 |
| | 300 | 3.81 | 6.44 | 6.36 | 12.69 |
| | 1 | 6.30 | 3.72 | 3.03 | 4.89 |
| | 15 | 8.17 | 5.70 | 7.29 | 6.03 |
| 300 | 30 | 5.03 | 0.65 | 6.78 | 6.72 |
| | 45 | 4.54 | 0.84 | 7.50 | 7.52 |
| | 60 | 4.60 | 0.99 | 8.42 | 7.59 |
| | 1 | 3.81 | 1.63 | 5.01 | 4.20 |
| | 15 | 4.78 | 1.02 | 6.28 | 5.57 |
| 350 | 30 | 3.60 | 1.60 | 4.43 | 4.17 |
| | 45 | 3.73 | 1.17 | 3.88 | 3.32 |
| | 60 | 6.99 | 2.15 | 4.50 | 3.75 |

Asghari and Yoshida (2010) compared the formation of useful chemicals of Japanese red pine wood in the absence and presence of dilute phosphate buffer at pH 2 in subcritical water. They found that higher the sugar yield was obtained with acid treatment and the rehydration of HMF was determined as a main levulinic acid formation pathway from Japanese red pine wood.

Apart from acid addition, several studies investigated the effect of solid catalyst or/and base concentration on the hydrothermal conversion of biomass. Catalytic degradation of

sawdust and cornstalk at 250-350 °C and 2 MPa $H_2$ in addition of $Ba(OH)_2$ and $RbCO_3$ catalyst (Tymchyshyn and Xu 2010). With both catalysts, the amount of phenolic compounds increased and the major phenolic compounds were found as 2-methoxy-phenol, 4-ethyl-2-methoxy-phenol and 2,6-dimethoxy-phenol. Moreover, Liu et al. (2006) studied the influence of both acid and base presence on the conversion of walnut shell between 200-300 °C. KOH and $Na_2CO_3$ led to higher conversion and more methoxy phenolic compounds, cyclopentene derivatives and C12-18 fatty acids whereas the mechanism of levulinic acid promoted, but conversion decreased with HCl treatment.

## 2.2. Total Phenolic Content and Total Antioxidant Activity

Hazelnut which is a plant derived product has phenolic content, minerals, vitamins, protein and carbohydrate. Therefore, hazelnut has been identified as an important agricultural product for human health. Different types of phenolic antioxidant including phenolic, caffeic acid, p-coumaric acid, gallic acid, sinapic acid, vanillic acid and ferulic acid are found in hazelnut (Altun et al. 2013). Shahidi et al. (2007) was evaluated the total phenolic content and total antioxidant activity of defatted hazelnut kernel and hazelnut byproducts (hazelnut skin, hazelnut hard shell, hazelnut green leafy cover and hazelnut tree leaf) extracts by 80:20 (v/v) ethanol/water mixture at 80 °C. The highest phenolic content was found in hazelnut skin with a value of 577.7 mg of catechin per gram of ethanol extract. Moreover, the total antioxidant acitivities of hazelnut byproducts was determined 4-5 fold more effective than that of hazelnut kernel. The content of phenolics and total antioxidant activities of hazelnut kernel and hazelnut byproducts are given in Table 2.2.

Table 2.2. The content of phenolics and total antioxidant activities of hazelnut kernel and hazelnut byproducts (Source: Shahidi et al. 2007)

| | **Total phenolic content** | **Total antioxidant acitivity** |
|---|---|---|
| hazelnut kernel | 13.7 | 29 |
| hazelnut skin | 577.7 | 132 |
| hazelnut hard shell | 214.1 | 120 |
| hazelnut green leafy cover | 127.3 | 117 |
| hazelnut tree leaf | 134.7 | 148 |

Alasalvar et al. (2009) extracted the total phenolics and total antioxidant activity of hazelnut skin by using 80:20 (v/v) acetone or methanol/water mixture at 50 °C for 30 min. The crude extracts were separated into low molecular weight phenolic fraction and tannin fraction. Total phenolic content and total antioxidant activities of hazelnut skin are shown in Table 2.3. In both solvent, total phenolics and total antioxidant activity of tannin fraction were higher than that of crude extract and low molecular weight phenolic fraction. Acetone was more favorable for total antioxidant activity whereas the content of total phenolics with methanol extraction was higher than those with acetone extraction.

Table 2.3. Total phenolics and total antioxidant activities in hazelnut skin (Source: Alasalvar et al. 2009)

| | | **acetone extraction** | **methanol extraction** |
|---|---|---|---|
| Total phenolics (mg CE/g) | crude extract | 686 | 701 |
| | low molecular weight phenolic fraction | 441 | 442 |
| | tannin fraction | 697 | 746 |
| Total antioxidant activity (mmol TE/g) | crude extract | 6.33 | 6.36 |
| | low molecular weight phenolic fraction | 4.77 | 4.02 |
| | tannin fraction | 6.77 | 6.47 |

Contini et al. (2008) studied the extraction of phenolic content from hazelnut shell, whole and chopped roasted hazelnut skins with 80:20 (v/v) acetone/methanol/ethanol and water mixture. For hazelnut shell, acetone was more effective to extract phenolic compounds with a value of 72.2 mg of GAE/gram of extract. However, affectivity of solvent type varied with respect to raw material (Table 2.4). The maximum phenol content amount was obtained from whole roasted hazelnut skin with 80:20 (v/v) ethanol-water mixture.

Table 2.4. Total phenolic amount of different material with respect to solvent type (Source: Contini et al. 2008)

| **Material Type** | **Solvent Type** | **Total Phenolic Content (mg GAE/g)** |
|---|---|---|
| Hazelnut shell | Methanol | 56.6 |
| | Ethanol | 59.6 |
| | Acetone | 72.2 |
| Whole roasted hazelnut skin | Methanol | 426.7 |
| | Ethanol | 502.3 |
| | Acetone | 466.8 |
| Chopped roasted hazelnut skin | Methanol | 97.7 |
| | Ethanol | 174.5 |
| | Acetone | 206.1 |

# CHAPTER 3

# EXPERIMENTAL

## 3.1. Chemicals

All chemicals used in this study were of analytical standards and used without purification. Information about these chemicals used during the experiments is given in Table 3.1. Moreover, de-ionized water was used to prepare solutions and cleaning.

Table 3.1. List of used chemicals in analytical standards and experiment

| Name | The Product Code | Producer |
|---|---|---|
| Furfural | 8.04012.0500 | Merck |
| Sulfuric acid | 84721 | Fluka |
| Lactic acid | 141034,1211 | Panreac |
| Acetic acid | 1,00063,2500 | Merck |
| Glucose | 1,08337,0250 | Merck |
| Formic acid | 1,00264,2500 | Merck |
| Fructose | F0127-1006 | Sigma Aldrich |
| Glycolic acid | 124737-256 | Sigma |
| Glycolaldehyde dimer | G6805-1G | Aldrich |
| Pyruvic acid | 107360-25G | Aldrich |
| 5-HMF | W501808-25G-K | SAFC |
| Levulinic acid | L2009-50G | Aldrich |
| DL-Glycerolaldehyde | G5001-500MG | Sigma |
| Glycerol | 141339,1212 | Pancreac |
| ABTS | 10102946001 | Sigma Aldrich |
| Potassium persulfate | 379824 | Fluka |
| Ethanol | 1009832511 | Merck |
| Folin Ciocalteu Reagent | 1090010500 | Merck |

**(Cont. on next page)**

| | | |
|---|---|---|
| Sodium carbonate | S2127 | Sigma Aldrich |
| Gallic acid | 842649 | Merck |

## 3.2. Experimental Apparatus

The reactions were carried out in a batch-type reactor (Parr 5500 High Pressure Compact Reactor). The maximum operating conditions of this reactor are 350 ºC of operating temperature, 3000 psi of operating pressure and 300 ml of reactor volume. The reactor is equipped with gas inlet and outlet valves, a pressure gage, a safety rupture disc, an internal thermocouple and an internal stirrer, is shown in Figure 3.1. Construction material of the reactor is Type 316 Stainless Steel. The reactor has a cooling system that utilizes water as coolant.

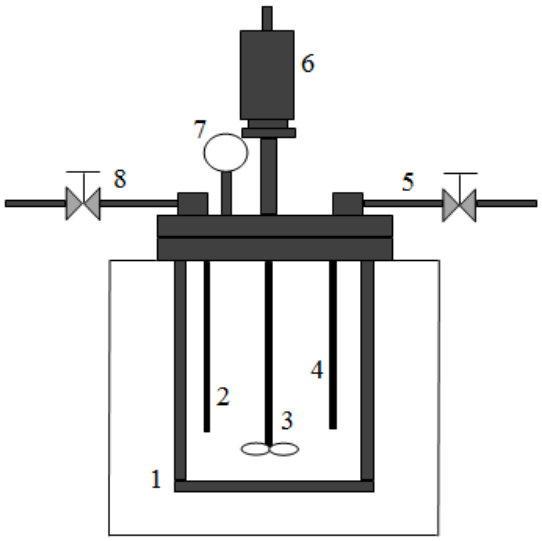


Figure 3.1. Hydrothermal conversion reactor: 1) stainless steel beaker, 2) thermocouple, 3) stirring impeller, 4) gas inlet, 5) input nitrogen gas, 6) magnetically driven Stirrer, 7) pressure gauge, 8) gas sample collecting valve

## 3.3. Experimental Procedure

Before the reaction, hazelnut shell was grinded to approximately 1 mm by a laboratory scale grinder. The reactor was initially loaded with 4 g of hazelnut shell and then the volume is completed to 100 ml by adding de-ionized water. For comparison, different concentration of acid ($H_2SO_4$ and $H_3PO_4$) was placed at the same reaction conditions. All the pins were tightened and then the reactor was purged with an inert gas ($N_2$) to remove air inside the reactor. After that, the reaction temperature was set to the desired reaction temperature with stirring rate of 200-250 rpm throughout the experiment. Temperature and pressures were recorded at every 5 minutes until the temperature reached the desired operating conditions. During heating period, temperature and internal pressure increased until reaching desired reaction temperature. The temperature-pressure profile of liquefaction process for 280 ºC and 60 min is given in Figure 3.2. At the end of the reaction time, the heater was turned off and the system let to be cooled since the reaction occurs at high pressures, pressure must come to safe levels before collecting the final sample.

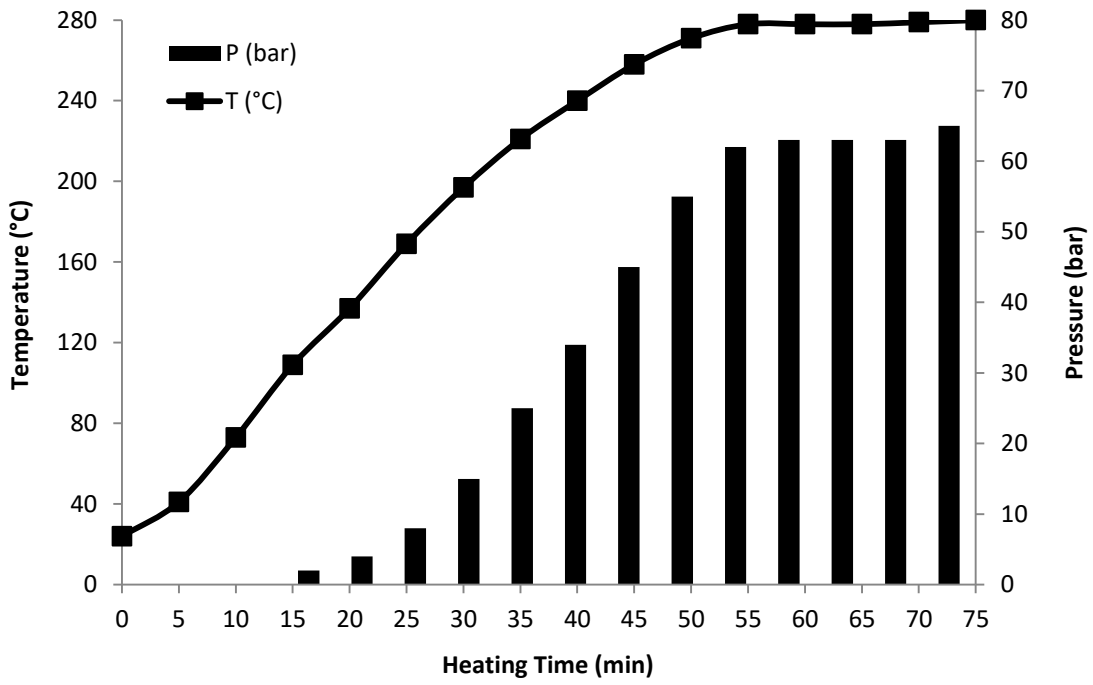


Figure 3.2. Temperature-pressure profile (280 ºC)

After the reaction, liquid, solid and gaseous products were obtained. Gaseous product was collected into gas bags. Solid and liquid product was separated with a filter paper

(quantitative paper, grade: 391) and the liquid product was defined as the water-soluble part (liquor). The remained solid residue was put in a forced oven (Daihan Wof 50) and a vacuum oven (Jsr jsvo-60T) to remove the moisture with set conditions as 50 ºC for 48 hours. And then, pH value of the liquid product was measured. The overall conversion of hazelnut shell was calculated relative to initial amount of dry hazelnut shell in regard to following equation:

$$Overall\ conversion\ (wt.\%) = \frac{Hazelnut\ shell\ (initial\ amount) - Solid\ residue}{Hazelnut\ shell\ (initial\ amount)} x100 \qquad Eqn\ (3.1)$$

The yield of each identified compounds by HPLC analyses was determined with following equation:

$$Yield\ of\ compounds\ (\%) = \frac{Concentration\ of\ compound\ (ppm)}{Degraded\ hazelnut\ shell\ (ppm)} x100 \qquad Eqn\ (3.2)$$

After the separation process, liquid products were analyzed by HPLC and GC-MS, and the gaseous products were analyzed qualitatively by GC-TCD analysis. The morphological structure of solid products was observed by SEM and FTIR analysis. The total organic carbon in the solid product was determined by TOC analyzer. In addition, antioxidant activity and total phenolic content were monitored by $ABTS^{+}$ Method and Folin Ciocalteu Method, respectively. The general diagram of experimental procedure is given in Figure 3.3.

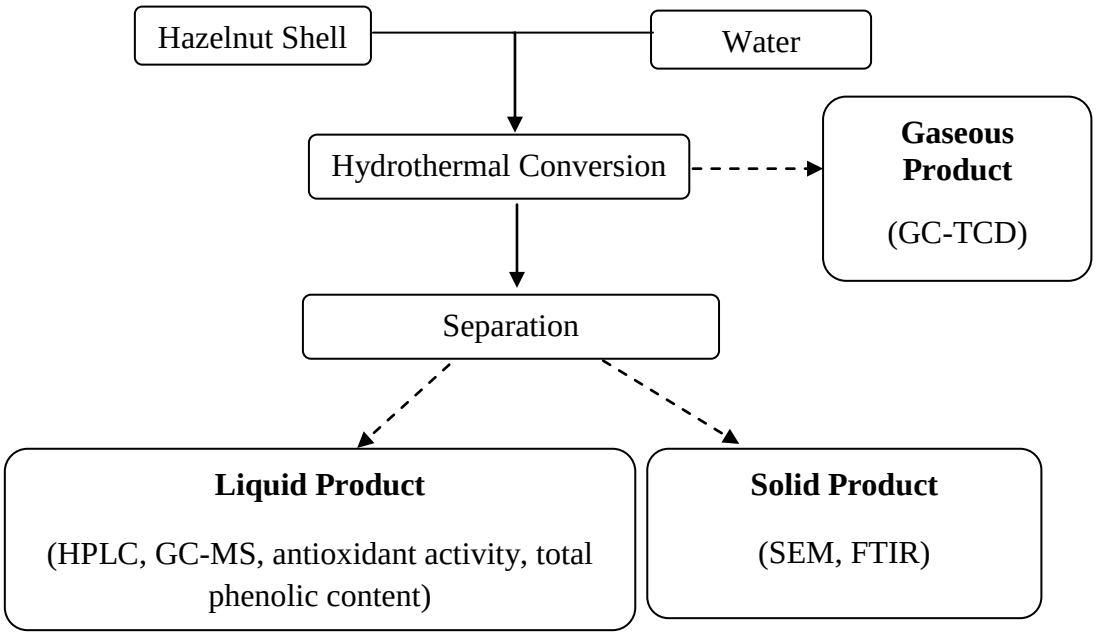


Figure 3.3. The general diagram of experimental procedure

The performed experimental conditions which were determined with using Analysis of Variance (ANOVA) are given in the Table 3.2.

Table 3.2. Experimental study of hazelnut shell conversion

| **Experiment Number** | **Acid Concentration (mM)** | **T (ºC)** | **t (min)** |
|---|---|---|---|
| | **$H_2SO_4$** | | |
| 1 | 0 | 150 | 15 |
| 2 | 0 | 200 | 15 |
| 3 | 0 | 250 | 15 |
| 4 | 0 | 280 | 15 |
| 5 | 0 | 150 | 60 |
| 6 | 0 | 200 | 60 |
| 7 | 0 | 250 | 60 |
| 8 | 0 | 150 | 90 |
| 9 | 0 | 200 | 90 |
| 10 | 0 | 250 | 90 |
| 11 | 5 | 200 | 60 |
| 12 | 50 | 150 | 15 |
| 13 | 50 | 200 | 15 |
| 14 | 50 | 250 | 15 |
| 15 | 50 | 280 | 15 |
| 16 | 50 | 150 | 60 |
| 17 | 50 | 200 | 60 |
| 18 | 50 | 250 | 60 |
| 19 | 50 | 280 | 60 |
| 20 | 50 | 150 | 90 |
| 21 | 50 | 200 | 90 |
| 22 | 50 | 250 | 90 |
| 23 | 50 | 280 | 90 |

**(Cont. on next page)**

| | | | |
|---|---|---|---|
| 24 | 50 | 150 | 120 |
| 25 | 50 | 280 | 120 |
| 26 | 0 | 150 | 120 |
| 27 | 0 | 200 | 120 |
| 28 | 0 | 280 | 60 |
| 29 | 0 | 280 | 90 |
| 30 | 0 | 280 | 120 |
| 31 | 0 | 250 | 120 |
| 32 | 50 | 200 | 120 |
| 33 | 50 | 250 | 120 |
| 34 | 50 | 150 | 15 |
| 35 | 25 | 200 | 60 |
| 36 | 75 | 200 | 60 |
| 37 | 100 | 200 | 60 |
| 38 | 125 | 200 | 60 |
| | **$H_3PO_4$** | | |
| 39 | 50 | 200 | 60 |
| 40 | 75 | 200 | 60 |
| 41 | 100 | 200 | 60 |
| 42 | 125 | 200 | 60 |

## 3.4. Product Analysis

### 3.4.1. Liquid Product Analysis

High performance liquid chromatography (HPLC) was performed for the identification of chemical compounds exists in the liquor. HPLC analysis was done in Environmental Development Application and Research Center of IZTECH and Biotechnology and Bioengineering Research and Application Center of IZTECH. The HPLC system equipped with Shodex Sugar Column (SH 1011) and refractive index (RI) detector. Dilute sulfuric acid (3.75 mM) was used as a mobile phase with a flow rate of 0.5 ml/min and the temperature of column was set 50 ºC.

To verify HPLC results and identify unidentified components, gas chromatography-mass spectrometry (GC-MS) (Agilent 6890 N/5973 N Network) with Restek Stabilwax-

DA column and Agilent 5973 Mass Selective Detector (S/SL inlet) were used. Helium at 1.3 ml/min of flow rate was used as an eluent gas at 240 ºC of operating temperature. Additionally, oven programme is 40 ºC (2 min with an increase of 8 ºC/min), 140 ºC (5 min with an increase of 10 ºC/min), and 220 ºC (10 min). This analysis was carried out in Environmental Development Application and Research Center of IZTECH.

### 3.4.1.1. Antioxidant Activity ($ABTS^+$ Method)

$ABTS^+$ solution was prepared by 14 mM ABTS solution and 4.9 mM potassium persulfate solution with the volume ratio of 1:1 and left for 16 hours at dark room. After 16 hours, $ABTS^+$ solution was diluted with ethanol with the volume ratio of 1:50 ($ABTS^+$ solution: ethanol). Then, 1 ml of liquid product was mixed with 4 ml of $ABTS^+$ solution and left in the dark at room temperature for 5 min. The absorbance was measured at 734 nm and water was used as blank. The calibration curve of $ABTS^+$ Method is given in the Figure 3.4.

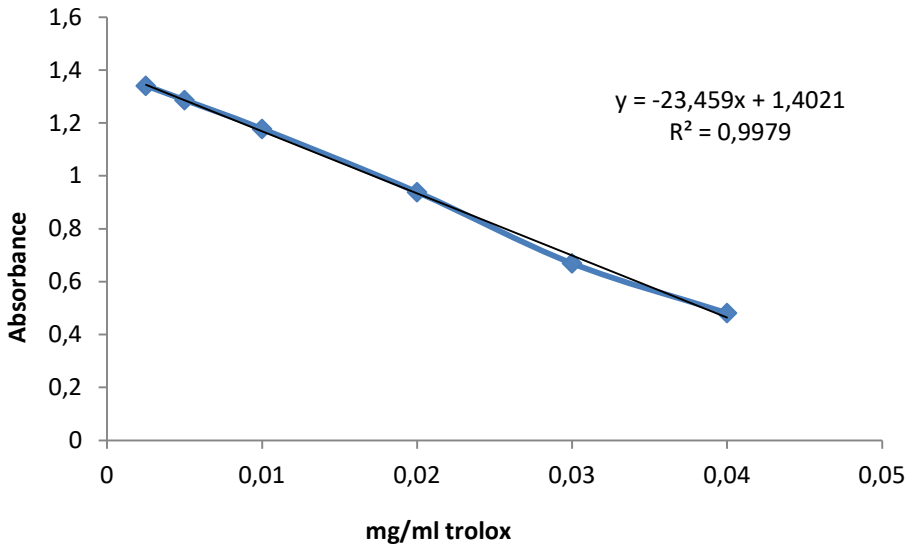


Figure 3.4. The calibration curve of $ABTS^+$ solution at 734 nm

### 3.4.1.2. Total Phenolic Content (Folin Ciocalteu Method)

Folin Ciocalteu reagent was diluted 10-fold with distilled water and 7.5% (75 g/L) of sodium carbonate solution as prepared with distilled water. 0.5 ml of Folin Ciocalteu reagent, 0.5 ml of liquid product and 1 ml of saturated sodium carbonate solution were mixed and then volume adjusted to 10 ml with distilled water. After mixing, the mixture was left in the dark at room temperature for 45 min. The absorbance was measured at 725 nm and water was used as blank. The calibration curve of Folin Ciocalteu Method is given in the Figure 3.5.

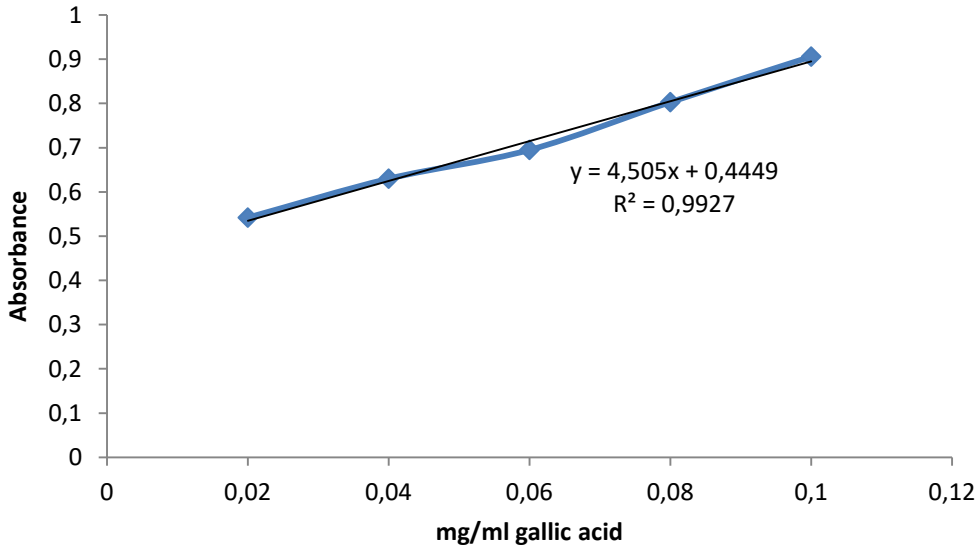


Figure 3.5. The calibration curve of Folin Ciocalteu Method at 725 nm

### 3.4.2. Solid Product Analysis

The remained solid residue was analyzed by SEM equipped with EDX detector and ATR-FTIR analyses. A scanning electron microscopy analyses were performed to observe morphological structure of solid product with a Quanta 250 SEM in Materials Research Center of IZTECH. Solid product samples were zoomed in 2000 (50 µm), 5000 (20 µm), 10000 (10 µm) and 20000 (5 µm). Fourier transform infrared spectroscopy was analyzed by using instrument of Perkin Elmer-Spectra Two in Biotechnology and Bioengineering Research and Application Center of IZTECH. Moreover, the total organic carbon in the solid product was determined by TOC

analyzer (TOC-VCPH, Shimadzu) in Environmental Development Application and Research Center of IZTECH.

### 3.4.3. Gaseous Product Analysis

Gaseous products were identified by using gas chromatography equipped with a thermal conductivity detector (Agilent 6890N Network GC System with Agilent 7683 Injector) in Environmental Development Application and Research Center of IZTECH.

# CHAPTER 4

# RESULTS AND DISCUSSION

Conversion of hazelnut shell was carried out at various reaction temperatures (150, 200, 250 and 280 ºC), reaction times (15, 60, 90 and 120 min), acid concentrations (0, 5, 25, 50, 75, 100 and 125 mM) and acid types ($H_2SO_4$, $H_3PO_4$). Dadenov (2015) investigated the effect of reaction pressure with values of 5, 10 and 15 bars on the degradation of cellulose in subcritical water. Chan et al. (2014) and Dadenov (2015) concluded that reaction pressure did not influence biomass conversion since degradation take places in liquid phase and pressure slightly changes the properties of water under hot compressed water (Kruse and Gawlik 2003). Therefore, hydrothermal degradation of waste hazelnut shell at different initial pressure did not studied in this study. Liquid, solid and gaseous products were analyzed after the hydrothermal treatment of hazelnut shell. HPLC analysis were performed to liquid product in order to determine the yields of pyruvic acid, monomers (glucose, fructose), glyceraldehydes, glycolic acid, glycolaldehyde, lactic acid, glycerol, formic acid, acetic acid, levulinic acid, 5-HMF, furfural and oligomers. The typical reflective index (RI) chromatogram is shown in Figure 4.1.

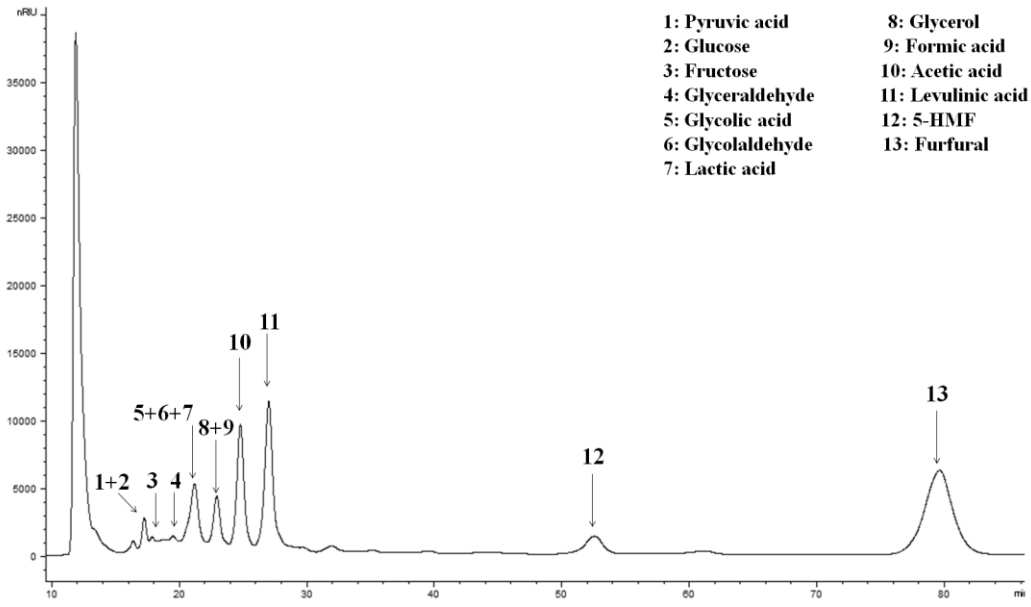


Figure 4.1. RI chromatogram of liquid products after degradation of hazelnut shell (200 °C, 60 min, 15 bar and with 50 mM $H_2SO_4$)

## 4.1. Effect of Reaction Temperature on Hazelnut Shell Conversion and Product Yields

The reaction temperature is the main reaction parameter on the conversion of hazelnut shell, which was also concluded by ANOVA Analysis. Conversion of hazelnut shell was carried out at 150, 200, 250 and 280 ºC. In literature, the reaction temperature was used as main operation condition for the production of bio-based chemicals from various biomasses (Cheng et al. 2009, Kruse and Gawlik 2003, Chan et al. 2014, Yan et al. 2008). The hazelnut shell conversion was calculated in regard to the initial amount of hazelnut shell and the weight of remained solid residue.

While the maximum hazelnut shell conversion was observed at 280 ºC and 120 min (65.40%), the least conversion of hazelnut shell was obtained at 150 ºC and 15 min (35.79%) in the presence of 50 mM $H_2SO_4$ concentration. As reaction temperature proceeded from 150 to 280 ºC, considerable increment of hazelnut shell conversion was observed at each reaction time. The conversion of hazelnut shell comparison with respect to reaction temperature and reaction time is shown in Figure 4.2. Furthermore, TOC conversion was also evaluated from solid residues as shown in Table 4.1. As the reaction temperature increased to 280 °C, the conversion of TOC was improved to 49.71% within 60 min. TOC conversion did not show increment with reaction time at several reaction temperatures except that 150 °C.

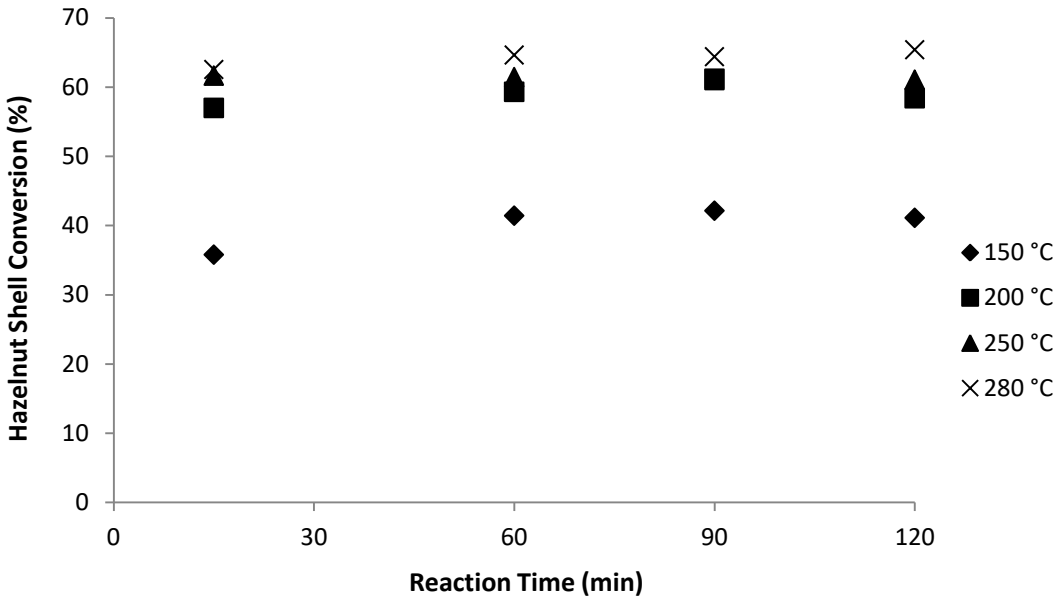


Figure 4.2. Hazelnut shell conversion at various reaction temperatures (150-280 ºC) and reaction times (0-120 min) in the presence of 50 mM $H_2SO_4$ concentration

Table 4.1. The effect of reaction temperature on TOC conversion at different reaction temperature with addition of 50 mM $H_2SO_4$ concentration

| T (°C) | t (min) | TOC Conversion (%) |
|---|---|---|
| 150 | 15 | 29.59 |
| | 60 | 38.49 |
| | 90 | 35.01 |
| | 120 | 32.61 |
| 200 | 15 | 47.73 |
| | 60 | 45.87 |
| | 90 | 46.08 |
| | 120 | 46.96 |
| 250 | 15 | 46.52 |
| | 60 | 47.30 |
| | 90 | 45.04 |
| | 120 | 47.41 |
| 280 | 15 | 43.39 |
| | 60 | 49.71 |
| | 90 | 48.26 |
| | 120 | 47.92 |

In subcritical water, firstly de-polymerization of cellulose is dominant to form oligosaccharides and monosaccharides (glucose). At further stage of the reaction, hydrolysis and rearrangement/decomposition of glucose and other monomer sugars take place to form several products such as fructose, 5- HMF, furfural, pyruvaldehyde, glyceraldehyde and glycolaldehyde. Moreover, hemicellulose is hydrolyzed into high molecular weight oligomers, low molecular weight oligomers, xylose, furfural, glycolaldehyde and glyceraldehydes. Re-polymerization, isomerization and fragmentation of these small products occur into liquid, gaseous and solid products at higher reaction temperatures (Pavlovic et al. 2013, Cardenas-Toro et al. 2014). Among various chemical compounds in the liquid product, the production of levulinic acid, acetic acid, 5-HMF and furfural were focused on. Product distribution of these compounds, which were identified by HPLC analysis and the conversion of hazelnut shell at different temperatures are given in Figure 4.3.

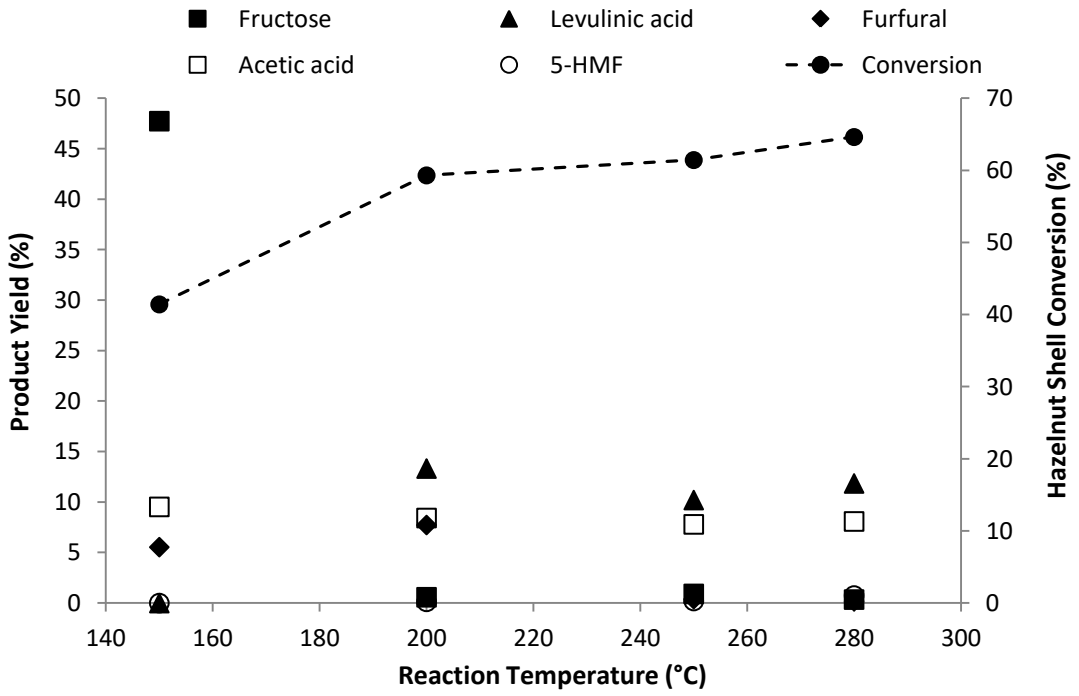


Figure 4.3. Product distribution of liquid compounds and conversion of hazelnut shell at different temperatures (50 mM $H_2SO_4$ and 60 min)

According to Figure 4.3, the conversion of hazelnut shell increased steadily from 41.42% (150 ºC) to 64.64 % (280 ºC). At 150 ºC, the yield of fructose was comparatively higher than the other compounds yields since hydrolysis and decomposition of glucose take place at low temperatures to form fructose (Cardenas-

Toro et al. 2014). With increasing reaction temperature, levulinic acid production increased while the production of 5-HMF dropped to nearly 0%. This result led to the conclusion that the main intermediate product of hexose sugar is 5-HMF which forms different final products like levulinic acid. Moreover, dehydration and hydrolysis reactions were favored at higher subcritical water temperatures to obtain levulinic acid (Asghari and Yoshida 2010). At all reaction temperatures, acetic acid was observed therefore, it was foreseen that the decomposition of furfurals and phenols form acetic acid (Akalin et al. 2012) and also it was formed from acetyl groups of hemicellulose (Rackemann and Doherty 2011). Additionally, the yield of furfural, produced by the dehydration of 5-carbon sugars of hemicellulose, was improved until 200 ºC and then, reduced considerably to 0.18% through higher reaction temperature (280 ºC).

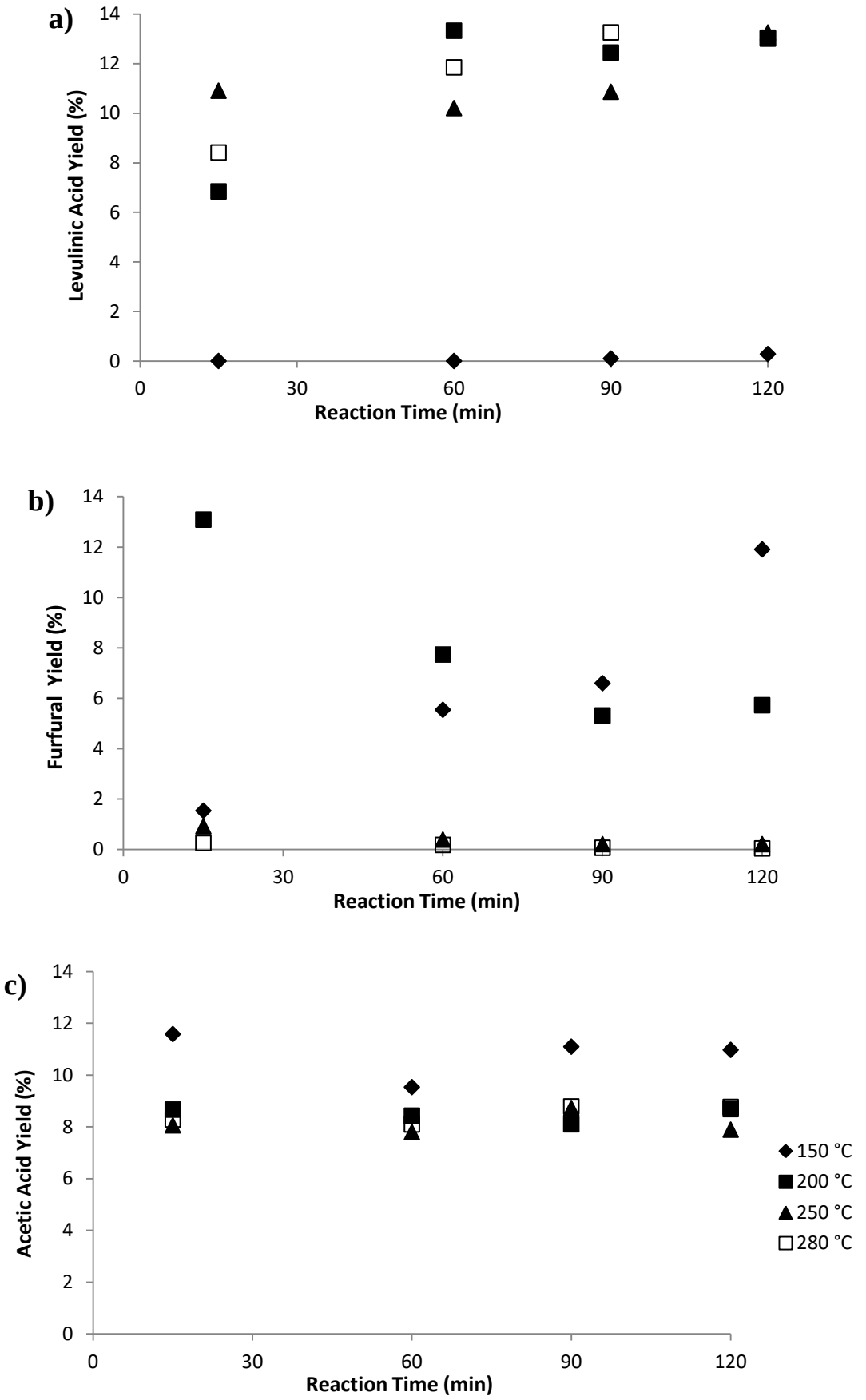


Figure 4.4. Effect of reaction temperature on the yields of **a)** levulinic acid, **b)** furfural, **c)** acetic acid with addition of 50 mM $H_2SO_4$ concentration

Levulinic acid, furfural and acetic acid were determined as major products of hazelnut shell conversion, therefore, the coupled effect of reaction temperature and reaction time of these products is given in Figure 4.4. Among them levulinic acid is the desired product. At low temperature (150 °C), the presence of levulinic acid was not observed until 90 min, whereas for longer reaction time, slight increase in the yield of levulinic acid was observed. The formation of levulinic acid was enhanced at higher process temperatures (200, 250 and 280 °C) and also the levulinic acid yield increased when subjected to longer reaction time. It can be seen from Figure 4.4a that the highest result of levulinic acid yield was achieved at 250 °C with 120 min with a value of 13.26%. This can be based on unique thermodynamic properties like dielectric constant and ion product of water since dielectric constant shows drastic decrease and the ion product is approximately three orders magnitude higher through the critical point. As a result, water becomes an acid or base catalyst precursor and ionic reaction can be boosted due to higher $H_3O^+$ and $OH^-$ ion concentration (Akiya and Savage 2002, Kruse and Dinjus 2007). Efremov et al. (1997) was reported similar observation about levulinic acid yield trend that increased with an increase in reaction temperature when adding 1 and 3 wt.% $H_2SO_4$. In contrast to levulinic acid yield, lower reaction temperatures (150 and 200 °C) were more favorable for the production of furfural (Figure 4.4b) since furfural yield increased up to 11.91% (120 min) from 1.54% (15 min) at 150 °C and observed 13.09% at 200 °C and 15 min whereas it decreased down to 0.04% at higher reaction temperature and reaction time (280 °C and 120 min). In the case of acetic acid, yield (Figure 4.4c) was higher at 150 °C, but it remained constant almost with a value of 8% at 200, 250 and 280 °C. Therefore, it can be said that acetic acid yield was not seriously affected from reaction temperature and time. Moreover, the liquid product was also analyzed by GC-MS (Figure 4.5) to verify the HPLC results and determine the unidentified compounds in HPLC analysis.

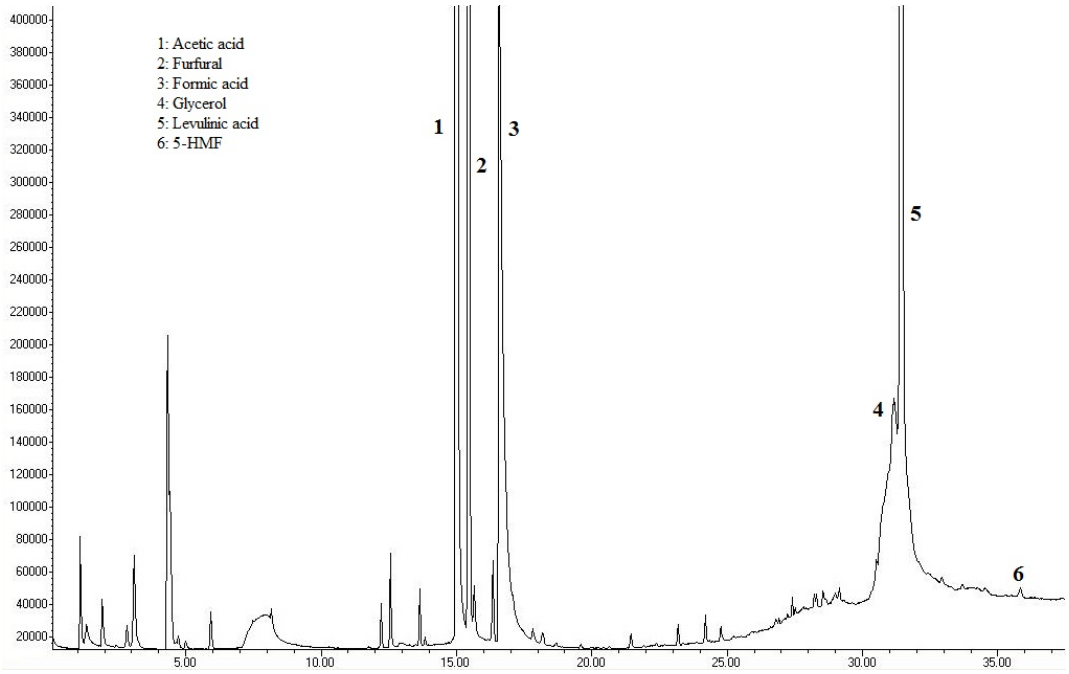


Figure 4.5. GC-MS chromatograms of liquid products after hydrothermal degradation of hazelnut shell (200 °C, 60 min, 15 bar and with 50 mM $H_2SO_4$)

To monitor the changes of surface morphology of untreated hazelnut shell and solid residues of each treatment conditions, scanning electron microscopy (SEM) analysis was applied which is given in Figure 4.6.

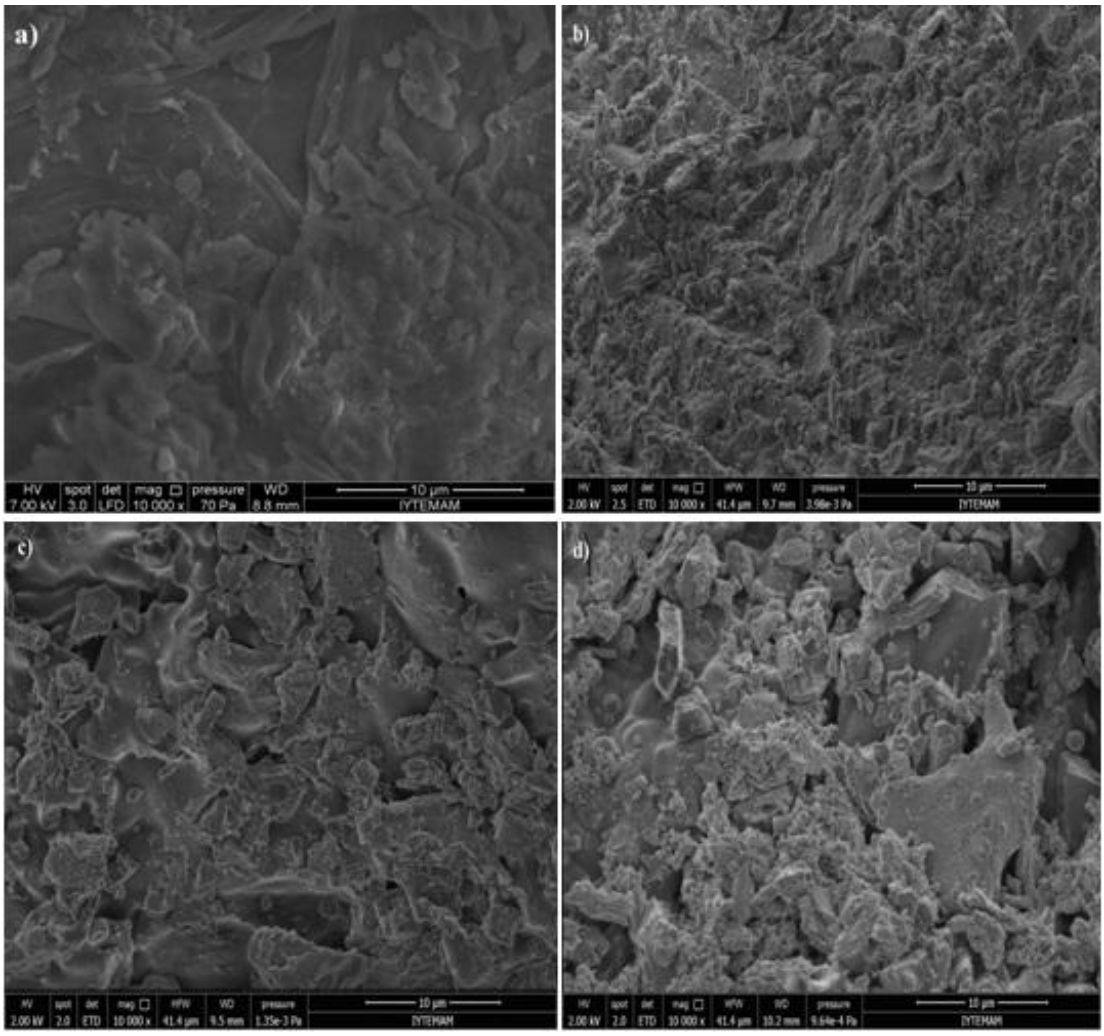


Figure 4.6. SEM images of **a)** untreated and solid residues after the treatment at **b)** 150 °C, **c)** 250 °C, **d)** 280 °C after 60 min wit 50 mM $H_2SO_4$ (at magnification of x10,000)

It can be seen from Figure 4.6, untreated hazelnut sample has a complex structure (Figure 4.6a). Applying 150 °C treatment led to start to the formation of small carbon spheres (Figure 4.6b). This indicates that higher diffusivity of water causes to easy cellulose and hemicellulose decomposition under subcritical water (Cheng et al. 2009). At higher reaction temperatures (250 °C and 280 °C), the amount of carbon spheres decreased and found in tarry structures (Figure 4.6c-d). The effect of reaction temperature on the functional group of hazelnut shell samples was also analyzed by FTIR spectrometry. FTIR spectrum of untreated hazelnut shell and solid residues at 150 ºC, 200 ºC, 250 ºC and 280 ºC are presented in Figure 4.7.

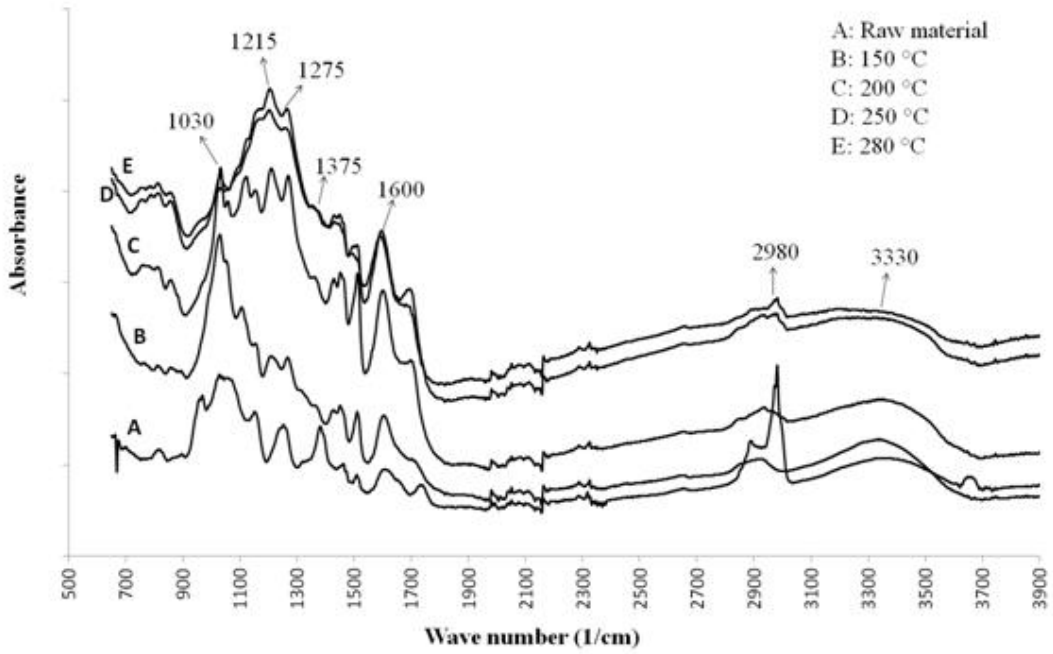


Figure 4.7. FTIR spectrum of untreated and treated hazelnut shell samples at different temperatures (60 min and 50 mM $H_2SO_4$)

As shown in Figure 4.7, the FTIR spectrum has several absorption peaks on hydro-treated solid samples because of the complex structure of biomass (hazelnut shell). The bands at 1030 $cm^{-1}$, 1375 $cm^{-1}$ and 2980 $cm^{-1}$ corresponds to C-O stretching of alcohols, carboxylic acids and esters, C-H bending of alkanes and saturated aliphatic C-H stretching, respectively which shows characteristic cellulosic and hemicellulosic structure (Cheng et al. 2009, Pavlovic et al. 2013). At 1375 $cm^{-1}$ and 2980 $cm^{-1}$, sharper peaks were observed for untreated hazelnut shell sample. In addition, the band of 1375 $cm^{-1}$ disappeared when reaction temperature was increased to 280 °C. Therefore, it can be said that higher temperature treatment resulted in more cellulosic and hemicellulosic component of hazelnut shell decomposition. The peaks at 1215-1275 $cm^{-1}$ indicate stretching of aliphatic C-H groups. Moreover, typical lignin structures which are stretching of C=C aromatic groups (at 1600 $cm^{-1}$) and hydrogen bonded O-H (at 3330 $cm^{-1}$) were observed (Wahyudiono et al. 2007, Cheng et al. 2009). For each case, lignin structures were detected, therefore; the cleavage of phenolic and alcoholic bonds is still difficult even operating at higher temperatures (Wahyudiono et al. 2007).

In this study, gas compounds were identified with gas chromatography thermal conductivity detector (GC-TCD) for conditions of higher reaction temperature (250 ºC and 280 ºC) and reaction time (120 min) since the rate of secondary decomposition

reactions of water-soluble products and the formation of gas compounds were enhanced under these conditions. The main gas products were carbon monoxide and carbon dioxide whereas hydrogen gas and methane were also formed in trace amounts (Table 4.2 and Figure 4.8). Carbon monoxide and carbon dioxide produce from decarbonylation of aldehydes and decarboxylation of carboxylic acids, respectively (Cheng et al. 2009). When the reaction temperature increased from 250 ºC to 280 ºC, the concentration of carbon monoxide improved to 200.47 µg/ml from 160.28 µg/ml whereas carbon dioxide amount decreased from 637.26 to 591.12 µg/ml. This points out that water gas shift reaction (Yakaboylu et al. 2015) shifts through left-hand side towards carbon monoxide when the reaction temperature increased. Comparatively, small amount of hydrogen gas was obtained and it decreased to 1.42 µg/ml because of interaction between cellulose and xylan with lignin when temperature was increased from 250 ºC to 280 ºC. This interaction decreases the generation of hydrogen gas since H atom is donated to lignin component of biomass (Resende 2009). Furthermore, the increment of methane concentration was observed with increase of reaction temperature and methane forms by methyl groups of lignin cleavage (Resende and Savage 2010).

Table 4.2. Gaseous product distribution for 250 ºC and 280 ºC, 50 mM $H_2SO_4$ addition and 120 min

| **Temperature (°C)** | **Gas composition (µg/ml)** | | | |
|---|---|---|---|---|
| | $H_2$ | CO | $CH_4$ | $CO_2$ |
| 250 | 2.77 | 160.28 | 0.29 | 637.26 |
| 280 | 1.42 | 200.47 | 1.78 | 591.12 |

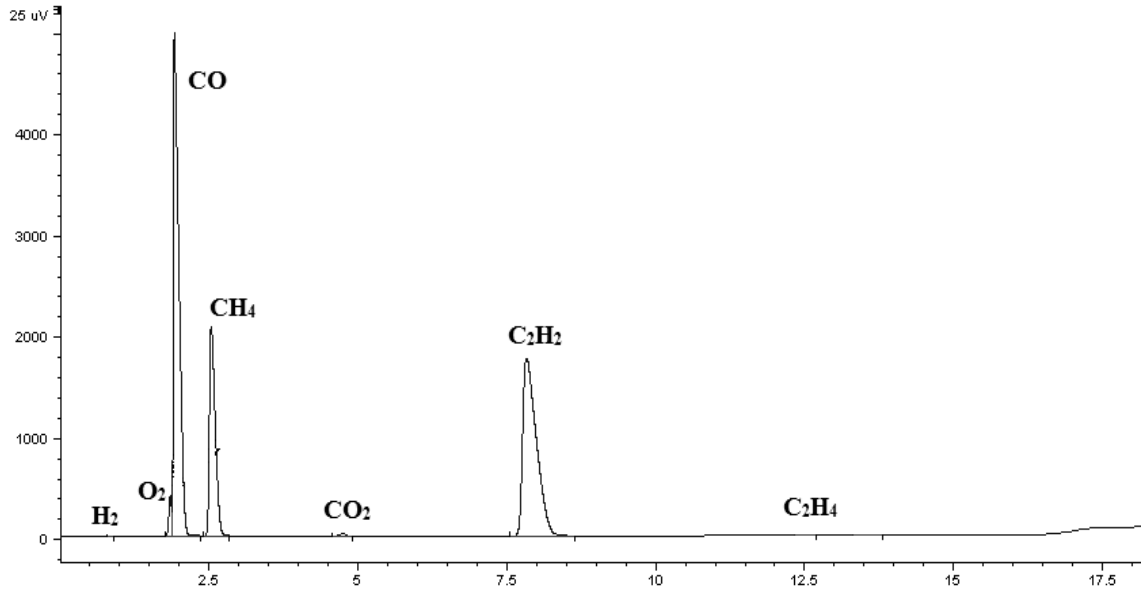


Figure 4.8. GC-TCD chromatogram of gas product at 280 ºC, 120 min and 65 bar in 50 mM $H_2SO_4$ concentration

## 4.2. Effect of Acid Addition on the Conversion of Hazelnut Shell and Product Yields

The investigation of the effect of dilute acid concentration on the hazelnut shell conversion and products yields was one of the main aims of this study. In literature, many previous studies were performed to convert biomass into value-added chemicals by using several acid types efficiently in the meaning of economy. In this way, high desired product yields can be obtained with comparatively low reaction temperature and reaction time that reduce energy consumption and cost. In hazelnut shell conversion, sulfuric acid was mainly preferred. In addition, it is concluded that usage of sulfuric acid improves levulinic acid yield which is our desired product (Fang and Hanna 2002). The comparison of hazelnut conversion in the presence and absence of sulfuric acid is shown in Figure 4.9.

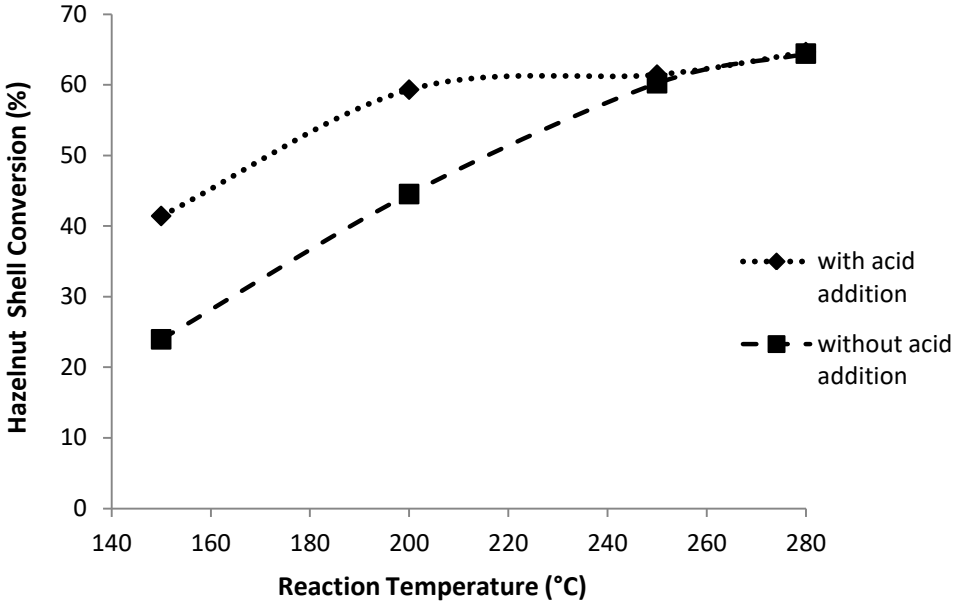


Figure 4.9. Effect of acid addition on the hazelnut shell conversion at different reaction temperatures (50 mM $H_2SO_4$ and 60 min)

As shown in Figure 4.9, the presence of dilute sulfuric acid enhances the degradation of hazelnut shell. At low temperature (150 ºC), the difference of hazelnut shell conversion between both treatments was clearly distinguishable, however; the conversion of hazelnut shell became nearly same at high temperatures (250 ºC and 280 ºC). The conversions were recorded as 59.32% in acidic treatment and 44.53% in the absence of sulfuric acid at 200 ºC, respectively. Efremov et al. (1997) reported nearly the same wood conversion results behavior with sulfuric acid addition at 200-250 ºC. The influence of dilute sulfuric acid on the product yields is given Figure 4.10.

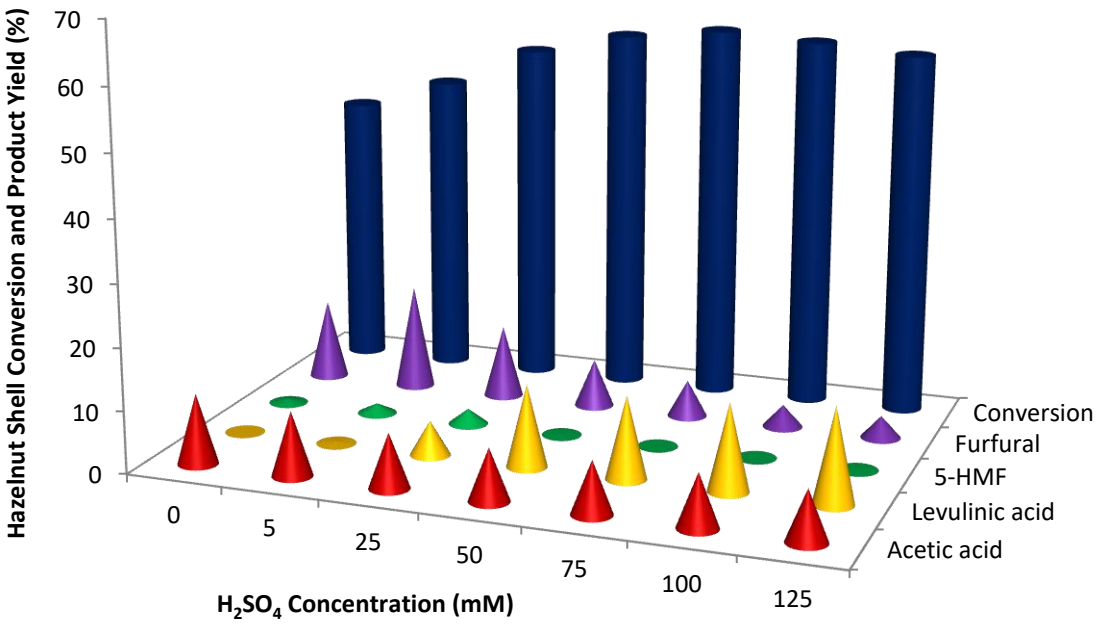


Figure 4.10. The influence of $H_2SO_4$ concentration on the product yield and hazelnut shell conversion (200 ºC, 60 min and 15 bar)

50 mM sulfuric acid concentration was mainly used in this study, besides 5, 25, 75, 100 and 125 mM sulfuric acid concentration were performed to evaluate product distribution trend. It can be concluded that addition of sulfuric acid showed positive effect on the hydrothermal conversion of waste hazelnut shell and levulinic acid formation. As seen in Figure 4.10, the yield of levulinic acid increased with the increment of $H_2SO_4$ concentration from 0.22% (with 5 mM $H_2SO_4$) to 15.40% (with 125 mM $H_2SO_4$). However, the other desired product (furfural) reduced sharply from 16.98% (with 5 mM $H_2SO_4$) to 3.58% (with 125 mM $H_2SO_4$). In the case of acetic acid in the liquor, it was observed that slightly remained constant with increasing $H_2SO_4$ concentration. Additionally, the formation of 5-HMF was so low compared with the other compounds. These trends of compounds can be concluded that the presence of $H_2SO_4$ concentration changes the mechanism of hazelnut shell and influences rate of different compounds. The yield of desired products (levulinic acid, furfural and acetic acid) in the presence and absence of $H_2SO_4$ at 150 ºC and 280 ºC is represented in Table 4.3.

Table 4.3. The yield of levulinic acid, furfural and acetic acid in presence and absence of sulfuric acid (50 mM) at different reaction time (150 and 280 ºC)

| | | Levulinic acid yield (%) | | |
|---|---|---|---|---|
| **Time (min)** | **150 ºC without acid addition** | **280 ºC without acid addition** | **150 ºC with acid addition** | **280 ºC with acid addition** |
| 15 | 0 | 0.40 | 0 | 8.42 |
| 60 | 0 | 0.89 | 0 | 11.85 |
| 90 | 0 | 1.22 | 0.10 | 13.26 |
| 120 | 2.17 | 1.05 | 0.28 | 13.05 |
| | | **Furfural yield (%)** | | |
| 15 | 0 | 1.85 | 1.54 | 0.25 |
| 60 | 0.08 | 0.76 | 5.54 | 0.18 |
| 90 | 0.389 | 0.40 | 6.60 | 0.07 |
| 120 | 0.77 | 0.23 | 11.91 | 0.04 |
| | | **Acetic acid yield (%)** | | |
| 15 | 1.17 | 9.30 | 11.58 | 8.28 |
| 60 | 2.07 | 10.64 | 9.53 | 8.09 |
| 90 | 1.80 | 9.51 | 11.09 | 8.78 |
| 120 | 1.94 | 8.65 | 10.97 | 8.76 |

As it seen in Table 4.3, the formation of levulinic acid was zero in the absence of sulfuric acid for shorter reaction times. However, under same conditions, the degradation of hazelnut shell to produce levulinic acid boosted with the addition of $H_2SO_4$. While significant improvement of acetic acid yield was observed with the addition of sulfuric acid at low temperature (150 ºC), it was not observed an excessive change at higher temperature (280 ºC). Fang and Hanna (2002) and Efremov et al. (1997) observed the comparable enhancement about levulinic yield with the increment of sulfuric acid amount. Efremov et al. (1997) found out 0% and 15.5% of levulinic acid yield at 200 ºC with 0 wt.% $H_2SO_4$ and 5 wt.% $H_2SO_4$, respectively. In the light of literature findings, the product yields in our study reflect the same behavior. Furthermore, $H_2SO_4$ addition showed its influence at 150 ºC by increasing up to 11.91%, but it did not affect at 280 ºC.

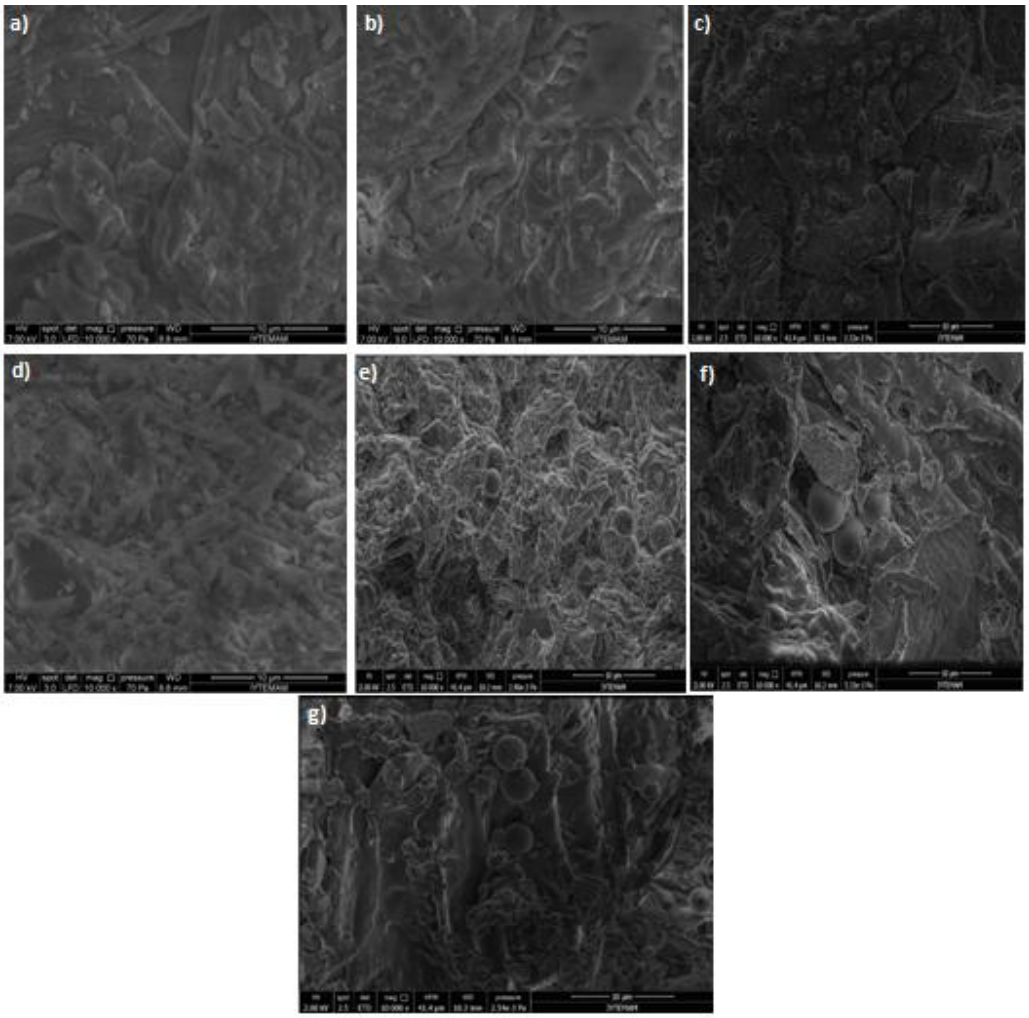


Figure 4.11. SEM images of **a)** raw hazelnut shell and solid residues after conversion (200 °C, 60 min and 15 bar) at **b)** 0 mM; **c)** 25 mM; **d)** 50 mM; **e)** 75 mM; **f)** 100 mM and **g)** 125 mM $H_2SO_4$ (at magnification of x10,000)

The SEM images of raw material and solid products after the hydrothermal treatment with respect to various $H_2SO_4$ concentrations are shown in Figure 4.11. Agglomerated small solid particles were observed at high dilute $H_2SO_4$ concentration (Figure 4.11f-g) when comparing with the treatment in the absence of $H_2SO_4$ concentration (Figure 4.11a).

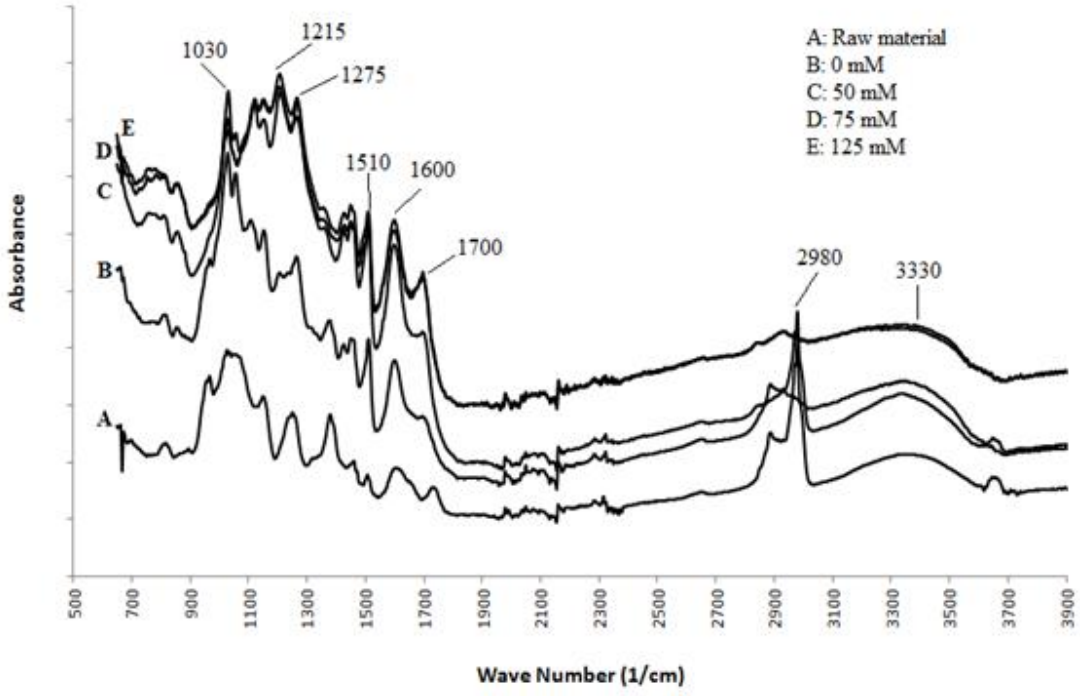


Figure 4.12. FTIR spectrum of solid product at raw material, 0, 50, 75 and 125 mM $H_2SO_4$ (200 °C, 60 min and 15 bar)

The solid residues' FTIR spectrum with the presence of different $H_2SO_4$ concentration is given in Figure 4.12. The same bands with the effect of reaction temperature part were observed, differently from these peaks, the band at 1700 $cm^{-1}$ was observed which is attributed to C=O stretching of α, β-unsaturated aldehydes and ketones. This band was not observed at untreated hazelnut shell sample and the presence of this band improved with a higher $H_2SO_4$ concentration treatment. The band at 2980 $cm^{-1}$, corresponds to saturated aliphatic C-H stretching, was not found at raw material sample and treatment of non- $H_2SO_4$. In addition, the bands at 1030 and 1215 $cm^{-1}$ were not observed at raw hazelnut shell sample. The band at 1510 $cm^{-1}$ corresponds to N-O symmetric stretching of nitro compounds.

## 4.3. Effect of Acid Type on Hazelnut Shell Conversion and Product Yields

Beside the effects of reaction temperature and acid addition were investigated in previous parts, in this section, the comparison of acid type on the conversion of hazelnut shell and product yields in subcritical water was studied. In various researches, different types of acids including $H_2SO_4$ (Efremov et al. 1997, Fang and Hanna 2002, Takeuchi et al. 2008), $H_3PO_4$ (Takeuchi et al. 2008, Asghari and Yoshida 2010), HCl (Yan et al. 2008, Takeuchi et al. 2008, Efremov et al. 1997), HBr (Efremov et al. 1997), $Ba(OH)_2$ and $Rb_2CO_3$ (Tymchyshyn and Xu 2010) were preferred for the hydrothermal degradation of biomass into value-added chemicals. With regard to literature survey, $H_3PO_4$ was selected for the comparison of the results obtained with $H_2SO_4$. Phosphoric acid-catalyzed treatment was performed at 200 ºC and 60 min with the amount of 50, 75, 100 and 125 mM. The comparison of acid type on the hazelnut shell conversion and pH of aqueous solution is shown in Figure 4.13.

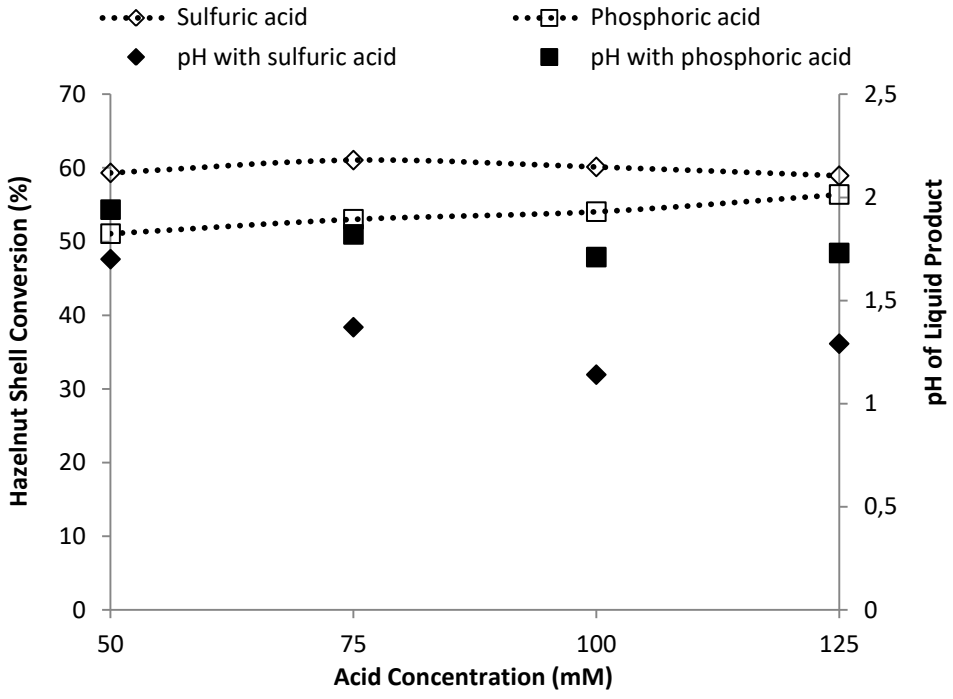


Figure 4.13. The comparison of acid type ($H_2SO_4$ and $H_3PO_4$) on the hazelnut shell conversion and pH of aqueous solution (200 ºC, 60 min and 15 bar)

As it seen from Figure 4.13, the conversion of hazelnut shell in the presence of $H_3PO_4$ was relatively lower than that of $H_2SO_4$. While the conversion value was found 54.05% with 100 mM $H_3PO_4$ addition, it reached to 60.12% within the same amount of $H_2SO_4$. pH of the aqueous solution was recorded as 3.23 without acid addition treatment. After hydrothermal conversion in the presence of 125 mM $H_2SO_4$ and 125 mM $H_3PO_4$ treatments, ph values were found as 1.29 and 1.73, respectively. The difference of pH is attributed to the organic acid formation amount from the decomposition of sugars and organic acid diversity. Identified organic acids were acetic, formic, lactic, pyruvic and glycolic acids from the degradation of hazelnut shell in the subcritical water treatment. The product distribution in the presence of $H_2SO_4$ and $H_3PO_4$ are given in Figure 4.14.

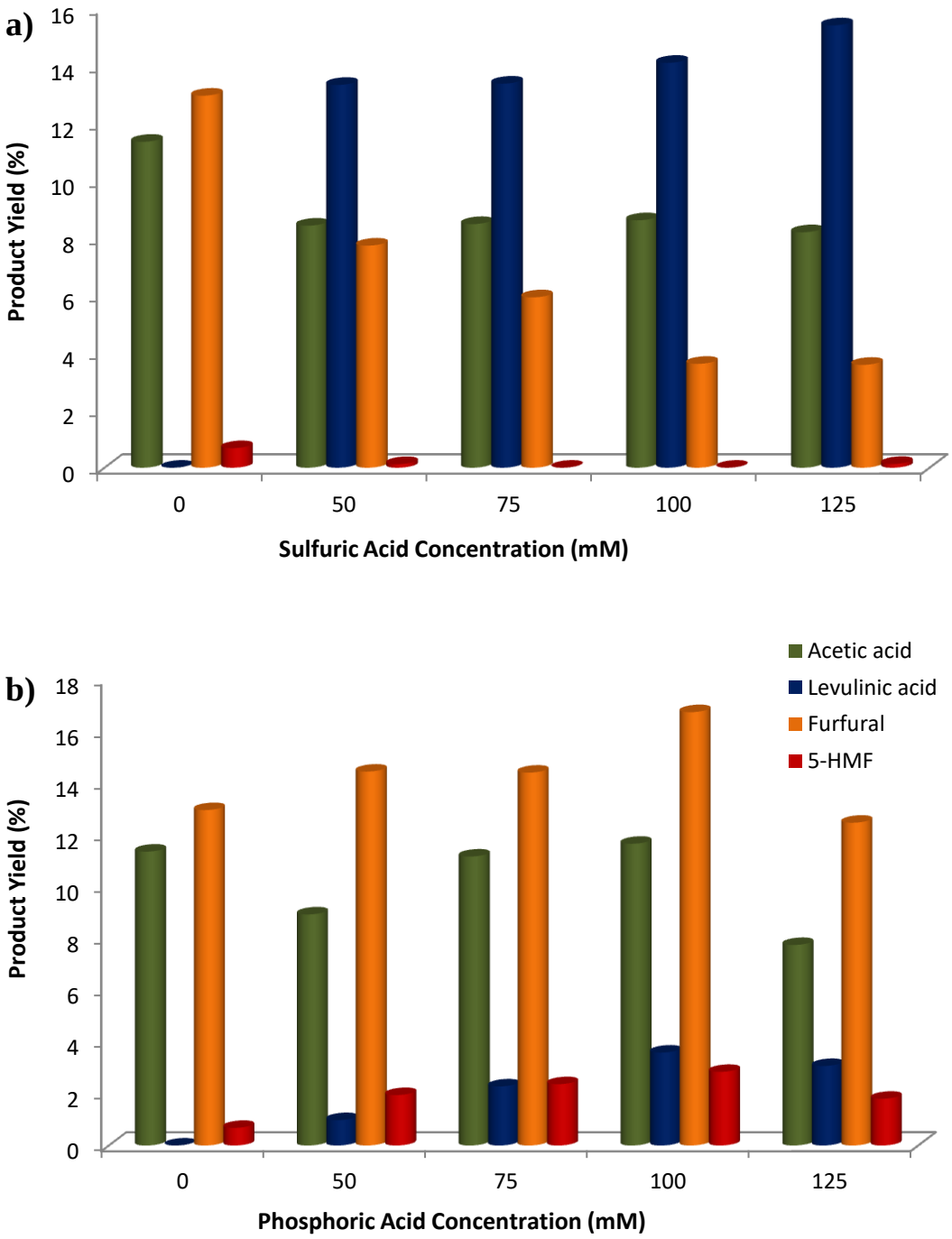


Figure 4.14. The product distribution in the presence of **a)** $H_2SO_4$ and **b)** $H_3PO_4$ at 200 ºC, 60 min and 15 bar

According to HPLC analyses (Figure 4.14), it can be concluded that acid type affected diversely to the product distribution. In the case of $H_3PO_4$, the yield of 5-HMF was higher than that of $H_2SO_4$ since the dehydration of glucose which is a highly reacting species occurs easily in the presence of low acid concentration (Takeuchi et al. 2008). On the other hand, the catalytic effect of $H_2SO_4$ was significantly higher than that of

$H_3PO_4$ in the formation of levulinic acid by accelerating the rate of rehydration of 5-HMF to levulinic acid. With adding more $H_2SO_4$ (125 mM), the yield of levulinic acid severely increased and reached to 15.40%, however; it was considerably low with a value of 3.07% in 125 mM $H_3PO_4$. Our results completely reflect the same findings with Takeuchi et al. (2008) which stated that $H_2SO_4$ is more effective for the production of levulinic acid whereas $H_3PO_4$ is preferred for 5-HMF formation. On the contrary, the use of weaker acids like $H_3PO_4$ was quite favorable in the formation of furfural since while the yield of furfural reached the highest value (16.74%) in the case of adding 100 mM $H_3PO_4$, 3.62% of furfural yield was observed in the same amount of $H_2SO_4$ concentration. This different behavior might cause by two reasons that are furfural can be degraded to furfuryl alcohol then converted to levulinic acid with acid-catalyzed treatment (Figure 4.15) (Rackemann and Doherty 2011) or polymerization of furfural can be caused char formation in hot compressed water (Promdej and Matsumura 2011). The other desired product yield, acetic acid yield, did not show significant difference between $H_2SO_4$ and $H_3PO_4$ addition. The GC-MS chromatogram of liquid product also is given in Figure 4.16.

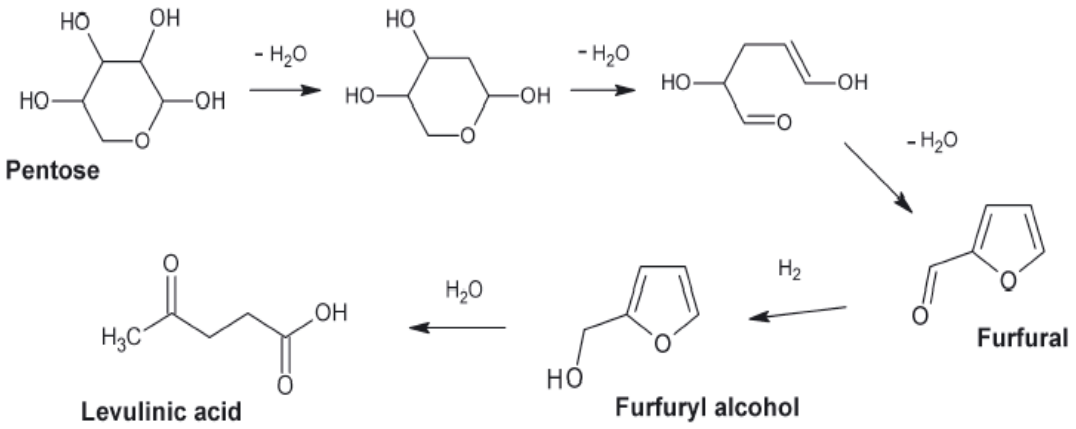


Figure 4.15. Reaction pathway of levulinic acid formation from pentose sugars (Source: Rackemann and Doherty 2011)

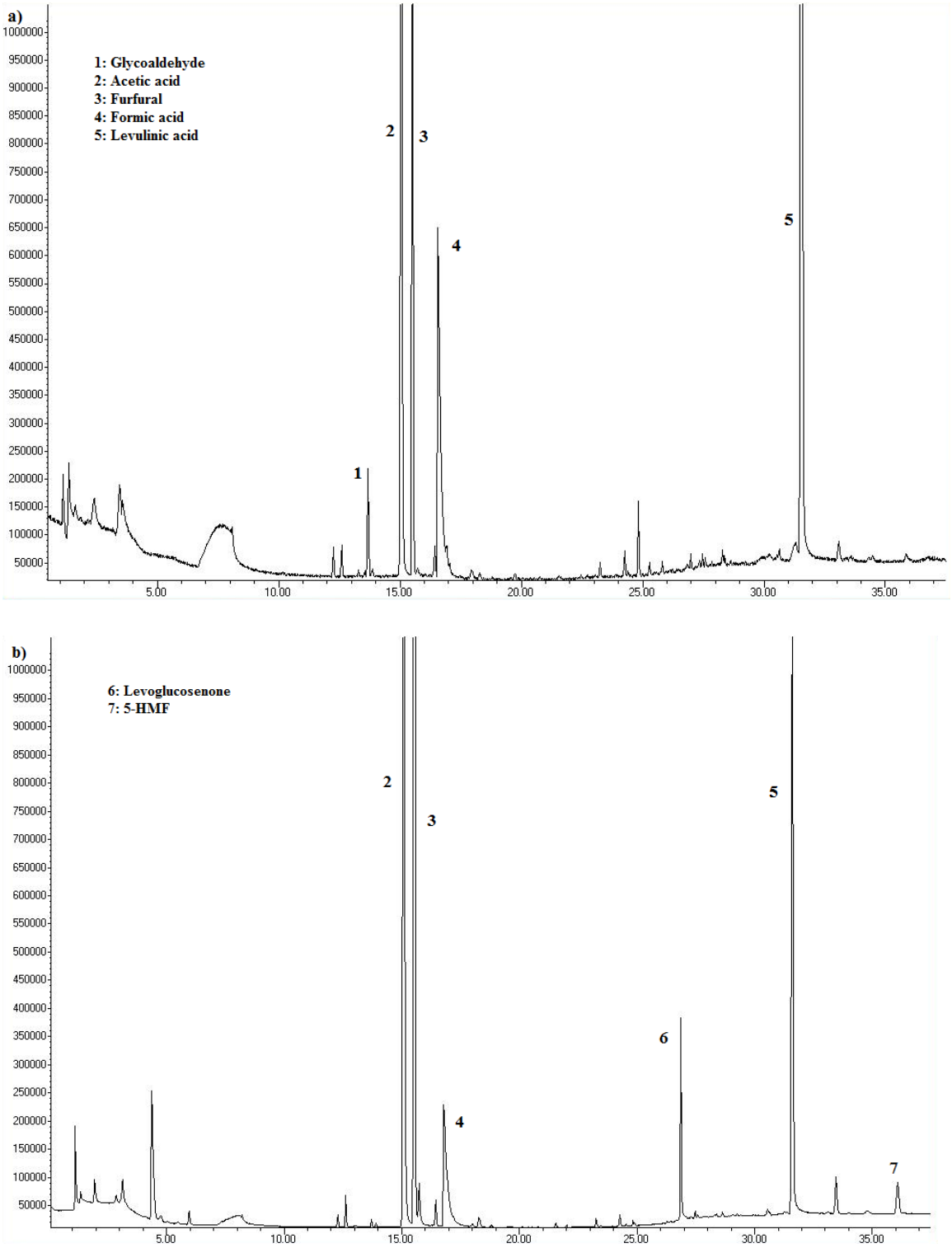


Figure 4.16. GC-MS spectrum of liquid products after treatment with **a)** 125 mM $H_2SO_4$ and **b)** 125 mM $H_3PO_4$ at 200 ºC, 60 min and 15 bar

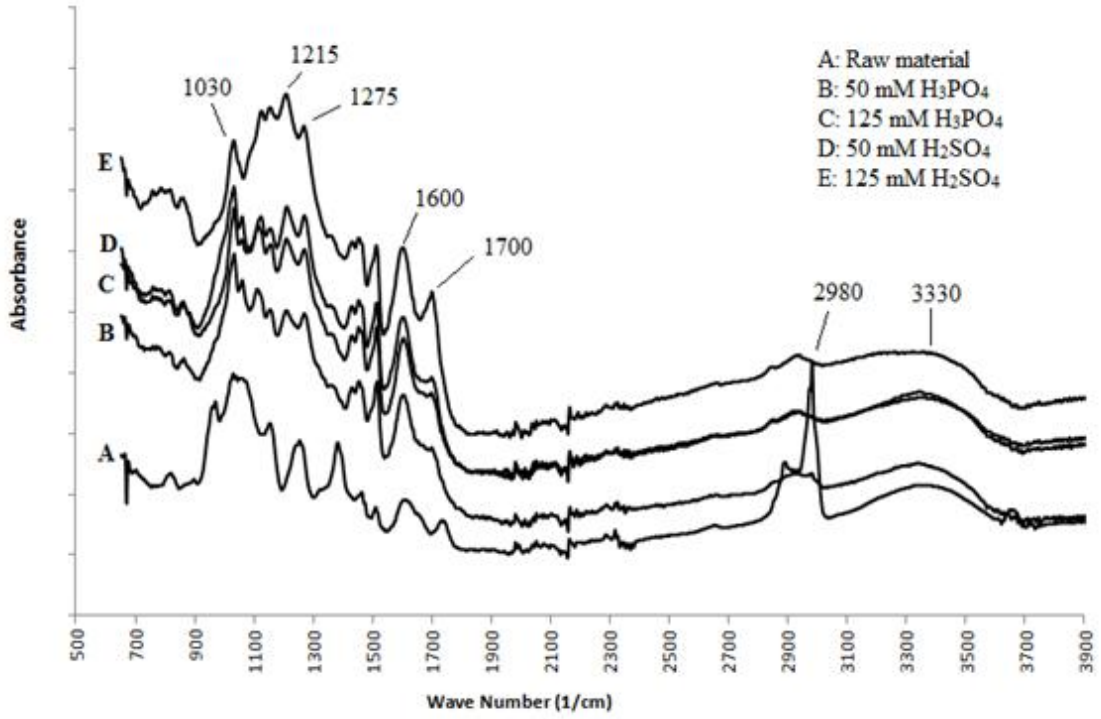


Figure 4.17. Comparison of FTIR spectrum of solid residue with different acid type at 200 ºC, 60 min and 15 bar

In Figure 4.17, the spectrum of FTIR analysis after hydrothermal treatment in the presence of $H_2SO_4$ and $H_3PO_4$ is shown. The 2980 $cm^{-1}$ band was not observed both $H_2SO_4$ and $H_3PO_4$ treatment because of cellulose degradation. The peak at 1700 $cm^{-1}$ refers to strong C=O stretching of carboxylic acids which was observed only in $H_2SO_4$ and $H_3PO_4$ treatments. The band at 1600 $cm^{-1}$ shows stretching of C-C aromatic ring. The peak at 1215-1275 $cm^{-1}$ corresponds to stretching of aliphatic C-H groups. Moreover, 1030 $cm^{-1}$ represents stretching of C-O alcohol esters.

## 4.4. Effect of Reaction Time on Hazelnut Shell Conversion and Product Yields

Although acid concentration and reaction temperature are more influential than the reaction time, optimization of reaction time is essential to obtain selective degradation of lignocellulosic biomasses to various value-added chemicals. Treatments were performed at 15, 60, 90 and 120 min for all reaction parameters. In literature, different studies were reported related to the effect of reaction time on the hydrothermal degradation of biomass (Yan et al. 2008, Takeuchi et al. 2008, Asghari and Yoshida

2010). In Figure 4.18, the conversion of hazelnut shell and the product yields are given at various reaction times at 200 ºC within 50 mM $H_2SO_4$ concentration.

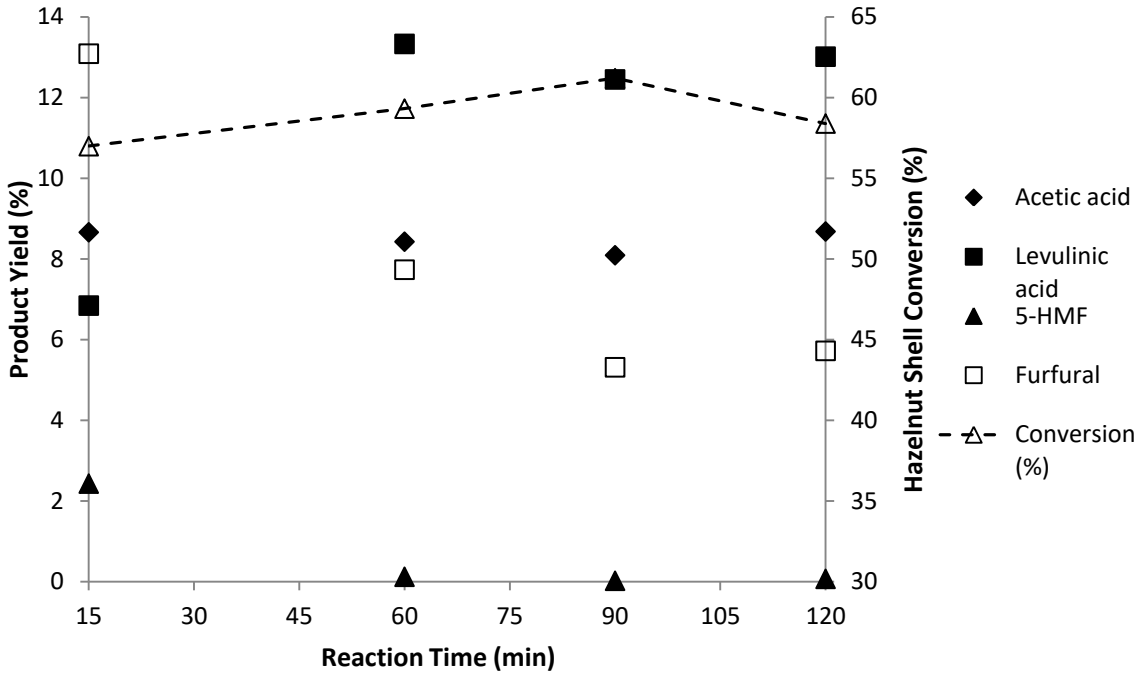


Figure 4.18. Effect of the reaction time on the conversion of hazelnut shell and the yield of product (200 ºC, 15 bar and 50 mM $H_2SO_4$)

As it seen from Figure 4.18, the conversion of hazelnut shell reached the highest value (61.20 wt.%) after 90 min treatment. When reaction time increased from 15 to 120 min, 2.43% of yield of 5-HMF reduced to nearly zero. On the contrary, levulinic acid yield, under same reaction conditions, doubled from 6.85% at 15 min to 13.01% at 120 min. This points out that the rehydration of 5-HMF to levulinic acid enhances with longer reaction time. Low reaction time (15 min) was favorable for furfural formation and furfural yield decreased to 5.72% (120 min). Furthermore, significant difference on the yield of acetic acid was not observed when reaction time proceeded to 120 min. Takeuchi et al. (2008) reported the similar levulinic acid and HMF production trends from the acid-catalyzed hydrothermal conversion of carbohydrate biomass (glucose) with our study with respect to reaction time. Beyond the 5 min, while HMF yield decreased to 1%, levulinic acid yield increased to 23% in $H_2SO_4$ (pH 1.5).

## 4.5. Possible Reaction Pathways of Hydrothermal Conversion of Hazelnut Shell

Possible reaction mechanisms of waste hazelnut shell degradation in subcritical water were evaluated according to HPLC results, as shown in Table 4.4. At low reaction temperature (150 °C), cellulose was hydrolyzed to oligomers (Zhu et al. 2014) and glucose was isomerized into fructose (Zhu et al. 2014) under hot compressed water. When reaction temperature increased to 200 °C, 5-HMF formation was enhanced in the presence of 75-100 mM $H_3PO_4$ concentration. Moreover, excess amount of $H_2SO_4$ (100-125 mM) and long reaction time (≥60 min) led to levulinic acid production from the rehydration of 5-HMF. In the case of hemicellulose, the pathway of acetic acid formation from the cleavage of acetyl (Zhu et al. 2014) dominated at 200 °C and the presence of low $H_2SO_4$ concentration (0-5 mM) or high $H_3PO_4$ concentration (75-100 mM). On the contrary, the production of furfural was effective at 200 °C and 15 min in the presence of 50 mM $H_2SO_4$. With further reaction temperature (250-280 °C) and reaction time (120 min), furfural transformed to char.

Table 4.4. Main proposed reaction pathways for hydrothermal conversion of hazelnut shell at different reaction temperature

| **Reaction Temperature** | **Possible Reaction Pathways** |
|---|---|
| 150 °C | Cellulose → Oligomers/Fructose<br>Hemicellulose → Oligomers/Xylose → Furfural (long reaction time) |
| 200 °C | Cellulose → Oligomers/Fructose → 5-HMF (high $H_3PO_4$ concentration); 5-HMF → Levulinic acid (high $H_2SO_4$ concentration / reaction time)<br>Hemicellulose → Oligomers/Xylose → Acetic acid (low $H_2SO_4$ / high $H_3PO_4$ concentration)<br>Oligomers/Xylose → Furfural (low $H_2SO_4$ / high $H_3PO_4$ concentration / short reaction time) |
| 250-280 °C | Cellulose → Oligomers/Fructose → 5-HMF → Levulinic acid (long reaction time)<br>Hemicellulose → Oligomers/Xylose → Furfural → Char (long reaction time) |

## 4.6. Antioxidant Activity Assay ($ABTS^+$ Method)

In antioxidant activity assay, oxidants including peroxyl radicals oxidize ABTS to radical cation of ABTS ($ABTS^+$) that has an intense blue color. $ABTS^+$ radical and the antioxidant compounds in the water soluble product react with each other, hence; blue color decreases which is used to determine the antioxidant capacity (Roudsari 2007). The antioxidant activity of liquor was performed with $ABTS^+$ method after the hydrothermal treatment of hazelnut shell. The results of antioxidant activity were measured at 734 nm and expressed as trolox equivalents (mg of TE/ml), in which the constants were calculated from the standard curve (Eqn. 4.1). The effect of reaction temperature (150 ºC, 200 ºC, 250 ºC and 280 ºC) and $H_2SO_4$ and $H_3PO_4$ concentration (50, 75, 100 and 125 mM) on the antioxidant activity were investigated.

$$Antioxidant\ activity\ (mg\ of\ TE/ml) = \frac{Absorbance - 1.4021}{-23.459} \qquad Eqn\ (4.1)$$

The influence of reaction temperature and acid concentration on the antioxidant activity for both $H_2SO_4$ and $H_3PO_4$ treatment is shown in Figure 4.19. When reaction temperature increased from 150 to 280 ºC, the antioxidant activity with the treatment of $H_2SO_4$ reduced from 0.045 to 0.038 mg of TE/ml. However, the antioxidant activity for $H_3PO_4$ case kept constant with a value of 0.044 mg of TE/ml under the same conditions. This can be related to hydrothermal treatment causes to the formation a number of antioxidative organic products with the cleavage of H-bonds of hazelnut shell and applying comparatively high reaction temperature and strong acid ($H_2SO_4$) treatment might lead to decrease in the antioxidant activity due to the degradation of antioxidative compounds (Watchararuji et al. 2008). Furthermore, acid concentration increase did not have a significant effect on antioxidant activity and it was recorded approximately as 0.045 mg of TE/ml.

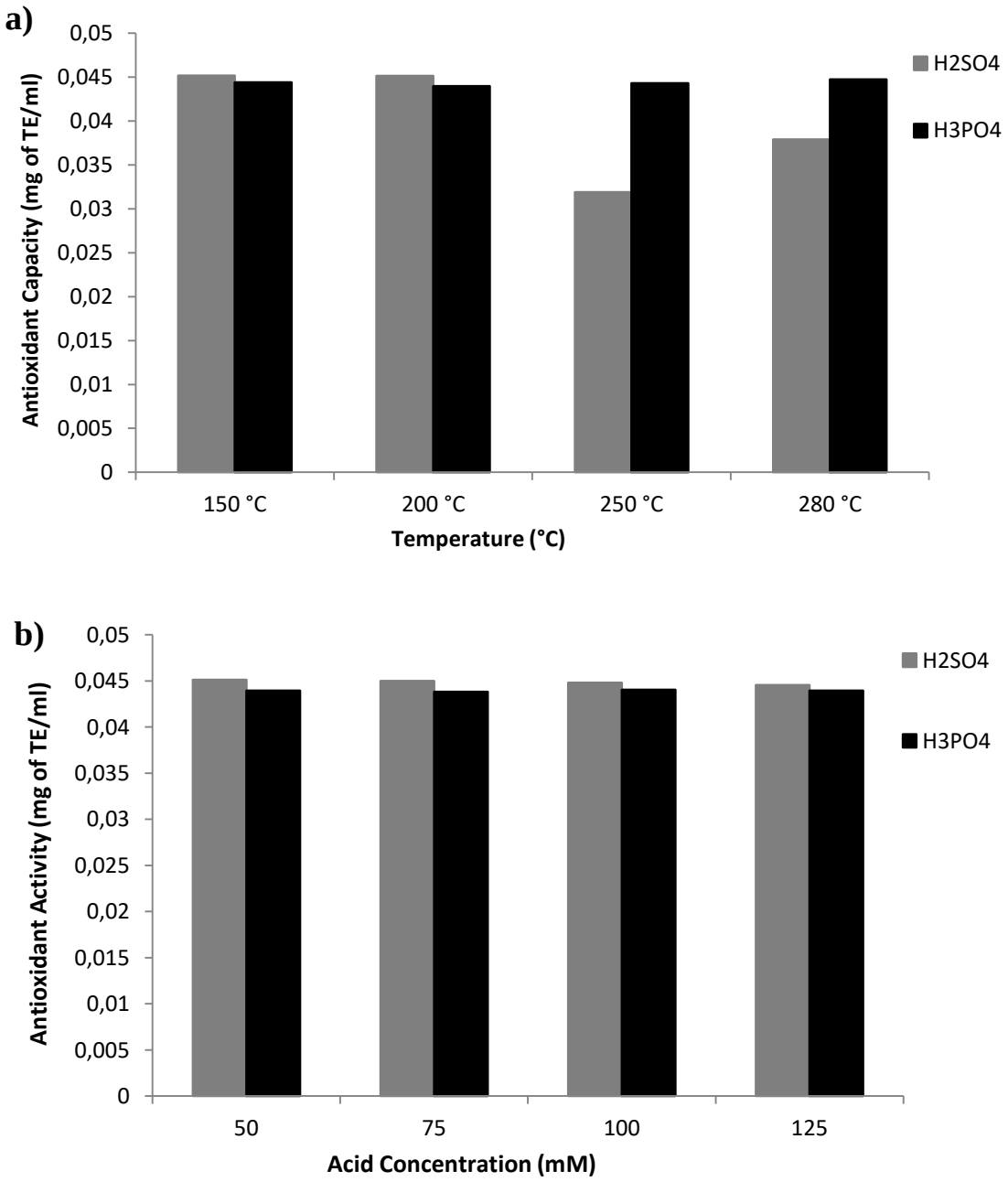


Figure 4.19. The effect of **a)** reaction temperature (60 min within 50 mM $H_2SO_4$ and $H_3PO_4$) and **b)** $H_2SO_4$ and $H_3PO_4$ concentration (200 °C, 60 min and 15 bar) on antioxidant activity

## 4.7. Total Phenolic Content Assay (Folin Ciocalteu Method)

As a result of reaction between Folin Ciocalteu reagent that has a yellow color and phenolic compounds in the liquor, a phenolate anion is formed due to the dissociation of a phenolic proton. Blue-colored compounds were formed by reversible

one or two electron reduction reactions between phenolate and Folin Ciocalteu reagent (Roudsari 2007). The phenolic content was analyzed at 725 nm and results were represented in gallic acid equivalents (mg of GAE/ml) in which the constants were obtained from the standard curve (Eqn. 4.2). The effect of reaction temperature (150 ºC, 200 ºC, 250 ºC and 280 ºC) and $H_2SO_4$ and $H_3PO_4$ concentration (50, 75, 100 and 125 mM) on the total phenolic content were examined, is given in Figure 4.20.

$$Total\ phenolic\ content\ (mg\ of\ GAE/ml) = \frac{Absorbance - 0.4449}{4.505} \qquad Eqn\ (4.2)$$

As seen from Figure 4.20a, total phenolic content increased up to 0.095 mg of GAE/ml, was the highest value, at 250 °C and 60 min within 50 mM $H_2SO_4$ and then decreased to 0.062 mg of GAE/ml at 280 °C. Increase in the total phenolic content at 250 °C can be explained by promoting hydrolysis reaction with increasing of the amount of $H^+$ and $OH^-$ ions (Fabian et al. 2010). In the case of $H_3PO_4$ treatment, the increment of total phenolic content was achieved through 280 °C that was 0.051 mg of GAE/ml. Despite this improvement, addition of $H_2SO_4$ was more favorable between 200-280 °C than $H_3PO_4$. Results showed that the total phenolic content showed different trends when the effect of $H_2SO_4$ and $H_3PO_4$ concentration was compared (Figure 4.20b). While the amount of phenolic compounds in the liquid product solution decreased with increase of $H_2SO_4$ concentration, 0.062 mg of GAE/ml of total phenolic content within 125 mM $H_3PO_4$ were obtained. These results can be caused by different acid strength of aqueous solutions. Pourali et al. (2010) reported that reaction temperature until 220 °C increases the total phenolic compound yield in the degradation of rice bran and defatted rice bran in subcritical water.

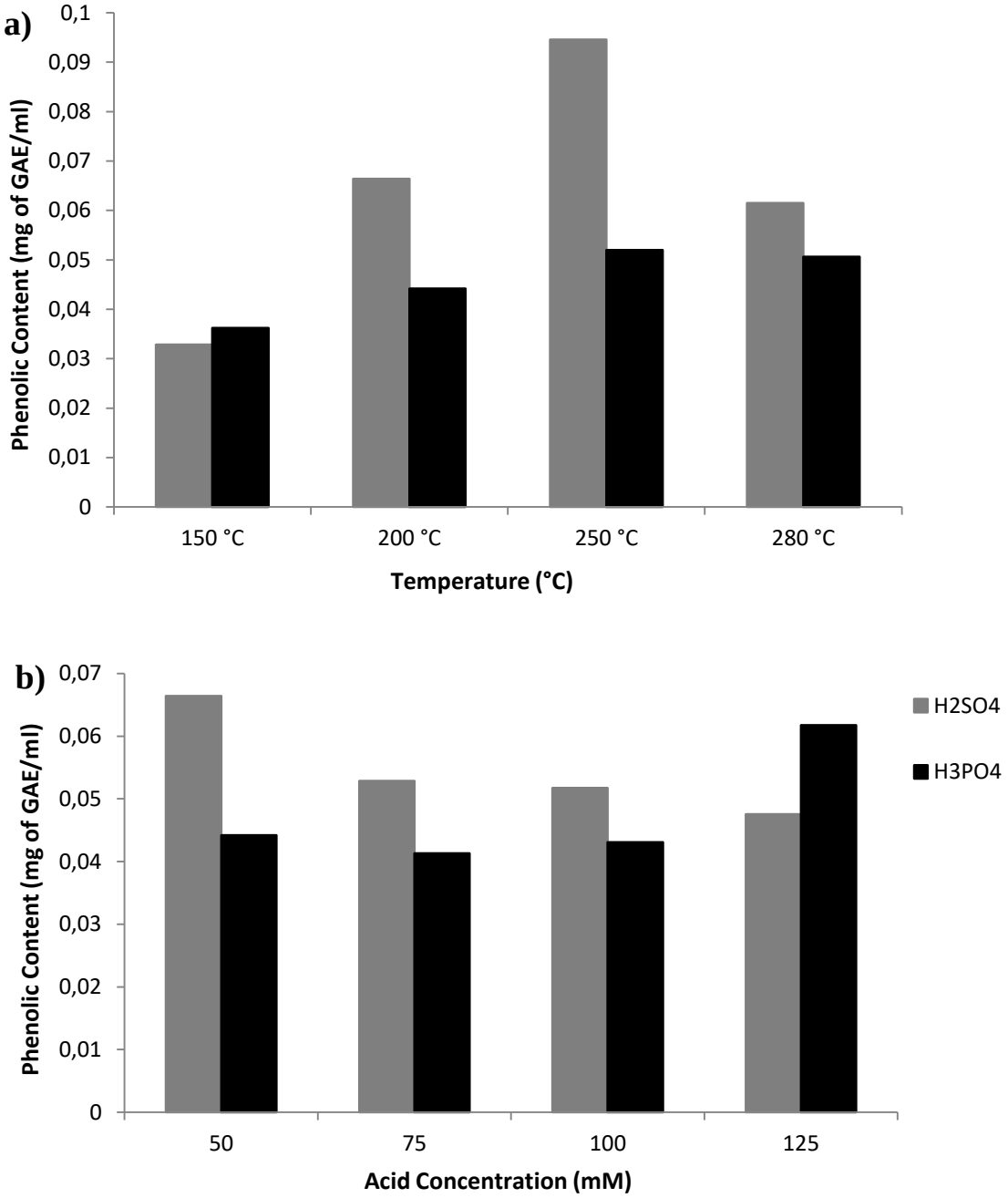


Figure 4.20. The effect of **a)** reaction temperature (60 min in 50 mM $H_2SO_4$ and $H_3PO_4$) and **b)** $H_2SO_4$ and $H_3PO_4$ (200 °C, 60 min and 15 bar) concentration on the total phenolic content at 200 °C

## 4.8. Analysis of Variance (ANOVA)

Significance of reaction temperature and $H_2SO_4$ concentration on the conversion of hazelnut shell and the yields of levulinic acid, acetic acid and furfural were performed by Analysis of Variance (ANOVA). Therefore, related experiments were repeated twice. In this study, acceptable p-values of each parameter were determined as $p \leq 0.05$. The p-values of individual effects of reaction temperature and $H_2SO_4$ concentration and quadratic reaction temperature for hazelnut shell conversion were 0.00, 0.10 and 0.00, respectively. Therefore, reaction temperature and $H_2SO_4$ concentration affected significantly to the conversion of hazelnut shell. In contrast, p-value of reaction time was 0.289 which is higher than confidence level so the influence of individual reaction time on hazelnut shell conversion was insignificant. Almost each individual reaction parameters affected significantly to the desired product yields but, only reaction temperature did not have significant effect on the acetic acid yield since its p-value was 0.088. The response surface plots of hazelnut shell conversion and the yields of desired products with respect to reaction temperature and $H_2SO_4$ concentration were shown in Figure 4.21. As seen in Figure 4.21, both waste hazelnut shell conversion (Figure 4.21a) and levulinic acid yield (Figure 4.21b) enhanced with increase up to 200 °C. In addition, addition of 50 mM $H_2SO_4$ concentration nearly increased the yield of levulinic acid with tripled value (9%). Response surface plot of acetic acid (Figure 4.21c) pointed out that $H_2SO_4$ treatment affected positively. The positive improvement of furfural yield (Figure 4.21d) was observed until 200 °C of reaction temperature; however, furfural production decreased remarkably with a further temperature increment.

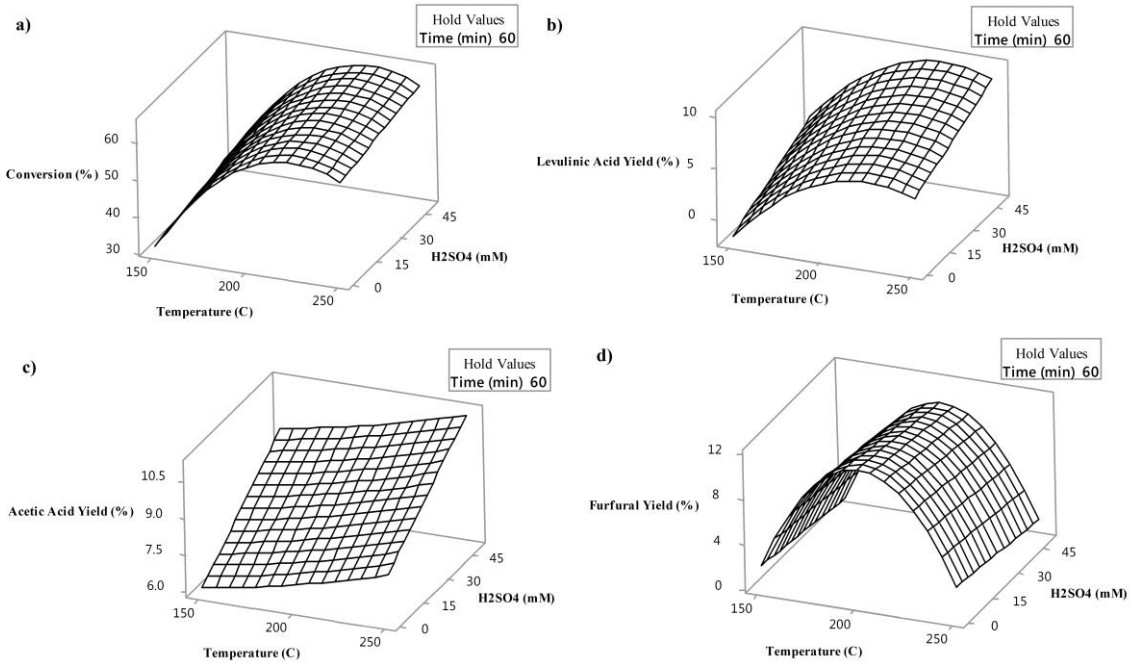


Figure 4.21. The surface plots of **a)** hazelnut shell conversion; yields of **b)** levulinic acid **c)** acetic acid and **d)** furfural with respect to reaction temperature and $H_2SO_4$ concentration

Maximum hazelnut shell conversion and the yields of desired products with the optimization of reaction parameters were given in Figure 4.22. 63.98% of maximum hazelnut shell conversion and 13.17% of maximum levulinic acid yield was obtained in the presence of 50 mM $H_2SO_4$ at 224.36 °C for 120 min. Optimized hazelnut shell conversion was recorded as 65.31% at 224.75 °C and 15 min in the addition of 50 mM $H_2SO_4$ and under the same conditions acetic acid yield was 12.87%. In addition, under the conditions of 201.52 °C reaction temperature for 15 min reaction time with 39.48 mM $H_2SO_4$, the conversion of hazelnut shell reached to maximum value of 61.53% and furfural yield was maximized as 11.60%.

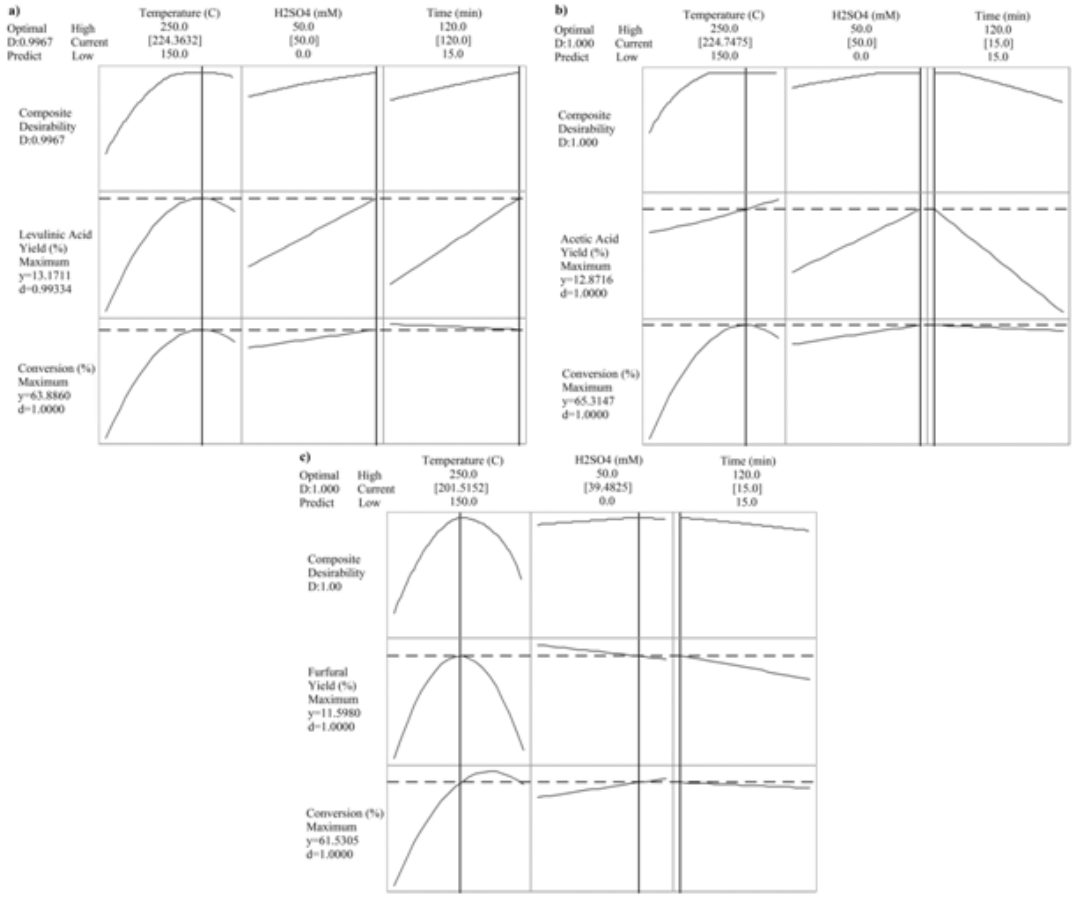


Figure 4.22. Optimized operating conditions for the maximum hazelnut shell conversion and the maximum yields of **a)** levulinic acid; **b)** acetic acid and **c)** furfural

# CHAPTER 5

# CONCLUSION

The hydrothermal conversion of waste hazelnut shell to value-added chemicals was investigated under hot compressed water in batch reactor that is equipped with agitation stirrer, temperature control, thermocouple and pressure gauge. Reactions were carried out at different reaction temperatures (150, 200, 250 and 280 °C), reaction time (15, 60, 90 and 120 min), acid type ($H_2SO_4$ and $H_3PO_4$) and acid concentrations (0, 5, 25, 50, 75, 100 and 125 mM). With hydrothermal acid-treatment, levulinic acid, furfural and acetic acid were determined as major compounds in liquid solutions; in addition, main gas products were carbon dioxide and carbon monoxide. Increase of reaction temperature led to significant improvement on the conversion of hazelnut shell and levulinic acid production with a value of 65.40% and 13.05% at 280 °C and 120 min in the presence of 50 mM $H_2SO_4$, respectively. In contrast, the yield of furfural reduced to 0.04% under the same reaction conditions. Addition of $H_2SO_4$ and $H_3PO_4$ promoted the different organic product formation mechanisms. While $H_2SO_4$ enhanced the production of levulinic acid, the formation of furfural was accelerated with $H_3PO_4$. Furthermore, bioactivity analysis to clarify antioxidant activity and phenolic content and ANOVA were performed. Therefore, hot compressed water as a reaction environment is a promising technology for adding value to waste hazelnut shell by producing bio-based chemicals such as levulinic acid, furfural and acetic acid.

# REFERENCES


Agreda, V.H. Acetic acid and its derivatives. New York: CRC Press. 1993.

Akalin, M. K., K. Tekin, and S. Karagoz. 2012. Hydrothermal liquefaction of cornelian cherry stones for bio-oil production. *Bioresource Technology* **110**:682-687.

Akiya, N., and P. E. Savage. 2002. Roles of water for chemical reactions in high-temperature water. *Chemical Reviews* **102** (8):2725-2750.

Alasalvar, C., M. Karamac, A. Kosinska, A. Rybarczyk, F. Shahidi, and R. Amarowicz. 2009. Antioxidant Activity of Hazelnut Skin Phenolics. *Journal of Agricultural and Food Chemistry* **57** (11):4645-4650.

Altun, M., S. E. Celik, K. Guclu, M. Ozyurek, E. Ercag, and R. Apak. 2013. Total Antioxidant Capacity and Phenolic Contents of Turkish Hazelnut (Corylus Avellana L.) Kernels and Oils. *Journal of Food Biochemistry* **37** (1):53-61.

Arai, Y., T. Sako, and Y. Takebayashi. Supercritical fluids: Molecular interactions, physical properties, and new applications. Heidelberg: Springer. 2002.

Asghari, F. S., and H. Yoshida. 2010. Conversion of Japanese red pine wood (Pinus densiflora) into valuable chemicals under subcritical water conditions. *Carbohydrate Research* **345** (1):124-131.

Cardenas-Toro, F.P., S.C. Alcazar-Alay, T. Forster-Carneiro, and M. A. A. Meireles. 2014. Obtaining oligo- and monosaccharides from agroindustrial and agricultural residues using hydrothermal treatments. *Food and Public Health* **4** (3):123-139.

Chan, Y. H., S. Yusup, A. T. Quitain, Y. Uemura, and M. Sasaki. 2014. Bio-oil production from oil palm biomass via subcritical and supercritical hydrothermal liquefaction. *Journal of Supercritical Fluids* **95**:407-412.

Cheng, L. M., X. P. Ye, R. H. He, and S. Liu. 2009. Investigation of rapid conversion of switchgrass in subcritical water. *Fuel Processing Technology* **90** (2):301-311.

Christensen, P.S. Hydrothermal liquefaction of waste biomass: Optimizing reaction parameters. Ph.D. Dissertation. Aarhus University. 2014.

Clark, J., and F. Deswarte. Introduction to chemicals from biomass. West Sussex: Wiley. 2015.

Contini, M., S. Baccelloni, R. Massantini, and G. Anelli. 2008. Extraction of natural antioxidants from hazelnut (Corylus avellana L.) shell and skin wastes by long maceration at room temperature. *Food Chemistry* **110** (3):659-669.

Dadenov, S. Hydrothermal treatment of biomass in hot-pressurized water. M. Sc. Thesis. İzmir Institute of Technology. 2015.

Efremov, A. A., G. G. Pervyshina, and B. N. Kuznetsov. 1997. Thermocatalytic transformations of wood and cellulose in the presence of HCl, HBr, and $H_2SO$. *Chemistry of Natural Compounds* **33** (1):107-112.

Fabian, C., N. Y. Tran-Thi, N. S. Kasim, and Y. H. Ju. 2010. Release of phenolic acids from defatted rice bran by subcritical water treatment. *Journal of the Science of Food and Agriculture* **90** (15):2576-2581.

Fang, Q., and M. A. Hanna. 2002. Experimental studies for levulinic acid production from whole kernel grain sorghum. *Bioresource Technology* **81** (3):187-192.

Fang, Z., and C. B. Xu. Near-critical and supercritical water and their applications for biorefineries. Dordrecht: Springer. 2014.

Gandini, A. 2011. The irruption of polymers from renewable resources on the scene of macromolecular science and technology. *Green Chemistry* **13** (5):1061-1083.

Girisuta, B. Levulinic acid from lignocellulosic biomass. Ph.D. Dissertation. University of Groningen. 2007.

Guney, M. S. 2013. Utilization of hazelnut husk as biomass. *Sustainable Energy Technologies and Assessments* **4**:72-77.

Jong, W.D., and J.R.V. Ommen. Biomass as a sustainable energy source for the future: Fundamentals of conversion processes. New Jersey: Wiley. 2015.

Kruse, A., and N. Dahmen. 2015. Water - A magic solvent for biomass conversion. *Journal of Supercritical Fluids* **96**:36-45.

Kruse, A., and E. Dinjus. 2007. Hot compressed water as reaction medium and reactant - Properties and synthesis reactions. *Journal of Supercritical Fluids* **39** (3):362-380.

Kruse, A., and A. Gawlik. 2003. Biomass conversion in water at 330-410 degrees C and 30-50 MPa. Identification of key compounds for indicating different chemical reaction pathways. *Industrial & Engineering Chemistry Research* **42** (2):267-279.

Lee, J.W. Advanced Biofuels and Bioproducts. New York: Springer. 2013.

Liu, A., Y. Park, Z. L. Huang, B. W. Wang, R. O. Ankumah, and P. K. Biswas. 2006. Product identification and distribution from hydrothermal conversion of walnut shells. *Energy & Fuels* **20** (2):446-454.

Machado, G., S. Leon, F. Santos, R. Lourega, J. Dullius, M.E. Mollmann, and P. Eichler. 2016. Literature review on furfural production from lignocellulosic biomass. *Natural Resources* **7**:115-129.

McKendry, P. 2002a. Energy production from biomass (part 1): overview of biomass. *Bioresource Technology* **83** (1):37-46.

McKendry, P. 2002b. Energy production from biomass (part 2): conversion technologies. *Bioresource Technology* **83** (1):47-54.

Moller, M., F. Harnisch, and U. Schroder. 2013. Hydrothermal liquefaction of cellulose in subcritical water-the role of crystallinity on the cellulose reactivity. *Rsc Advances* **3** (27):11035-11044.

Moller, M., P. Nilges, F. Harnisch, and U. Schroder. 2011. Subcritical Water as Reaction Environment: Fundamentals of Hydrothermal Biomass Transformation. *Chemsuschem* **4** (5):566-579.

Pandey, A., C. Larroche, S.C. Ricke, C.G. Dussap, and E. Gnansounou. Biofuels: Alternative feedstocks and conversion processes. San Diego: Academic Press. 2011.

Pavlovic, I., Z. Knez, and M. Skerget. 2013. Subcritical Water - a Perspective Reaction Media for Biomass Processing to Chemicals: Study on Cellulose Conversion as a Model for Biomass. *Chemical and Biochemical Engineering Quarterly* **27** (1):73-82.

Peleteiro, S., S. Rivas, J. L. Alonso, V. Santos, and J. C. Parajo. 2016. Furfural production using ionic liquids: A review. *Bioresource Technology* **202**:181-191.

Pourali, O., F. S. Asghari, and H. Yoshida. 2010. Production of phenolic compounds from rice bran biomass under subcritical water conditions. *Chemical Engineering Journal* **160** (1):259-266.

Promdej, C., and Y. Matsumura. 2011. Temperature Effect on Hydrothermal Decomposition of Glucose in Sub- And Supercritical Water. *Industrial & Engineering Chemistry Research* **50** (14):8492-8497.

Rackemann, D. W., and W. O. S. Doherty. 2011. The conversion of lignocellulosics to levulinic acid. *Biofuels Bioproducts & Biorefining-Biofpr* **5** (2):198-214.

Resende, F. L. P. Supercritical water gasification of biomass. Ph.D. Dissertation. The University of Michigan. 2009.

Resende, F. L. P., and P. E. Savage. 2010. Kinetic Model for Noncatalytic Supercritical Water Gasification of Cellulose and Lignin. *Aiche Journal* **56** (9):2412-2420.

Roudsari, M. H. Subcritical water extraction of antioxidant compounds from canola meal. Master of Science. University of Saskatchewan. 2007.

Saxena, R. C., D. K. Adhikari, and H. B. Goyal. 2009. Biomass-based energy fuel through biochemical routes: A review. *Renewable & Sustainable Energy Reviews* **13** (1):167-178.

Sengupta, D., and R.E. Pike. Chemicals from biomass: Integrating bioprocesses into chemical production complexes for sustainable development. Boca Raton: CRC Press. 2013.

Shahidi, F., C. Alasalvar, and C. M. Liyana-Pathirana. 2007. Antioxidant phytochemicals in hazelnut kernel (Corylus avellana L.) and hazelnut byproducts. *Journal of Agricultural and Food Chemistry* **55** (4):1212-1220.

Shakhashiri http://scifun.chem.wisc.edu/chemweek/pdf/aceticacid.pdf; Acetic acid & Acetic anhydride. Retrieved in 15 October 2016.

Takeuchi, Y., F. M. Jin, K. Tohji, and H. Enomoto. 2008. Acid catalytic hydrothermal conversion of carbohydrate biomass into useful substances. *Journal of Materials Science* **43** (7):2472-2475.

Tekin, K., S. Karagoz, and S. Bektas. 2014. A review of hydrothermal biomass processing. *Renewable & Sustainable Energy Reviews* **40**:673-687.

Timokhin, B. V., V. A. Baransky, and G. D. Eliseeva. 1999. Levulinic acid in organic synthesis. *Uspekhi Khimii* **68** (1):80-93.

Toor, S. S., L. Rosendahl, and A. Rudolf. 2011. Hydrothermal liquefaction of biomass: A review of subcritical water technologies. *Energy* **36** (5):2328-2342.

Tymchyshyn, M., and C. B. Xu. 2010. Liquefaction of bio-mass in hot-compressed water for the production of phenolic compounds. *Bioresource Technology* **101** (7):2483-2490.

Wahyudiono, M. Sasaki, and M. Goto. 2007. Noncatalytic liquefaction of tar with low-temperature hydrothermal treatment. *Journal of Material Cycles and Waste Management* **9** (2):173-181.

Watchararuji, K., M. Goto, M. Sasaki, and A. Shotipruk. 2008. Value-added subcritical water hydrolysate from rice bran and soybean meal. *Bioresource Technology* **99** (14):6207-6213.

Yakaboylu, O., G. Yapar, M. Recalde, J. Harinck, K. G. Smit, E. Martelli, and W. de Jong. 2015. Supercritical Water Gasification of Biomass: An Integrated Kinetic Model for the Prediction of Product Compounds. *Industrial & Engineering Chemistry Research* **54** (33):8100-8112.

Yan, K., G. S. Wu, T. Lafleur, and C. Jarvis. 2014. Production, properties and catalytic hydrogenation of furfural to fuel additives and value-added chemicals. *Renewable & Sustainable Energy Reviews* **38**:663-676.

Yan, L. F., N. K. Yang, H. Pang, and B. Liao. 2008. Production of levulinic acid from bagasse and paddy straw by liquefaction in the presence of hydrochloride acid. *Clean-Soil Air Water* **36** (2):158-163.

Zhu, G. Y., X. Zhu, Z. B. Xiao, R. J. Zhou, Y. L. Zhu, and X. L. Wan. 2014. Kinetics of peanut shell pyrolysis and hydrolysis in subcritical water. *Journal of Material Cycles and Waste Management* **16** (3):546-556.